UNIVERSITY OF KWAZULU-NATAL ™

INYUVESI YAKWAZULU-NATALI

THE ANTIPROLIFERATIVE AND APOPTOSIS INDUCING EFFECTS OF *MORINGA OLEIFERA* AQUEOUS LEAF EXTRACT AND ITS SYNTHESISED GOLD NANOPARTICLES - MODULATION OF ONCOGENES AND TUMOUR SUPPRESSOR GENES IN HUMAN CANCER CELL LINES

BY

CHARLETTE TILOKE

B.Sc., B.Med.Sc. (Hons) University of KwaZulu-Natal

Submitted in fulfilment of the requirements for the degree of

Doctor of Philosophy

in the

Discipline of Medical Biochemistry and Chemical Pathology

School of Laboratory Medicine and Medical Sciences

College of Health Sciences

University of KwaZulu-Natal

2015

PREFACE AND DECLARATION

For centuries, plants have been utilised for dietary supplementation and medicinal properties. These medicinal plants play a pivotal role in the traditional treatment of a variety of diseases. One such plant is *Moringa oleifera* (MO), an indigenous tree to India, found throughout South Africa (SA). Almost all parts of the tree are used either for dietary supplementation or medicinal properties. However the nutritious leaves possess a wide range of bioactive compounds that display anticancer, anti-inflammatory and antimicrobial activity among several others. In SA, majority of the population are relatively poor and rely on traditional medicines of which MO forms part of their remedy. Lung and oesophageal cancers are the leading causes of death in SA. Current cancer therapies are expensive with many side-effects therefore cheap, alternate traditional plant therapies are being actively investigated. Nanoparticles are also showing potential as a cancer therapeutics and can be easily synthesised using plant extracts such as MO leaf extract (MOE). This green chemistry can be advantageous especially in large scale production. Gold nanoparticles (AuNP's) was successfully synthesised from MOE (ML_{AuNP}). This study established the use of MOE as a complementary and alternate medicine in the treatment of both lung and oesophageal cancers. In addition, ML_{AuNP} also showed potential in the treatment of lung cancer. Their mode of action was to induce cancer cell apoptosis with minimal effect on normal healthy cells. It can be concluded that SA's traditional tree can be used as an antiproliferative agent against cancer.

I, **Charlette Tiloke** declare that:

(i) The research reported in this thesis, except where otherwise indicated, is my original work.

(ii) This thesis has not been submitted for any degree or examination at any other university.

(iii) This thesis does not contain other persons' data, pictures, graphs or other information, unless specifically acknowledged as being sourced from other persons.

(iv) This thesis does not contain other persons' writing, unless specifically acknowledged as being sourced from other researchers. Where other written sources have been quoted, then:

a) their words have been re-written but the general information attributed to them has been referenced;

b) where their exact words have been used, then their writing has been placed inside quotation marks, and referenced.

(v) Where I have reproduced a publication of which I am author, co-author or editor, I have indicated in detail which part of the publication was actually written by myself alone and have fully referenced such publications.

(vi) This thesis does not contain text, graphics or tables copied and pasted from the Internet, unless specifically acknowledged, and the source being detailed in the thesis and in the References sections.

Signed:

Charlette Tiloke **03/03/2016**

Charlette Tiloke **Date**

DEDICATION

I dedicate this thesis

to my family

Ramesh Tiloke, Romitha Tiloke, Noelin Tiloke, Nicolette Tiloke

and

Ethan Isaiah Tiloke

for all the support, encouragement and unconditional love

ACKNOWLEDGEMENTS

Prof A.A. Chuturgoon

I am grateful for your guidance and advice throughout the study. Without your valuable suggestions, the study would have not been possible. I am also grateful for the skills that I have developed and the opportunities you have given me to develop into a better researcher. I beam with pride to have a supervisor like you who is inspiring, motivating and dedicated in sharing your knowledge with us. Thank you for all your efforts in bringing out the best in your students. Thank you for your assistance in the manuscript preparations. The journey through PhD has been incredible and I am grateful and proud to be part of the Medical Biochemistry family.

Dr A. Phulukdaree

The guidance and support through the study is appreciated. Your assistance, experience, dedication and flexibility have inspired and motivated me to be the best that I can be. Your scientific advice, knowledge, insightful discussions and contributions are also greatly appreciated. Thank you for the assistance in the manuscript preparations. You are a dear friend and the best role model that I could ask for. Your enthusiasm and love for teaching has been an inspiration to me.

Professor R.M. Gengan and Dr K. Anand

Thank you for the synthesis and characterisation of the gold nanoparticles. Your technical guidance is appreciated.

Discipline of Medical Biochemistry and Chemical Pathology (2012-2015)

Great appreciation goes to staff and postgraduate students. Thank you for the support and motivation throughout the years. The endless discussions and positive criticism is duly appreciated.

Scholarships

I am thankful to the National Research Foundation, South Africa for the prestigious Doctoral scholarship. The study was also supported by the College of Health Sciences research scholarship from UKZN. Thank you for recognising the importance of research and providing resources to complete the study.

My family

Thank you for the patience and encouragement. The unwavering support and confidence has motivated me to achieve my goals. I will like to especially thank my hard-working parents - for all the sacrifices, motivation and unconditional love.

TABLE OF CONTENTS

LIST OF PUBLICATIONS

1) Tiloke, C., Phulukdaree, A., Chuturgoon, A.A. 2013. The antiproliferative effect of *Moringa oleifera* crude aqueous leaf extract on cancerous human alveolar epithelial cells. BMC Complementary and Alternative Medicine 13, 226: 1-8. DOI: 10.1186/1472-6882-13-226

(Top 100 publication in journal, highly accessed, 21 citations) (Original article)

2) Tiloke, C., Phulukdaree, A., Chuturgoon, A.A. 2015. The antiproliferative effect of *Moringa oleifera* crude aqueous leaf extract on human oesophageal cancer cells. Journal of Medicinal Food.

***In press*.** (Manuscript number JMF-2015-0113) (Original article)

3) Tiloke, C., Phulukdaree, A., Anand, K., Gengan, R.M., Chuturgoon, A.A. 2015. *Moringa oleifera* gold nanoparticles modulate oncogenes, tumor suppressor genes and *caspase-9* splice variants in A549 cells. Journal of Cellular Biochemistry. DOI: 10.1002/jcb.25528 (Original article)

4) Tiloke, C., Phulukdaree, A., Chuturgoon, A.A. 2015. Chemotherapeutic potential of gold nanoparticles obtained by green synthesis in human carcinomas. Therapeutic Nanostructures (I-V) Multi-Volume SET (published by Elsevier)

Edited by: Alexandru Mihai Grumezescu (http://grumezescu.com/)

(Invited review - submitted on 20 September 2015)

5) Tiloke, C., Chuturgoon, A.A. 2015. The antiproliferative and anti-bacterial effect of *Moringa oleifera* mediated gold nanoparticles: A review. Strategies for metabolic engineering in bioactive compounds and processes (published by Springer)

Edited by: Dr Adesh K. Saini, Dr Reena V. Saini, Dr Deepak K. Sharma and Dr V.C. Kalia.

(Invited review - submitted on 25 November 2015)

LIST OF PRESENTATIONS

The paper titled: The effects of *Moringa oleifera* on transformed human alveolar epithelial cells (A549) *in vitro* by Tiloke, C., Phulukdaree, A., Chuturgoon, A.A was presented at the local conference (Poster):

1) College of Health Science Research Symposium 12th -13th September, University of KwaZulu-Natal, Durban, South Africa, 2012

The paper titled: Induction of apoptosis by gold nanoparticles of *Moringa oleifera* leaf extract in human lung cancer *in vitro* by Tiloke, C., Phulukdaree, A., Anand, K., Gengan, R.M., Chuturgoon, A.A was presented at the local conference (Oral):

1) College of Health Science Research Symposium 12th -13th September, University of KwaZulu-Natal, Durban, South Africa, 2013

The paper titled: The antiproliferative effect of *Moringa oliefera* leaf extract on human oesophageal cancer cells by Tiloke, C., Phulukdaree, A., Chuturgoon, A.A was presented at the following local and international conferences (Oral):

1) College of Health Science Research Symposium 11th -12th September, University of KwaZulu-Natal, Durban, South Africa, 2014 - won 1st prize in best oral presentation category
2) 2nd International Congress of Society for Ethnopharmacology (SFEC - 2015) - Focal theme: Validation of Medicinal Plants and Traditional Medicines - Global Perspectives 20-22nd February, Chitnavis Convention Centre, Civil Lines Nagpur, India, 2015. Affiliated to the International Society of Ethnopharmacology, UK

The paper titled *Moringa oleifera* gold nanoparticles modulate oncogenes, tumor suppressor genes and caspase-9 splice variants in human lung carcinoma cells by Tiloke, C., Phulukdaree, A., Anand, K., Gengan, R.M., Chuturgoon, A.A was presented at the local conference (Oral):

1) College of Health Science Research Symposium 10th -11th September, University of KwaZulu-Natal, Durban, South Africa, 2015

LIST OF FIGURES

Page

CHAPTER 1

CHAPTER 2

CHAPTER 3

CHAPTER 4

LIST OF TABLES

LIST OF APPENDICES

LIST OF ABBREVIATIONS

Ag	Silver
AIDS	Acquired immune deficiency syndrome
AIF	Apoptosis inducing factor
Apaf-1	Apoptotic protease activation factor-1
ARE	Antioxidant response element
ATP	Adenosine triphosphate
Au	Gold
AuNP's	Gold nanoparticles
BCA	Bicinchoninic acid assay
BH	Bcl-2 homology
Bid	BH3-interacting domain death agonist
BIR	Baculovirus IAP repeat
BSA	Bovine serum albumin
CAM	Complementary and alternative medicines
CARD	Caspase activation and recruitment domain
Caspases	Aspartate-specific cysteine proteases
CAT	Catalase
C_{AuNP}	Trisodium citrate gold nanoparticles
CCM	Complete culture media
cDNA	Copy DNA
c-FLIP	FADD-like interleukin-1β-converting enzyme (FLICE)-inhibitory protein
Cyt c	Cytochrome c
DED	Death effector domain
DISC	Death-inducing signal complex
DLS	Dynamic light scattering
DMSO	Dimethyl sulphoxide
DNA	Deoxyribonucleic acid
ds	Double-strand
EGFR	Epidermal growth factor receptor
EMEM	Eagle's minimum essential medium
EtBr	Ethidium bromide
FACS	Fluorescence-activated cell sorting
FADD	Fas-associated death domain

Fbw7	F-box and WD repeat domain-containing 7
Fbw7α	F-box and WD repeat domain-containing 7 α
GPx	Glutathione peroxidase
GSH	Glutathione
Gsk3	Glycogen synthase kinase 3
Gsk3β	Glycogen synthase kinase 3β
GSR	Glutathione reductase
GSSG	Glutathione disulphide
GST	Glutathione-S-transferase
H_2O_2	Hydrogen peroxide
$HAuCl_4.3H_2O$	Gold (III) Chloride trihydrate
HIV	Human immunodeficiency virus
hnRNP	Heterogeneous nuclear ribonucleoprotein
HRP	Horse radish peroxidase
Hsp	Heat shock proteins
IAP	Inhibitor of apoptosis
IAP's	Inhibitor of apoptosis proteins
IC_{50}	Concentration of half the maximum inhibition
IL	Interleukin
Keap1	Kelch-like epichlorohydrin-associated protein 1
LMPA	Low melting point agarose
MDA	Malondialdehyde
MDR	Multi drug-resistant
MF_{AuNP}	Gold nanoparticles mediated by *Moringa oleifera* flower extract
Min	Minutes
ML_{AuNP}	AuNP's synthesised from MOE
MO	*Moringa oleifera*
MOE	MO leaf extract
MPTP	Mitochondrial permeability transition pore
mRNA	Messenger RNA
MtB	*Mycobacterium tuberculosis*
MTT	Methyl thiazol tetrazolium/ 3-(4, 5-Dimethyl-2-thiazolyl)-2, 5-diphenyl-2H-tetrazolium bromide
NAD^+	Nicotinamide adenine dinucleotide
NMD	Nonsense-mediated mRNA decay

NO^-	Nitroxyl anion
NO^+	Nitrosonium cation
$NO^\bullet$	Nitric oxide
NP's	Nanoparticles
Nrf2	Nuclear factor - erythroid 2 p45 - related factor 2
NSCLC	Non-small cell lung cancer
OC	Oesophageal cancer
OD	Optical density
PAK2	p21-activated kinase 2
PARP-1	Poly (ADP ribose) polymerase-1
PBMCs	Peripheral blood mononuclear cells
PBS	Phosphate buffered saline
PGE_2	Prostaglandin E_2
PI	Propidium iodide
PS	Phosphatidylserine
qPCR	Quantitative polymerase chain reaction
RBD	Relative band density
RLU	Relative lights units
RNA	Ribonucleic acid
RNS	Reactive nitrogen species
ROS	Reactive oxygen species
RPMI	Roswell park memorial institute
RT	Room temperature
RT cocktail	Real time cocktail
RT buffer 3	Real time buffer 3
SA	South Africa
SCF	Skp1/Cull/F-box
SCLC	Small cell lung cancer
SD	Standard deviation
SEM	Standard error of the mean
Skp2	S-phase kinase-associated protein 2
Smac/DIABLO	Second mitochondria-derived activator of caspase/direct inhibitor of apoptosis binding protein with low pI
SOD	Superoxide dismutase
SPR	Surface Plasmon Resonance

SR proteins	Serine/arginine-rich proteins
ss	Single-strand
TB	Tuberculosis
TBA/BHT	Thiobarbituric acid (1%)/0.1 mM butylated hydroxytoluene solution
TBARS	Thiobarbituric acid assay
tBid	Truncated Bid
TEM	Transmission electron microscopy
Thr58	Threonine 58
TIC	Total ion chromatogram
TNF-α	Tumour necrosis factor alpha
TRADD	TNFR-associated death domain
TTBS	Tris-buffered saline containing 0.5% Tween20
USA	United States of America
VDAC	Voltage-dependent anion channel
VEGF	Vascular endothelial growth factor
WHO	World Health Organisation
XDR	Extremely drug-resistant
xIAP	X chromosome encoded IAP
ΔΨm	Mitochondrial depolarization
11-MUA	11-mercaptoundecanoic acid

ABSTRACT

Cancer is one of the leading causes of global mortality. In South Africa (SA), the burden of cancer (lung and oesophageal) continues to increase. *Moringa oleifera* (MO), indigenous to India, is found widely in SA and used in traditional treatments of cancer. Gold nanoparticles (AuNP's) are showing potential in cancer therapies and can be synthesised using plants extracts such as MO leaf extract (MOE). This study investigated the antiproliferative effect of MOE and AuNP's synthesised from MOE (ML_{AuNP}) in A549 lung and SNO oesophageal cancer cells.

MO crude aqueous leaf extract was prepared and cytotoxicity (MTT assay) was assessed in A549, SNO cells and normal peripheral blood mononuclear cells (PBMCs) (24h). Oxidative stress, DNA fragmentation and apoptotic markers were determined. A one-pot green synthesis technique using MOE to synthesise ML_{AuNP} was then conducted. A549, SNO cells and PBMCs were also exposed to ML_{AuNP} and C_{AuNP} to evaluate cytotoxicity and apoptotic markers.

MOE was cytotoxic to A549 cells. MOE (IC_{50}: 166.7µg/ml, 24h) significantly increased lipid peroxidation, decreased glutathione (GSH) and Nrf2 levels leading to DNA fragmentation. MOE induced apoptosis by significantly increasing p53, caspase-9, enhancing caspase-3/7 activities and Smac/DIABLO expression. MOE significantly cleaved PARP-1 into 89kDa and 24kDa fragments.

MOE was not cytotoxic to PBMCs but in SNO cells (IC_{50}: 389.2µg/ml, 24h), it significantly increased lipid peroxidation, DNA fragmentation, decreased GSH, catalase and Nrf2 levels. Apoptosis was confirmed by the significant increase in phosphatidylserine (PS) externalisation, caspase-9, enhanced caspase-3/7 activities and significant decrease in ATP levels. MOE significantly increased p53, Smac/DIABLO and cleavage of PARP-1, resulting in an increase in the 24kDa fragment.

ML_{AuNP} was successfully synthesised. ML_{AuNP} and C_{AuNP} were not cytotoxic to PBMCs, whilst its pro-apoptotic properties were confirmed in A549 (IC_{50}: ML_{AuNP} - 98.46µg/ml; C_{AuNP} - 121.4µg/ml) and SNO (IC_{50}: ML_{AuNP} - 92.01µg/ml; C_{AuNP} - 410.4µg/ml) cells. ML_{AuNP} significantly increased caspase activity in SNO cells while ML_{AuNP} significantly increased PS externalisation, mitochondrial depolarisation, caspase-9, caspase-3/7 activities and decreased ATP levels. Also, ML_{AuNP} significantly increased p53, Bax, Smac/DIABLO, PARP-1 24kDa fragment and enhanced SRp30a levels. Conversely, ML_{AuNP} significantly decreased Bcl-2,

Hsp70, *Skp2*, *Fbw7α*, *c-myc* levels and activated alternate splicing with *caspase-9a* splice variant being increased.

These findings indicate that MOE exerts antiproliferative effects in cancerous A549 and SNO cells by increasing oxidative stress, DNA fragmentation and inducing apoptosis. ML_{AuNP} also possessed antiproliferative properties in SNO cells and induced apoptosis in A549 cells by modulating oncogenes, tumour suppressor genes and activating alternate splicing of *caspase-9*. MOE and ML_{AuNP} showed potential use as a complementary and alternative treatment for lung and oesophageal cancer. MOE fractionation studies are further recommended to identify the bioactive compounds responsible for the antiproliferative effect seen in A549 and SNO cells. In addition, membrane transport proteins as well as cell cycle analysis will provide further insight into MOE and ML_{AuNP} antiproliferative effect.

INTRODUCTION

Cancer is amongst the major noncommunicable diseases causing death worldwide [1, 2]. Cancer alone accounts for 21.7% of all noncommunicable diseases. In 2012, approximately 8.2 million deaths occurred due to cancer. The annual cancer mortality is expected to increase to 12.6 million by year 2030. The burden of cancer is increasing in both developed and developing countries as a result of increased tobacco use, alcohol consumption, physical inactivity, diet and lifestyle [3]. In addition, inhalation of air-borne pollutants, occupational exposure to chemicals and toxins, family history and burden of infectious diseases are also factors associated with cancer pathogenesis [4, 5].

In South Africa (SA) the healthcare burden is compounded by the presence of infectious diseases such as Human immunodeficiency virus (HIV)/Acquired immune deficiency syndrome (AIDS), *Mycobacterium tuberculosis* (MtB) infections in addition to cancer and other noncommunicable diseases [6]. HIV causes immune dysfunction, disease progression and susceptibility to secondary infections e.g. tuberculosis (TB) [7] with multi drug-resistant (MDR) and extremely drug-resistant (XDR) TB accounting for 10% of all TB cases. The majority of South Africans are at a higher risk of developing cancers (especially lung and oesophageal) due to lifestyle changes and high burden of these infectious diseases [8]. In SA, lung and oesophageal cancers commonly have high mortality rates which are a major concern.

Cellular homeostasis is maintained via cell proliferation and apoptosis (programmed cell death) [9]. Cancer cells evade apoptosis and proliferate through activation of oncogenes e.g. c-myc, and inactivation of tumour suppressor genes e.g. p53. Apoptosis occurs via two pathways namely the death receptor - mediated procaspase - activation (extrinsic) pathway or mitochondrion - mediated procaspase - activation (intrinsic) pathway [10, 11]. The pathways are activated via apoptotic stimuli i.e. reactive oxygen species (ROS), decreased antioxidant response and DNA damage [9]. In addition, the aspartate-specific cysteine proteases (caspases) cause the cleavage of proteins and execution of the apoptotic cascade.

Overexpression of c-myc is seen in many cancers which result in cancer cell proliferation and evasion of apoptosis [12]. It is post-translationally regulated by S-phase kinase-associated protein 2 (Skp2) and F-box and WD repeat domain-containing 7 α (Fbw7α) which forms subunits of SCF-type E3 ligase responsible for proteasomal degradation. Skp2 and Fbw7α can also act as oncogenes and tumour suppressor genes respectively. Targeting their expression can

be effective for cancer therapeutics. In addition, regulation of genes and proteins determines cellular fate which can also aid in the development of chemotherapeutic agents. This is evident by the alternate splicing mechanism which determines which variant of a gene is translated resulting in differing protein expression. Caspase-9, an initiator caspase, undergoes alternate splicing via SRp30a, causing two splice variants - *caspase-9a* (pro-apoptotic) and *caspase-9b* (anti-apoptotic) [13-15]. The variant expression is a determinant of the activation of the intrinsic pathway to ensure cellular death.

The health care policies in SA have not been beneficial to all South Africans especially in the rural areas [6]. The quality of health care is relatively low as well as access to these services are inadequate. Traditional medicine has therefore been the only access for maintenance and management of various diseases. *Moringa oleifera* (MO) commonly known as Drumstick tree is consumed widely in SA and is used in traditional medicine [16, 17]. Almost all parts of the tree are used in traditional treatments, however the leaves possess high levels of vitamins, amino acids, proteins and antioxidants [18, 19]. There are many bioactive compounds such as niazimicin, gallic acid, glucosinolates and isothiocyanates present in the extract which possess anticancer and anti-inflammatory properties [16, 20, 21]. Traditional healers in SA, utilise MO as part of their treatment of various ailments however their mode of action have not been elucidated.

Nanoparticles (NP's) are showing huge promise in cancer therapy [22] because they have characteristic properties of being very small (1-100nm). Metals such as gold (Au) are readily available for use in the synthesis of NP's. These NP's can be synthesised using plant extracts such as MO - in a cost effective and environmentally friendly synthesis.

Currently there are no reports for the anti-cancer effects of MO leaf extract (MOE). In addition, the use of MOE to synthesise novel gold nanoparticles (AuNP's) have not been conducted. This study determined the antiproliferative and apoptosis inducing effects of MOE and its synthesised AuNP's (ML_{AuNP}) on human carcinomas - A549 lung and SNO oesophageal cancer cells *in vitro.* The study provides a biochemical mechanism underlying the use of SA's traditional plant and its synthesised novel AuNP's in cancer drug development.

RESEARCH RATIONALE, AIM, HYPOTHESIS AND OBJECTIVE

Research rationale

Despite the major advances in medicine, many people still depend on natural remedies. Due to SA's limited healthcare services especially in our rural areas, traditional medicine has been the only access to treatment of various diseases. MO has both nutritional and medicinal properties and is used traditionally to treat malnutrition, diabetes mellitus - type 2, cardiovascular and liver diseases [16, 23]. MO trees grow well in both rural and urban areas and its leaves are readily available for use. Traditional healers in SA therefore utilise MO as part of their treatment regime. Cancer mortality rates are increasing and global burden is expected to increase even further [8]. MOE possesses anticancer properties and can be used to synthesise AuNP's however their exact pharmacological action has not been investigated and established.

Aim

The aim of the study was to determine the antiproliferative properties of MOE (crude aqueous extract) and its synthesised AuNP's (ML_{AuNP}) (exposed singly) in selected cancerous cell lines.

Hypothesis

MOE and ML_{AuNP} possess antiproliferative properties in cancerous cells *in vitro* with minimal cytotoxic effects on normal healthy cells.

Objective

The objectives of this study were designed to assess the antiproliferate effects of MOE and ML_{AuNP} (exposed singly) on carcinoma cell lines (A549 lung and SNO oesophageal cancer cells) to determine whether it:

1) Increased oxidative stress and apoptosis in A549 lung cancer cells

2) Increased oxidative stress and apoptosis in SNO oesophageal cancer cells

3) Increased apoptosis in SNO oesophageal cancer cells and influenced oncogenes, tumour suppressor genes and *caspase-9* splice variants to induce apoptosis in A549 lung cancer cells

CHAPTER 1
LITERATURE REVIEW

1.1. *Moringa oleifera* - 'The tree of life'

Ancient medicinal systems have extensively utilised natural resources such as trees and plants in alleviating, managing and treating a variety of ailments. The evolution of mankind has therefore depended tremendously on these ancient traditional medicinal systems. As nature provided a storehouse of natural remedies, their traditional uses have been passed on from generations having a positive impact on human health.

A versatile tree with a vast range of therapeutic potential, *Moringa oleifera* (MO), is an indigenous tree to India but found widely in other parts of the world, including SA [20]. This multipurpose and rapid-growing tree is cultivated for medicinal and industrial purposes increasing its utilisation among many communities (Figure 1.1) [16]. Often known as the 'Tree of life', it is also referred to as the Drumstick tree, Soanjna and Murungai [16, 17]. *Moringa oleifera* leaves, flowers, seedpod (drumstick), seeds and bark are edible and has been part of the conventional diet of many communities [20, 24].

Figure 1.1 A branch of leaves from the *Moringa oleifera* tree [25]

1.1.1. Taxonomy

Moringa oleifera, a natural reservoir for nutrition and medicine, is used in many traditional therapies [26]. The tree has been scientifically classified accordingly into the Kingdom - Plantae, Division - Magnoliphyta, Class - Magnoliopsida, Order - Brassicales, Family - Moringaceae, Genus - *Moringa* and Species - *oleifera* [26].

In both rural and urban areas, MO trees are grown and utilised for nutritional as well as medicinal properties. The various parts of this tree are consumed and utilised on a regular basis. Figure 1.2 shows images of the MO tree with various parts readily available as food sources as well as traditional medicinal use.

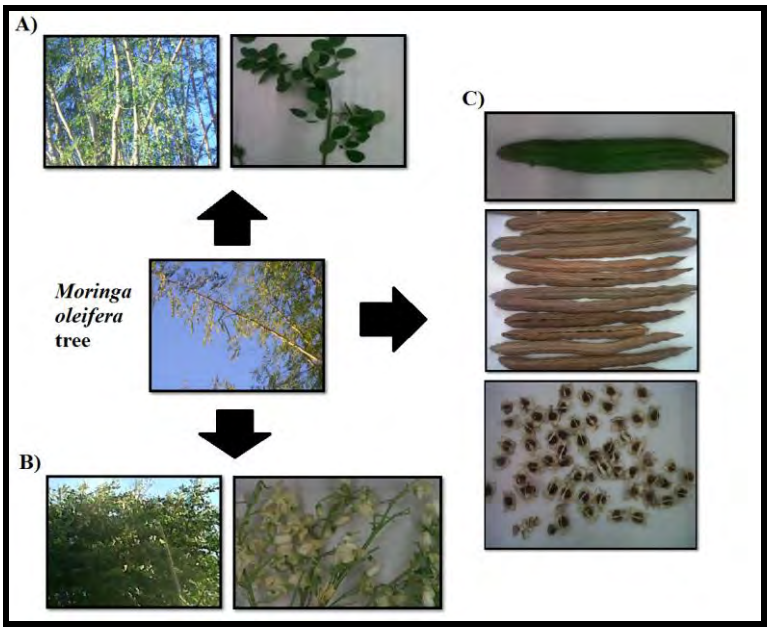

Figure 1.2 Images of the *Moringa oleifera* tree found locally [MO leaves **(A)**, MO flowers **(B)**, MO seedpod and seeds **(C)**]

1.1.2. Habitat

Indigenous to the Indian subcontinent, MO is also found in warmer regions including SA. The tree grows well in dry loamy soil which is slightly alkaline [24], however it is very adaptable to varying conditions. It thrives in dry to moist climates, with rainfall ranging from 25-300cm annually with temperatures of 19-28°C [25].

1.1.3. Traditional herbal medicine

In developing countries such as SA, traditional medicine has played a vital role in managing and treating various diseases [27]. According to the World Health Organisation (WHO), traditional medicine is defined as 'health practices, approaches, knowledge, and beliefs incorporating plant, animal and mineral based medicines, spiritual therapies, manual techniques and exercises, applied singularly or in combination to treat, diagnose and prevent illnesses and, maintain wellbeing' [28]. A wide range of plants have been utilised in traditional medicine to treat a variety of ailments even those non-responsive to western medicine. In SA, approximately 75% of people living with HIV/AIDS use traditional medicine [28]. *Moringa oleifera* is becoming

extensively used as almost all parts of the tree namely the leaves, seedpods (drumstick), seeds, flowers and bark possess medicinal properties. The rural areas of SA often have limited financial resource as well as health care services therefore many people rely on traditional healers for treatment of which the MO medicinal tree forms part of their treatment regime.

1.1.4. Nutritional value of *Moringa oleifera*

All parts of the tree possess medicinal properties however MO leaves display high nutritional value as they contain high levels of vitamin A, vitamin C, potassium, proteins, calcium and iron [18]. Studies show that the concentration of vitamin A is higher than carrots (four times), vitamin C is higher than oranges (seven times), calcium and protein is higher than milk (four and two times respectively) and potassium is higher than bananas (three times) [29, 30]. This high nutritional value of MO is particularly important in developing countries where malnutrition is prevalent.

1.1.5. Biological properties

The Drumstick tree displays many biological properties as it is used in folk medicine for the treatment of inflammation, diabetes mellitus - type 2, cardiovascular and liver disease [18, 23, 31, 32]. The leaf extract is used to treat hypertension and displays hypoglycaemic, hypocholesterolaemic, antitumour, antioxidant and hepatoprotective properties [30, 33]. These properties can be attributed to MOE's constituents as it possesses a high indigenous source of vitamins and phytochemicals like carotenoids (β-carotene), alkaloids and flavonoids [20]. It is rich in amino acids such cystine, lysine, methionine and tryptophan [34, 35].

1.1.6. Phytochemistry of *Moringa oleifera*

Dietary intake of plants, fruits and vegetables are beneficial, improving overall health [36]. A poor diet has been associated to 30-40% of cancer development [37]. Increasing the dietary intake of plants, fruits and vegetables have shown to lower the incidence of cancer. The lowered cancer incidence is due to the chemopreventive effects of phytochemicals of which these natural products contain [36, 37]. They affect the tumour microenvironment, cell proliferation and apoptosis displaying its anticancer effect. Epigallocatechin-3-gallate (isolated from green tea) and resveratrol (isolated from grapes and red wine) are examples of phytochemicals which have been identified to display anticancer effects and have entered clinical trials.

Phytochemicals have three structural classes namely glucosinolates (contains β-thioglucoside *N*-hydroxysulfate motif), flavonoids (contains two aromatic rings joined by three carbon links) and

phenolic acids (contains benzoic acid and cinnamic acid with hydroxyl groups) [38]. The MO leaves contain glucosinolates which has a benzyl-glycoside group linked to a single carbon. The enzymatic hydrolysis of glucosinolates results in the formation of isothiocyanates, thiocyanates or nitriles. Myrosinase (thioglucoside glucohydrolase) is an enzyme responsible for cleavage of the thio-liked glucose in glucosinolates [39]. The remaining aglycone rearranges to form isothiocyanates. Glucosinolates are also converted to isothiocyanates by host gut microbiota. Isothiocyanates from MO leaves are similar to those from crucifers however they are present at higher concentrations and more chemically stable thereby increasing their anticancer potential.

Phytochemical properties of MO contributes to its action against diseases [20]. It contains a rich source of rhamnose, glucosinolates and isothiocyanates. The compounds present in MO are responsible for its anticancer effects. These include 4-(α-L-rhamnopyranosyloxy) benzyl glucosinolate, 4-(α-L-rhamnopyranosyloxy) benzyl isothiocyanate, benzyl isothiocyanate and niazimicin (Figure 1.3). The leaves contain quercetin-3-O-glucoside and kaempferol-3-O-glucoside which play a role in antioxidant defence by scavenging free radicals and reducing oxidative stress [16]. The bioactive compound, niazimicin, can be utilised as agent for chemoprevention [40-42]. It also has antibacterial, hypotensive and bradycardiac activity [43]. Fractional studies of MO leaf extract (MOE) showed it is composed of flavonoids, hyperosid, rutosid, terpenoids, oleanoic acid and β-sitosterol which attributed to its antioxidant properties [44]. Chlorogenic acid, gallic acid, ferulic acid and ellagic acid are present in the leaves [25, 38]. MO leaves also contain nitrile glycosides, niaziridin and niazirin [45]. These compounds increase bio-availability of drugs which enables a reduction in drug associated toxicity and reduces the period for chemotherapy.

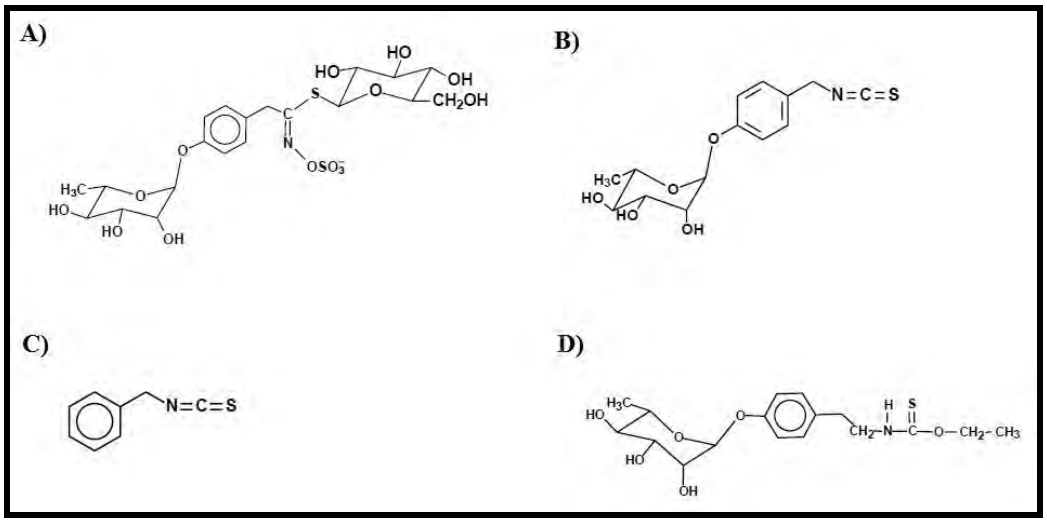

Figure 1.3 The phytochemical constituents of MO 4-(α-L-rhamnopyranosyloxy) benzyl glucosinolate **(A)**, 4-(α-L-rhamnopyranosyloxy) benzyl isothiocyanate **(B)**, benzyl isothiocyanate **(C)** and niazimicin **(D)** [20]

Several studies on MO used solvent extracts to assess their biological activities [40, 46-49]. Solvent extraction isolates bioactive compounds with methanol, ethanol, acetone, ethyl acetate, hot, cold water and buffers [40, 46-50]. Anticancer drug chemical structures have hydrophobic groups which make them insoluble in water [50, 51]. Intravenous administration of poorly soluble drugs results in poor absorption. This causes precipitation of the drugs with severe complications including embolism and respiratory system failure. Therefore increasing water solubility can be beneficial for anticancer agents. Limited scientific evidence is available for the use of aqueous leaf extract of MO as an anticancer agent.

1.1.7. Pharmacological action of *Moringa oleifera*

Antioxidant and anticancer properties of MO are known to induce apoptosis and disrupt proliferation of cancer cells. Previous studies have shown MOE to inhibit lipid peroxidation by scavenging free radicals thus reducing oxidative stress. MOE also offered protection against oxidative DNA damage [52]. The bioactive components of MO have shown to be effective in Burkett's lymphoma as it inhibited the activation of early antigen of phorbol ester (TPA)-induced Epstein-Barr virus [53]. Cytotoxic activity of MOE was seen in human hepatocellular carcinoma cells. Asare et al., 2012 assessed MOE's cytotoxic and genotoxic effects using Sprague-Dawley rats and showed that doses higher than 3,000 mg/kg b.wt can be genotoxic [33].

Toxicology studies on MOE also showed that the aqueous leaf extract is relatively safe when administrated orally [54]. Acute toxicity tests were conducted on male Wistar albino mice and showed no significant changes in biochemical and haematological markers rendering the aqueous leaf extract to be relatively safe. Radiotherapy has been used in treatment of cancers but has many side effects [55]; MOE counteracted these side effects, demonstrating a protective effect. An ethanol-water extract of MOE were used in HeLa cells to determine the cytotoxic effects [56]. HeLa cells were exposed to the extract for 48h which caused a dose-dependent decline in cell viability. MOE contains a wide range of phenolic compounds thereby causing a decline in cell viability. The effect of MOE and seedpod (drumstick) extracts *in vitro* and *in vivo* were investigated [57]. The aqueous extracts decreased malondialdehyde levels and increased glutathione levels displaying its antioxidant potential. The effects of MOE on human macrophages after exposure to cigarette smoke extract were investigated and showed that the ethyl acetate fraction decreased tumour necrosis factor alpha (TNF-α), interleukin (IL)-6 and IL-8 response [58]. It also decreased *RelA* gene expression responsible for inflammation. The decrease in cytokine production results in decreased tissue damage.

The bioactive compound, chlorogenic acid, has shown to induce apoptosis in Bcr-Abl+ chronic myeloid leukaemia [59]. There was an increase in reactive oxygen species, mitochondrial dysfunction and subsequent release of cytochrome c which led to the activation of caspases and the induction of apoptosis in the leukaemic cells. Ovarian cancer is now becoming resistant to treatment with cisplatin therefore alternate therapies are being investigated [60]. Kaempferol, also a bioactive compound, have shown potential in ovarian cancer as it decreased vascular endothelial growth factor (VEGF) in the cancer cells. Kaempferol also sensitised the ovarian cancer cells to cisplatin treatment. Kaempferol and cisplatin worked synergistically to inhibit a member of the ABCC family, ABCC6, which are membrane transport proteins. The ABCC family of proteins cause the efflux of anticancer drugs leading to drug resistance. Kaempferol and cisplatin also synergistically inhibited *c-myc* mRNA levels thereby inducing apoptosis. Although natural products and their bioactive components are showing huge potential in cancer therapeutics, further investigation into cancer cell target therapy is necessary.

1.2. Nanoparticles

Nanoscience has revolutionised modern science and medical research as it is being utilised to improve the quality of life [22]. Nanotechnology is a novel approach to medicine as it enables early detection, diagnosis and treatment of diseases [61]. Nanoparticles have their potential use in anticancer drug delivery systems however, their mechanism of action still remains to be

determined [62]. Metals such as gold are readily available. AuNP's were developed as they are biocompatible and stable with therapeutic application in various diseases such as Rheumatoid arthritis, Diabetes mellitus - type 2, Hepatitis B, HIV, TB and Alzheimer [63]. Due to the size of these nanoparticles (approximately 10 thousand times smaller than the human cell) - they are able to interact with cell molecules both on the surface and intracellularly [64]. Nanoparticles are stabilised chemically or via the use of plants [22]. The use of plant extracts in the synthesis of nanoparticles can be cost effective and advantageous in large scale production. It is a good alternative as chemical synthesis involves toxic chemicals which can be detrimental to the environment [65]. Nanoparticles facilitate the recognition of the cancer cell, binding to it and ultimately carrying out its therapeutic effect with minimal or no effect on normal healthy cells.

The one-pot green synthesis technique used for the synthesis of nanoparticles involves a redox reaction which is facilitated by plant extracts [65, 66]. In addition, the green synthesis of NP's are also facilitated by fungi, bacteria, yeast and algae [67]. They have the ability to cause the reduction of metal ions into NP's. Plant extracts such as leaves and flowers are favourable for the synthesis of NP's as it does not require any preparation or isolation, in addition to the low cost associated with its cultivation [22, 68]. Plant extracts such as MOE contains many bioactive compounds such as phenolic acids and flavonoids [57, 69]. Flavonoids play a role in chelation and the reduction of metal ions for the synthesis of nanoparticles [67]. This occurs due to their conversion from enol- to keto- form which releases a hydrogen atom. It has been shown that MO seedpod causes the reduction of chloroauric acid which resulted in the synthesis of AuNP's [69]. The AuNP's protected $HepG_2$ cells against the toxicity associated with the exposure to acetaminophen and carbon tetrachloride. Gold nanoparticles have been synthesised using "green" capping agents that are derived from medicinal plants such as *Hibiscus rosa sinensis* and *Ocimum sanctum* [70, 71].

Silver (Ag) nanoparticles were synthesised by *Albizia adianthifolia* leaf extract. It caused the redox reaction - Ag^+ ions were reduced to Ag^0 [66]. The silver nanoparticles induced A549 lung cancer cell death [72]. A one-pot green synthesis technique was also used for the synthesis of gold nanoparticles mediated by *Moringa oleifera* flower extract (MF_{AuNP}). It also showed the redox reaction by which Au^+ ions were reduced to Au^0 [65]. The synthesis of silver nanoparticles using MO aqueous leaf extract for the reduction of the silver ions showed potential use of MO in the synthesis of nanoparticles [22]. Therefore green synthesis of nanoparticles is more efficient and environmentally friendly.

1.2.1. Gold nanoparticles - Emerging benefits in medicine

Nanoparticle sizes range between 1-100nm and are showing promise in cancer therapeutics [73, 74]. Gold nanoparticles (AuNP's) have been used in diagnosis, drug delivery and treatment however limited scientific evidence is available as an anticancer agent. Gold is biologically inert facilitating its biocompatibility and non-cytotoxicity [75, 76]. In addition, according to the shape and size of the synthesised AuNP's, they are easily distributed to various parts of the body further enhancing their therapeutic effect. AuNP's induced DNA damage, cytokinesis arrest and apoptosis in human oral squamous cell carcinoma showing potential as an anticancer agent [62]. AuNP's are favoured over silver nanoparticles as they are more stable, biocompatible and the synthesis is cost-effective and environmentally friendly [74]. AuNP's can enter the cell and bind strongly to amine and thiol groups [77]. AuNP's have been utilised in medicine as there are minimal side-effects seen in patients [65]. In addition, AuNP's have many diagnostic applications [78]. AuNP's have a high surface area which enable them to bind to their targets efficiently. They are utilised in diagnostics due to their colour change upon aggregation for the detection of nucleic acid sequences. They also used as selective nanoprobes and signal enhancement for electrochemical methods of diagnosis.

MF_{AuNP} has been synthesised (Figure 1.4) [65]. MF_{AuNP} induced a dose-dependent decline in A549 cell viability with minimal effect on normal healthy peripheral blood mononuclear cells (PBMCs). MOE can also be used for the synthesis of AuNP's (ML_{AuNP}) as it causes the reduction of chloroauric acid producing stabilised gold nanoparticles [79]. The AuNP's produced were 20-60nm in size and stable up to 30 days. This environmentally friendly synthesis enabled biocompatible and stable nanoparticles which can be useful in anticancer therapies.

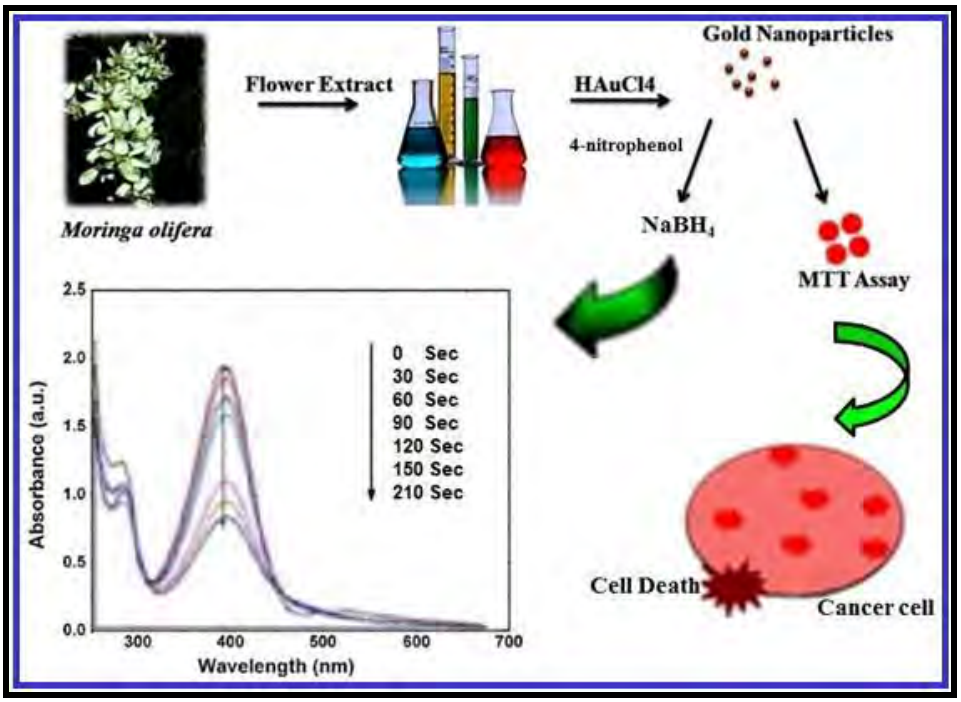

Figure 1.4 An example of gold nanoparticles mediated by *Moringa oleifera* flowers [65]

Nanoparticles induce a variety of cellular responses [80]. Gold nanoparticles selectively target cancer cells as citrate-capped AuNP's selectively targeted and induced apoptosis in human lung epithelial cells (A549) without an effect on BHK21 kidney cells and $HepG_2$ liver cells [81]. Similarly it has been shown that citrate and 11-mercaptoundecanoic acid (11-MUA)-coated AuNP's induced DNA damage in $HepG_2$ cells [82]. AuNP's mode of action depends on the size, shape, charge and surface conjugation [80]. Therefore different cancer cell types will respond differently to AuNP's. Positively charged nanoparticles remain longer in the blood stream and are advantageous for an intravenous route of administration [83]. The conventional mode of administration of anticancer drugs is intravenously. Oral administration has been used for the delivery of drugs and this mode of administration has been used for chitosan nanoparticles. In addition, delivery of nanoparticles to the lungs can be conducted via inhalation. Nanoparticle bioavailability is a concern as investigations on rats showed that the size of the nanoparticle determined its distribution in the body [84]. AuNP's size of 10nm had a widespread distribution whereas AuNP's sizes 50-250nm where only distributed to the blood, spleen and liver. Nanoparticles, in general, function by inducing oxidative stress, increasing reactive oxygen species and decreasing antioxidants to create an imbalance of cellular redox state. This ultimately leads to apoptotic cell death which is important as cancer cells evade apoptosis.

1.3. Oxidative stress

The mitochondrion, an energy producing intracelluar organelle with a double membrane [85], contains its own circular deoxyribonucleic acid (DNA) [86]. The energy produced [adenosine triphosphate (ATP)] is via oxidative phophorylation. The inner mitochondrial membrane consists of five complexes (I-V) (Figure 1.5) which are responsible for oxidative phosphorylation. The mitochondria are vital in ATP generation, reactive oxygen species (ROS) formation and regulation of apoptosis.

Oxidative stress, an imbalance between ROS, reactive nitrogen species (RNS) and antioxidant systems i.e. glutathione (GSH), catalase (CAT) and superoxide dismutase (SOD) levels leads to apoptosis [87]. ROS has an unpaired electron rendering them unstable and are produced during metabolic processes. When oxidative stress exceeds the antioxidant capacity of the cell - then macromolecules such as lipids, protein and DNA are oxidised by ROS [85]. The mitochondrion is the main source of production of ROS (Figure 1.5) [88]. ROS production is increased when the mitochondrial membrane potential is affected. The mitochondrial complex I releases superoxides in the matrix. The release of superoxides into the matrix and intermembrane space is also via complex III. The cell responds to increased ROS production by elevating antioxidant levels. The antioxidant, manganese SOD converts superoxides to hydrogen peroxide (H_2O_2) which is further converted to water by glutathione peroxidase (GPx) [89]. However when this does not occur H_2O_2 reacts with transition metals via the Fenton reaction to produce highly reactive hydroxyl radicals. ROS produced near membrane phospholipids leads to peroxidation of polyunsaturated fatty acid molecules leading to lipid peroxidation [87]. ROS also causes damage to proteins and DNA. The production of ROS can occur via mitochondrial respiration, xanthine/xanthine oxidase and NADPH oxidase system [88].

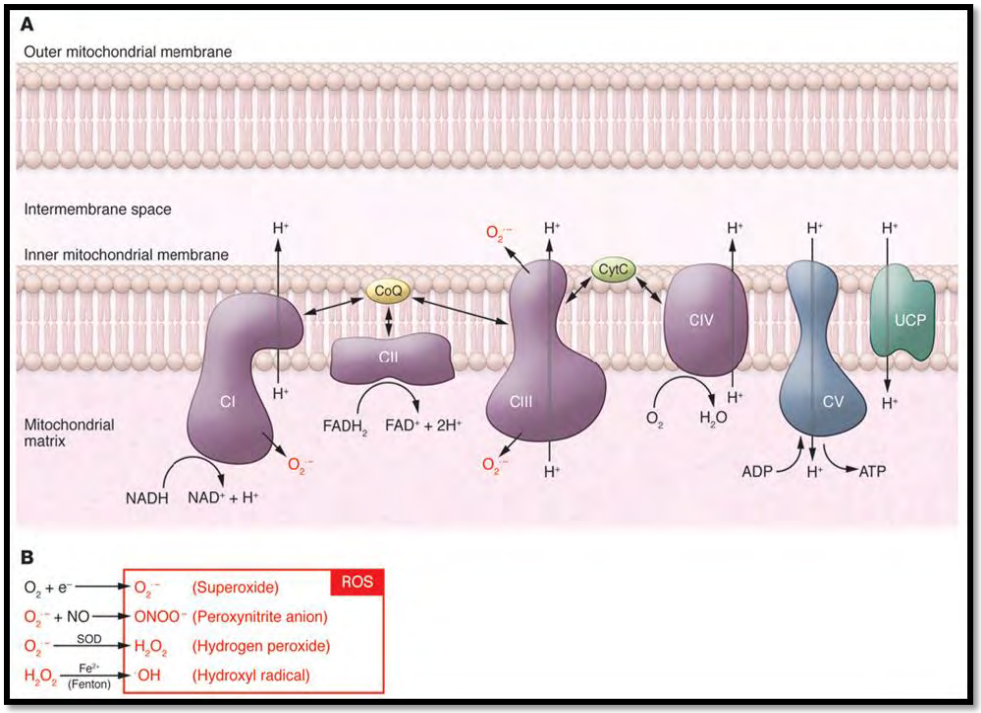

Figure 1.5 The electron transport chain found on the inner mitochondrial membrane **(A)** and the production of reactive oxygen species **(B)** [89]

When nitric oxide ($NO^{\bullet}$), nitroxyl anion (NO^{-}) and nitrosonium cation (NO^{+}) further exceeds the antioxidant capacity, it results in nitrosative stress [90]. Superoxides can react with nitric oxide to produce peroxynitrite [85, 91, 92]. Peroxynitrite targets thiol groups found in GSH. GSH, an important antioxidant, scavengers free radicals and reduces oxidative stress [93]. Present at high levels in the cell ranging from 1-10mM and 10-30µM in plasma, the active form, reduced GSH maintains the cellular redox milieu [9]. GSH is a tripeptide comprising of glycine, cysteine and glutamate.

Reduced GSH forms from glutathione disulphide (GSSG) via a redox reaction catalysed by glutathione reductase (GSR) which utilises NADPH as a cofactor [9, 94-96]. In addition, GSH can become oxidised back to GSSG (catalysed by GPx) maintaining the redox balance. During oxidative stress, there is an imbalance between ROS, RNS and the antioxidant system. Also during oxidative stress the GSH: GSSG ratio is decreased.

Nuclear factor - erythroid 2 p45 - related factor 2 (Nrf2) is a transcription factor that offers protection against oxidative insult [96-98]. When there is oxidative stress, Nrf2 dissociates from Kelch-like epichlorohydrin-associated protein 1 (Keap1) and translocates to the nucleus due to Keap1 cysteine residue modification [99]. Nrf2 regulates antioxidant gene transcription by

binding to antioxidant response element (ARE) in promoter regions of antioxidant genes. In mice, changes in Nrf2 resulted in oxidative damage and inflammation. Nrf2 regulates GSH homeostasis by regulating biosynthesis as well as the cysteine/glutamate exchange transporter. Intracellular GSH levels are thus maintained by the cysteine influx by the transporter.

Cancer cells have higher metabolic activity with increased energy demand [100]. With an enhanced metabolic activity, ROS levels increase which can either stimulate metabolic pathways or if severe can induce oxidative damage. An adaptive response to oxidative damage is the up-regulation of antioxidants and cytoprotective genes. However, when these are unable to offer protection, it leads to apoptosis [85].

1.4. Apoptosis - Mechanism of cell death

Apoptosis or programmed cell death is a vital process in embryonic development and tissue homeostasis and is regulated by aspartate-specific cysteine proteases (caspases) [9, 10, 53]. The progression of apoptosis is due to signal cascades. Apoptosis occurs through two pathways namely: death receptor - mediated procaspase - activation pathway (extrinsic pathway) and mitochondrion - mediated procaspase - activation pathway (intrinsic pathway). Homeostasis is maintained by following a process of cell growth, division and death. This ensures a healthy state by regulating cell number and tissue size [11]. Cells that threaten homeostasis are signalled for cell death. Abberation to this process results in the initiation of cancer as abnormal cells are not removed and continue to proliferate.

1.4.1. Morphology of apoptosis

When apoptosis is induced, the cell undergoes characteristic morphological changes and result in cell shrinkage, membrane blebbing, cytoskeletal disruptions and chromatin condensation (Figure 1.6) [101-103]. Nuclear shrinkage and budding occurs as the nuclear lamins are cleaved [11, 104]. The change in morphology of the cell is due to the cleavage of cytoskeletal proteins which include gelsolin and fodrin; p21-activated kinase 2 (PAK2) is responsible for the cellular blebbling.

Phosphatidylserine (PS) externalisation occurs as PS translocates from the inner leaflet to outer plasma membrane which is an early marker of apoptosis [105]. The cell loses its membrane phospholipid asymmetry. It has been shown that PS externalisation occurred in apoptotic lymphocytes and this feature was not seen in normal healthy lymphocytes [106]. PS externalisation serves as a recognition site for macrophage engulfment of apoptotic cells.

Chromatin margination and nuclear fragmentation by endonuclease occurs to degrade the DNA [102]. The cell breaks down into smaller membrane-bound apoptotic bodies which become easier to be phagocytosed by the macrophages [9]. This prevents damage to neighbouring cells and the induction of inflammation.

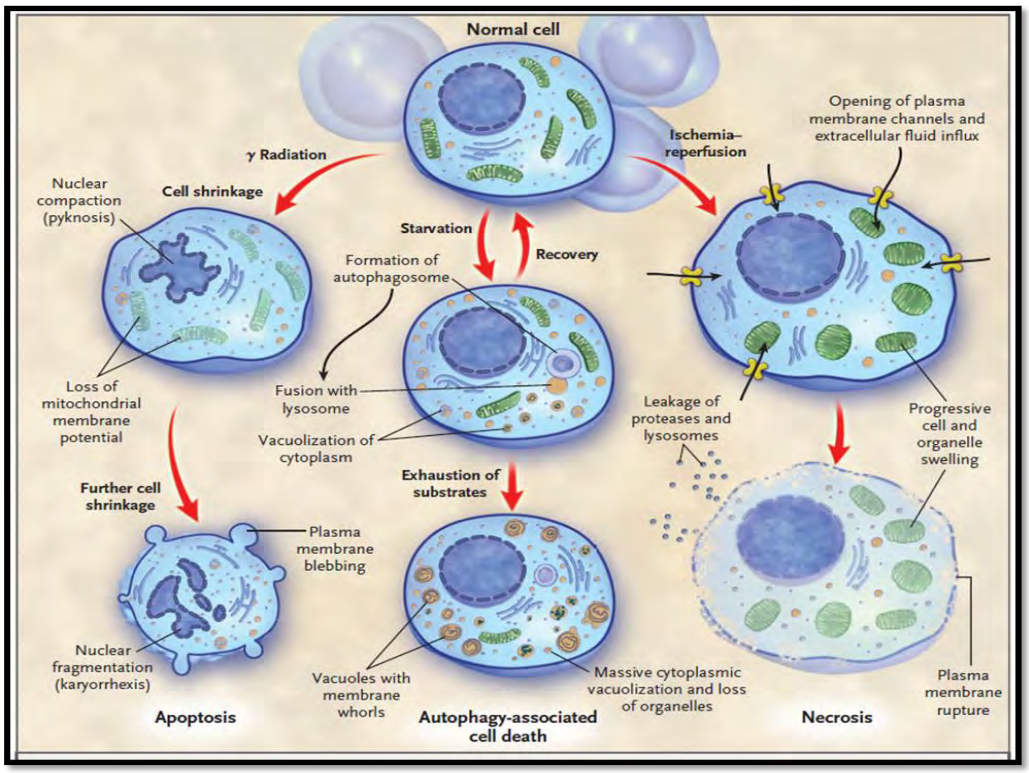

Figure 1.6 The morphological changes occurring during cell death [103]

1.4.2. Mediators of apoptosis - Caspases

Caspases play a vital role in apoptosis. Caspases are enzymatically inert zymogens which comprise of three domains namely an N-terminal prodomain, a p20 and p10 domain [11]. There are three main mechanisms of activation for these molecules which include activation by upstream caspases, induced proximity and association with a regulatory subunit. The cleavage of the zymogen between the prodomain and p20 domain or between the p20 and p10 domain leads to the activation of the caspases.

Once upstream initiator caspase-8 and caspase-9 becomes activated, they signal for downstream effector caspase-3/7 to be activated [11]. The initiator caspases are activated via protein-protein interactions and induce the apoptotic mechanism. When the death receptor is stimulated, upon the binding of ligands to its corresponding receptors, it results in the aggregation of procaspase-8. Due to procaspase-8 close proximity, it results in the cleavage and activation of the molecule.

Caspase-9 activation is more complicated as it requires other regulatory subunits such as apoptotic protease activation factor-1 (Apaf-1), cytochrome c (cyt c) and ATP to form an apoptosome. Caspase-8 and caspase-9 are the mediators of the two apoptotic pathways.

1.4.3. Apoptotic pathways

1.4.3.1. Death receptor - mediated procaspase - activation pathway

The extrinsic pathway of apoptosis occurs via two ligands namely CD95 (Fas) and TNF-α (Figure 1.7) [10]. The Fas or TNF ligand binds to its corresponding receptor, Fas-associated death domain (FADD) or TNFR-associated death domain (TRADD) respectively which leads to the activation of the death domain. The death-inducing signal complex (DISC) is formed and activated leading to the recruitment of many procaspase-8 molecules. The induced proximity causes procaspase-8 cleavage and activation [11]. Caspase-8 contains a death effector domain (DED) and can be inhibited via FADD-like interleukin-1β-converting enzyme (FLICE)-inhibitory protein (c-FLIP). The caspase-8 activation directly leads to the activation of executioner caspase-3/7 or signals apoptosis via the mitochondria. It does this by cleaving a pro-apoptotic molecule BH3-interacting domain death agonist (Bid) which is found in the cytosol and translocates as truncated Bid (tBid) to the mitochondria. The mitochondrion is targeted as tBid binds to cardiolipin, a mitochondrial specific lipid, through its helices 4-6 [107]. Its active form, tBid, is responsible for triggering the mitochondrial release of cyt c thus leading to cell death.

1.4.3.2. Mitochondrion - mediated procaspase - activation pathway

When cellular DNA is damaged or there is an increase in reactive oxygen species, the cell induces apoptosis via the mitochondria (Figure 1.7) [10]. A pro-apoptotic molecule from the Bcl-2 family (Bax, Bad, Bid), which localises in the cytoplasm, translocates to the mitochondrial outer membrane and binds to voltage-dependent anion channel (VDAC) and influences its activity [11, 108]. The VDAC protein then forms a subunit of the mitochondrial permeability transition pore (MPTP). When there is mitochondrial swelling, changes in ion channels and depolarisation of the mitochondrial membrane, it results in the opening of MPTP releasing cyt c into the cytoplasm and together with ATP, Apaf-1 and procaspase-9 forms an apoptosome. The interaction of caspase activation and recruitment domain (CARD) on the N-terminal of Apaf-1 and the prodomain of procaspase-9 leads to the activation of caspase-9. This activates executioner caspase-3/7 resulting in apoptosis as well as a positive feedback mechanism by activating more procaspase-9.

Anti-apoptotic molecules from the Bcl-2 family include Bcl-2 and Bcl-x_L [11]. They contain four Bcl-2 homology (BH) domains and a C-terminal hydrophobic tail. The proteins localise on the outer surface of the mitochondria thereby preventing apoptosis and ensuring cell survival. They bind to prevent the oligomerisation of pro-apoptotic molecules such as Bax [107]. Thus, the regulation between pro- and anti- apoptotic molecules is a determinant of cellular fate.

There are regulators of the mitochondrial apoptotic pathway such as heat shock proteins (Hsp) which act as chaperones [109]. Upon acute or chronic stress, proteins become misfolded and Hsp are then expressed to restore protein homestasis. It possess cytoprotective effects ensuring cell survival. Under normal physiological conditions, Hsp expression is fairly low. Hsp prevents the execution of apoptotic cascade as Hsp27 and Hsp70 sequests cyt c and Apaf-1 respectively. This prevents the apoptosome formation and the subsequent caspase-3/7 activation. In cancerous cells, Hsp expression is high further preventing the progression of apoptosis. This can be a potential target in chemotherapy.

Inhibitor of apoptosis proteins (IAP's) contain baculovirus IAP repeat (BIR) domains which target, bind and inhibit caspase-3/7 activity further preventing the execution of apoptosis [11, 107]. Second mitochondria-derived activator of caspase/direct inhibitor of apoptosis binding protein with low pI (Smac/DIABLO) is concurrently released from the mitchondria with cyt c and antagonises IAP's thus ensuring the execution of apoptosis [9, 110]. Smac/DIABLO binds to X chromosome encoded IAP (xIAP) at BIR 2 and 3 domain, the bindng site for caspase-3/7 thus inhibiting its function [107]. Through Smac/DIABLO functionality, the mitochondria enables the effective progression of the apoptotic cascade.

Cytochrome c (cyt c) is a key molecule in the mitochondrion as it is a water-soluble component of the electron transport chain [107, 111]. When cyt c is released during apoptosis, the electron transport chain, ATP synthesis and mitochondrial membrane potential is affected. In the electron transport chain, cyt c is responsible for transferring electrons from cytochrome c reductase (complex III) to cytochrome c oxidase (complex IV). During this process water is formed by the reduction of oxygen. Due to the release of cyt c, it affects this step in the electron transport chain thus leading to the formation of ROS. An increase in ROS results in oxidative stress, oxidative damage to lipids (lipid peroxidation), protein and DNA ultimately leading to apoptosis.

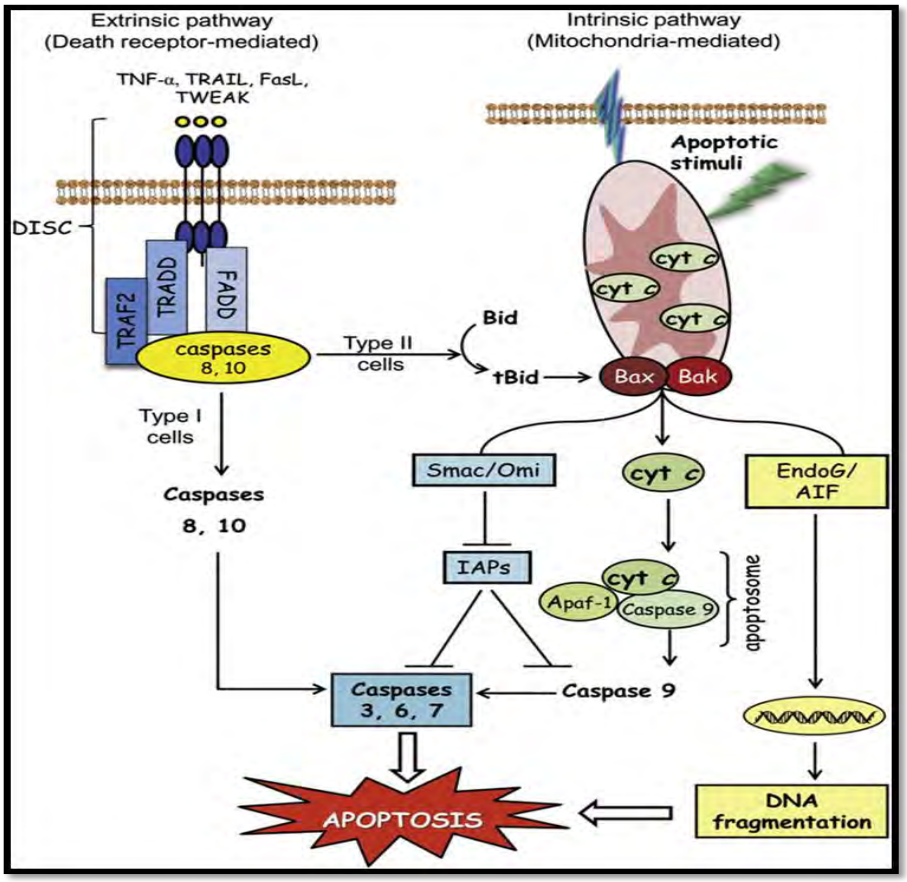

Figure 1.7 Caspases and its regulating factors in the apoptotic pathways [9]

1.5. Messenger ribonucleic acid (RNA), protein synthesis and alternate splicing of *caspase-9*

The Central Dogma of Biology is a process that is important for all living cells. It involves the replication of DNA and conversion of important genetic information into protein. Messenger RNA (mRNA) transfers this genetic information from the cell nucleus to ribosomes [112]. It is complementary to the gene sequence in DNA. Genetic information is coded by DNA and the ribosomes are found in the cytoplasm of cells where it utilises the genetic information as a template for the synthesis of proteins. The mRNA becomes translated to protein, stored or can be degraded [113]. The synthesis of proteins is important in many physiological processes and aberrations to the synthesis can result in disease. In addition, alternate pre-mRNA splicing enables a diverse expression of protein isoforms from a single gene [114]. These proteins often have differing functionality. Approximately 90% of human genes have alternate spliced isoforms resulting in diverse protein expression [114, 115]. Under normal physiological conditions, inappropriate alternate splice forms are removed via the nonsense-mediated mRNA decay (NMD) pathway. However in disease states, such as cancer, these splice forms are

maintained to ensure cell survival. Therefore targeting alternate pre-mRNA splicing can be beneficial in cancer therapies.

A human gene is made up of coding regions (exons) and non-coding regions (introns) [114]. Alternate pre-mRNA splicing removes introns and joins together exons. The newly spliced mRNA leaves the nucleus and enters the cytoplasm for translation into protein. Through alternate pre-mRNA splicing, various mRNA are produced which is translated into proteins with various biological effects. RNA *trans*-acting splicing factors are responsible for activating alternate splicing in the cell. Serine/arginine-rich proteins (SR proteins) regulate the processing of pre-mRNA [13, 114].

Alternate splicing of *caspase-9* produces two splice variants viz. *caspase-9a* and *caspase-9b* (Figure 1.8). SRp30a is an important RNA *trans*-acting factor for alternate slicing of *caspase-9* pre-mRNA [13]. The activation of *caspase-9* gene pro-apoptotic function involves an increase in pro-apoptotic splice variant *caspase-9a* (exon 3, 4, 5, 6 cassette inclusion) with a decrease in anti-apoptotic splice variant *caspase-9b* (exon 3, 4, 5, 6 cassette exclusion). The *caspase-9b* competes with *caspase-9a* splice variant for binding to the apoptosome. *Caspase-9b* splice variant does not have the catalytic activity but has the interacting domains (CARD) [14]. Shultz et al., 2010 showed that through alternate splicing of *caspase-9*, ceramide was able to induce apoptosis in A549 lung cancer cells [14]. The regulation of the alternate splicing is vital in the interaction with APAF-1 for apoptosome formation and the downstream activation of effector caspase-3/7. Through the down-regulation of SRp30a, it induces the *caspase-9b* splice variant and halts the apoptotic machinery. It has been shown that MCF-7 cells were not able to undergo apoptosis when *caspase-9b* splice variant was expressed [116]. In addition, this expression also disrupted the apoptosome formation [117] conferring resistance irrespective of apoptotic stimuli [15]. Therefore regulation of the inclusion/exclusion of the exon cassette will determine cell fate.

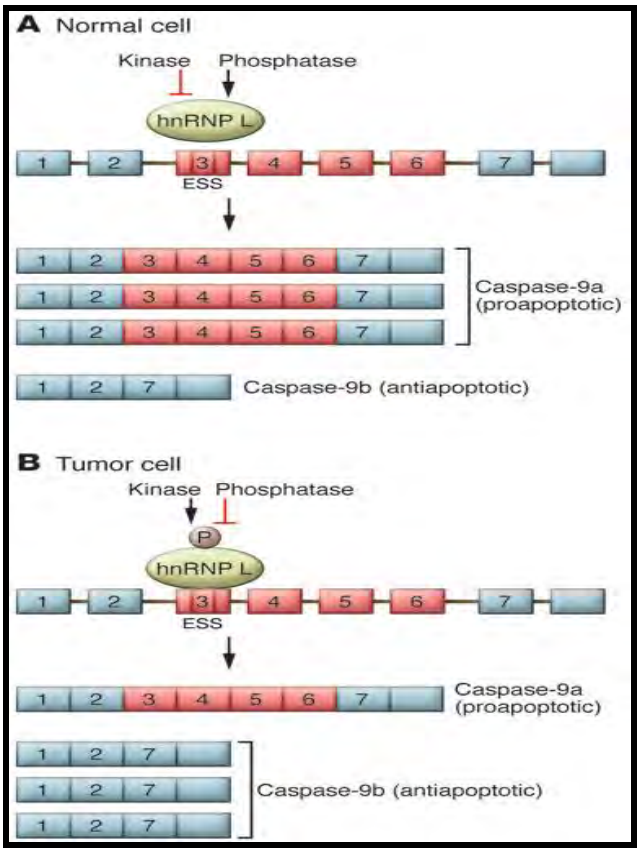

Figure 1.8 Regulation of *caspase-9* gene expression by alternate mRNA splicing in a normal cell **(A)** and tumour cell **(B)** [115]

A member of the heterogeneous nuclear ribonucleoprotein (hnRNP) family, hnRNP L, is also a regulator of *caspase-9* and has been implicated in the exclusion of the exon cassette thus favouring the *caspase-9b* splice variant expression [14] (Figure 1.8). Splice variant expression of *caspase-9* is imperative for the induction and execution of the apoptotic cascade and the subsequent cleavage and inactivation of regulating proteins such as poly (ADP ribose) polymerase-1 (PARP-1).

1.6. The role of poly (ADP ribose) polymerase-1 in apoptosis

Certain cellular proteins are lysed by caspases during apoptosis. These proteins include PARP-1. During apoptosis, caspases are activated and caspase-3 cleaves PARP-1 (Figure 1.9) [118, 119]. PARP-1, a nuclear enzyme, is proteolysed to a 24 kDa N-terminal DNA-binding domain and an 89 kDa C-terminal catalytic fragment rendering PARP-1 inactive [120-122]. The N-terminal DNA-binding domain has two zinc fingers [123]. The cleavage prevents cell survival function as it conserves ATP for use during the apoptotic cascade. PARP-1 also causes

apoptosis inducing factor (AIF) release from the mitochondria causing DNA damage and caspase-independent apoptotic cell death.

PARP-1 responds to low levels of DNA damage by cleaving nicotinamide adenine dinucleotide (NAD^+) to nicotinamide and ADP-ribose [123, 124]. ADP-ribose is utilised to form ADP-ribose polymers on nuclear proteins including endonucleases, topoisomerase and histones. PARP-1 plays a role in DNA base excision repair, maintenance of the integrity of the genome thus ensuring cell survival [125]. PARP-1 has a high affinity to single-strand (ss) or double-strand (ds) breaks in DNA via the two zinc fingers and facilitates base excision repair [125, 126]. It recruits DNA repair proteins such as DNA ligase III, XRCC-1 and DNA polymerase β thus the cell is able to recover. However when there is cleavage of PARP-1, the 24 kDa fragment (the DNA binding domain which irreversibly binds to DNA strand breaks) inhibits DNA repair enzymes from accessing the damage sites preventing repair and cell survival function [127]. It is also seen that when there is DNA damage, the 89 kDa fragment is unable to be stimulated [124]. When there is an extremely high level of DNA damage, PARP-1 decreases NAD^+ and the production of ATP substantially [123]. This ultimately leads to necrosis (Figure 1.9).

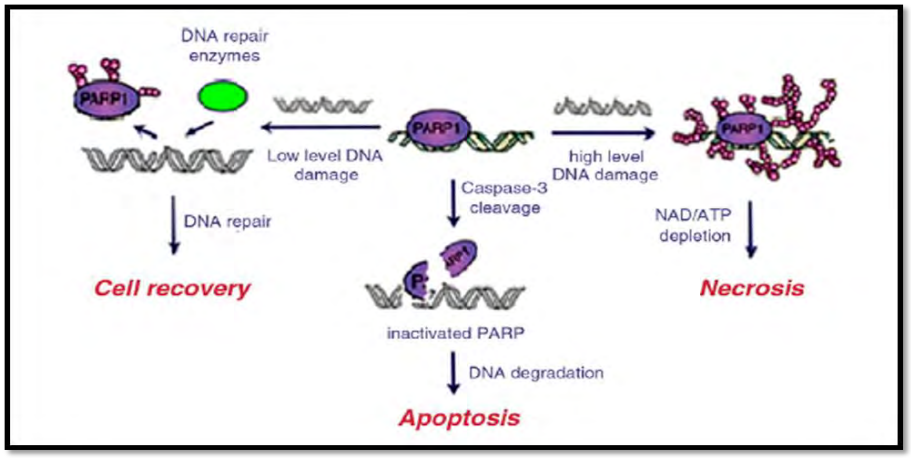

Figure 1.9 Poly (ADP ribose) polymerase-1 response in cell survival and cell death [123]

PARP-1 has been implicated in cancers as it plays a role in cell survival [123]. Current anticancer agents induce DNA damage however PARP-1 is also activated for DNA repair. Therefore, inhibiting PARP-1 activity can be a therapeutic target in cancer as it will delay the DNA repair response and facilitate apoptosis via tumour suppressor gene, p53, which also responds to the DNA damage.

1.7. p53 - 'The guardian of the genome'

p53, a tumour suppressor gene and transcription factor, is a regulator of the apoptotic cascade [119, 128]. A defective p53 gene is generally seen in more than 70% of cancers thereby affecting the cell cycle checkpoint resulting in cell proliferation [129]. p53 responds to a variety of stimuli such as ROS, DNA damage and lesions, inappropriate oncogene activation and anoxia. It also monitors telomere length.

Cancer is genetically unstable with the loss of p53 function [130]. An assessment of the role of p53 in lung cancer, mice were injected with C8 fibroblasts containing either wild-type or mutant p53. The lungs were isolated within 2 to 4 hours and showed that lung macrometastases possessed the mutant p53 alleles. The loss of p53 function is the basis for metastasis and can be a therapeutic target. Previous studies have shown that lung and prostate cancers which contained mutant p53 gene resulted in cancer cell apoptosis via the introduction of the wild-type p53 showing potential in gene therapy by p53 targeting [129]. Using a retroviral vector also showed potential in patients who were non-responsive to conventional chemotherapy. There are limitations to gene therapy as the mutant variant may be more dominant as well as sufficient copies of the gene needs to be delivered to target cells. Also, the differentiation between normal healthy cells and cancer cells is imperative.

Under normal physiological conditions p53 is bound to Mdm2 rendering it inactive [128]. Upon stimuli viz. oxidative DNA damage, p53 becomes phosphorylated, releasing Mdm2, causing p53 activation (Figure 1.10). p53 then signals for cell cycle arrest by activating p21 which inhibits the cyclin-CDK complex and the progression from G1 to S phase in the cell cycle. The damaged cell undergoes repair and those cells which have irreparable damage are then signalled for apoptosis via the mitochondrial pathway. This prevents defective cells from continuing in the cell cycle resulting in tumour formation. If p53 function is lost, p21 gene is not transcribed to inhibit the cyclin-CDK complex thereby allowing increased cell cycle activity with subsequent cell proliferation [129].

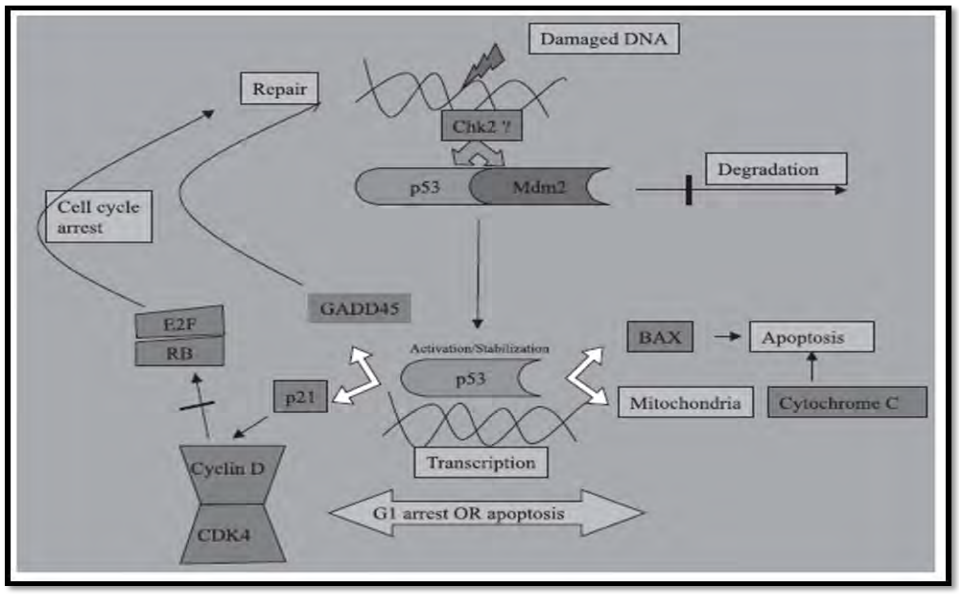

Figure 1.10 Schematic model of the activation of p53 and its signalling pathway [129]

Irreparable cells are signalled by p53 to undergo apoptosis via the mitochondria [128, 131]. Upon stimuli, p53 increases the transcription and activation of pro-apoptotic molecule Bax. Bax translocates from the cytoplasm to the mitochondria were it undergoes oligomerisation. It binds to the outer mitochondrial membrane causing mitochondrial depolarisation, opening of MPTP and subsequent release of cyt c into the cytoplasm. The formation of the apoptosome (cyt c, ATP, APAF-1 and procaspase-9) activates caspase-9 and downstream executioner caspase-3/7 resulting in apoptosis. Therefore targeting p53 expression in cancers which have increased oncogene expression will ultimately lead to apoptosis and can be beneficial in therapy.

1.8. Oncogenic role of c-myc

Oncogenes are responsible for cell growth and proliferation leading to tumour formation [129]. Activated oncogenes initiates cancer and maintains a cell in its proliferative state therefore has been a target for anticancer therapies [132]. c-Myc is an oncogene involved in the process of tumourigenesis [133]. c-Myc belongs to the family of myc genes [134]. The myc family contains c-myc, L-myc and N-myc with neoplastic properties. c-Myc is made up of an N-terminal regulatory and transactivational domain [135]. This domain contains Myc-box motifs, MBI and MBII. There is a C-terminal basic helix-loop-helix leucine zipper and a DNA-binding domain. It is responsible for tumour formation because when activated [134], there is an increase in cell proliferation. Generally c-myc is under homeostatic control however in human cancers, translocation from chromosome 8q24 to chromosome 2, 14, or 22 in B cells results in its activation. In Burkitt's lymphoma, there is chromosomal translocation of the *c-myc* gene

[129]. Lung, breast and colon cancers express high levels of c-myc. Approximately 70% of human cancers have dysregulated c-myc expression [136]. The gene encodes transactivating factors controlling cell differentiation, proliferation and apoptosis [134, 137]. The increased stability of c-myc has shown to induce carcinogenesis [138].

Nutrients, growth factors and mitogenic stimuli activate signal transduction pathways resulting in a phosphorylation cascade and the activation of c-myc. The RAS/RAF/MEK/ERK pathway phosphorylates myc at serine 62, stabilising it whereas glycogen synthase kinase 3β (Gsk3β) phosphorylates myc at threonine 58 (Thr58) which results in its destabilisation [138]. c-Myc is expressed in S-phase of the cell cycle and is tightly regulated [129]. In cancer there is overexpression of c-myc resulting in cell cycle progression.

Chromosomal rearrangements and increased transcriptional pathways activate c-myc [139]. c-Myc targets rate-limiting enzymes and is involved in ROS production. c-Myc is also involved in cell cycle as it causes G1 to S phase progression. It is able increase transcription of cyclins and reduces inhibitors of cyclin/CDK complexes. c-Myc inhibits p27 resulting in the activation of cyclin E/CDK2 complex. The decreased p27 has been noted in various cancers enabling cells to continue in the cell cycle. The Skp1/Cull/F-box (SCF) ligase complex ubiquitinates p27 for proteasomal degradation. c-Myc can further activate Cull in the complex which leads to the degradation of p27. Through the activation of the cyclin/CDK complex, c-myc is able to promote cell progression irrespective of the Rb checkpoint in the cell cycle.

1.9. c-Myc/Skp2/Fbw7α pathway

c-Myc stability and function is regulated by ubiquitin mediated pathways which include ubiquitin ligases [138]. The F-box ubiquitin ligases are S-phase kinase-associated protein 2 (Skp2) and F-box and WD repeat domain-containing 7 (Fbw7) which recognise substrates for proteasomal degradation. They form subunits of the SCF-type E3 ligase [SCF (Skp1/Cull/F-box protein) complexes] [12] which is also involved in proteasomal degradation. In the SCF complex, the F-box proteins recognise the substrates and Cull ubiquitinates it for proteasomal degradation [138]. Skp2 and Fbw7 cause the ubiquitination and degradation of c-myc [138]. Fbw7 and Skp2 targets the MBI and MBII domains of c-myc respectively. Skp2 binds to MBII via the leucine-rich repeats which results in ubiquitination and degradation. In addition, c-myc increases Skp2 expression which also acts as a co-factor increasing c-myc's transcriptional activity [138]. Skp2 can also act as an oncogene and is often overexpressed in cancers [138, 140].

Skp2 also targets p27 and p57 involved in inhibiting cell cycle progression [140]. Through the downregulation of Skp2, it results in the accumulation of p27 therefore causing cell cycle arrest. Studies have shown that quercetin, curcumin and epigallocatechin-3-gallate possess anticancer effects by inhibiting Skp2 expression. It has been shown that Skp2 expression is increased via c-myc activation in K562 myeloid leukaemia cells [141]. Bone marrow samples from chronic myeloid leukaemia patients had also shown the correlation. In addition, silencing of Skp2 prevented c-myc's inhibition of p27.

The degradation of c-myc by Fbw7 requires additional steps [12, 138]. c-Myc is phosphorylated by Gsk3β at Thr58 which causes destabilisation. This further facilitates the degradation as Fbw7 recognises the phosphorylated site in the MBI domain. The decreased expression of Fbw7 confers drug resistance in cancers as Fbw7 can act as a tumour suppressor gene [140]. Fbw7 have different isoforms α, β and γ which are located in the nucleus, cytoplasm and nucleolus respectively. Fbw7 is regulated by upstream genes including p53.

The apoptosis inducing effects of bioactive compound wogonin on A549 cells were investigated [12]. Natural products and their bioactive compounds are showing potential in cancer therapies however their mechanism of action is required to be identified. Wogonin decreased A549 cell viability and increased the cleavage of PARP-1. In addition it caused the release of AIF and cyt c from the mitochondria which resulted in apoptosis via the intrinsic pathway. Studies show that the c-Myc/Skp2/Fbw7α pathway promotes cancer progression [12]. Wogonin decreased c-myc protein expression but not mRNA expression. Fbw7α and Gsk3β expression were also decreased. Wogonin decreased Skp2, HDAC1 and HDAC2 protein expression. The study suggested that wogonin had multiple anticancer effects and was able to induce apoptosis irrespective of the decreased Fbw7α expression. This is important especially in drug-resistant cancers therefore targeting the pathway will be beneficial for cancer therapies. The effects of Oridonin, a bioactive compound, on apoptosis in K562 myeloid leukaemia cells were determined [142]. Oridonin increased Gsk3β and Fbw7 which resulted in a reduction in c-myc expression and the induction of apoptosis in the cancer cells.

1.10. Cancer

Under normal conditions, a cell functions optimally thereby maintaining homeostasis in the body. During carcinogenesis, the physiological functioning of normal cells are disrupted leading to abnormal growth, proliferation and evasion of apoptosis [143]. Normal genes called proto-oncogenes become altered to oncogenes affecting cell division. Cancer cells are able to grow

uncontrollably by causing the formation of new blood vessels (angiogenesis) which allows nutrients to be delivered to the site of the tumour.

There are also other factors which aids in cancer cell growth including sustaining a proliferative signal, evasion of growth suppressors, activation of invasion and metastasis, enabling replicative immortality and resisting cell death (apoptosis) (Figure 1.11) [143]. Cancer cells have a high metabolic rate and they utilise glucose through increased glycolysis (Warburg effect) [144]. Cellular metabolism is also affected as cancer cells dysregulates cellular energetics and evades the immune system [143]. Often there is dysregulation in oncogenes and tumour suppressor genes leading to carcinogenesis and therefore can be a potential target in chemotherapy. In SA, the rate of cancer incidence (lung and oesophageal cancer) is increasing [5]. The rate of incidence for lung cancer is 5.8 per 100,000 and oesophageal cancer is 32.7 per 100,000 which is a growing concern.

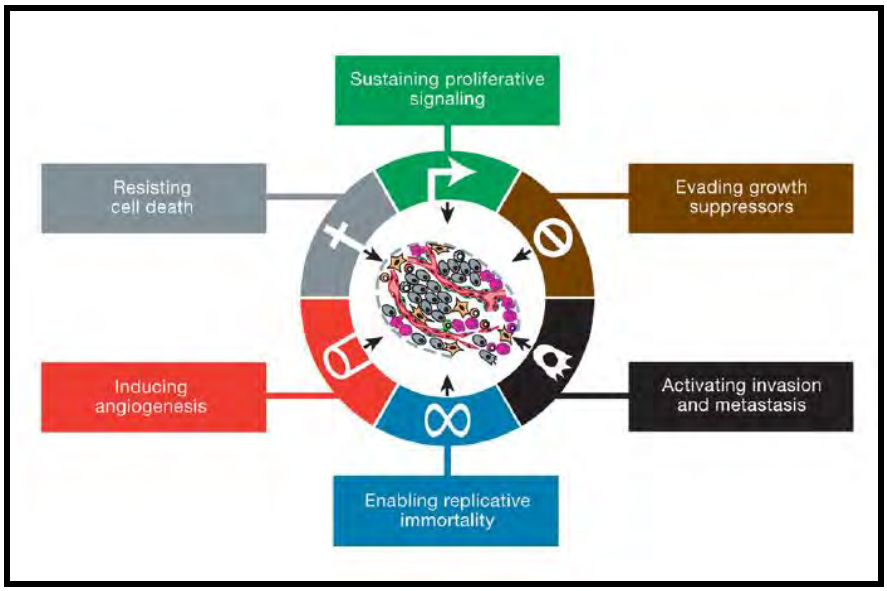

Figure 1.11 Cancer hallmarks [143]

1.10.1. Lung cancer

Lung cancer is a leading cause of death in many countries [119] and is the result of pollutants, toxins and cigarette smoking [87]. Non-smokers that are constantly exposed to tobacco smoke are at risk of developing lung cancer [145]. Surviving HIV positive individuals have a higher risk of lung cancer which previously has not been associated with the disease [8]. Diagnosis of lung cancer is expected to increase thus research into anticancer agents are imperative [146]. Lung cancer affects the quality of life and the outcome upon diagnosis is poor due to the rapid

progression [147, 148]. Genetics play a role in predisposition to lung cancer as it affects absorption of tobacco smoke as well as its metabolism [145].

Cancer in the lung originates from the basal epithelial cells [149]. There are two types viz. non-small cell lung cancer (NSCLC) and small cell lung cancer (SCLC). It is estimated that 85% of diagnosed lung cancers are NSCLC. A549 cell line is a lung cancer cell line (NSCLC) derived from human pulmonary adenocarcinoma [150]. The cells were collected through explant culture from a Caucasian 58 year old male [151]. A549 cells retain the biochemical activities of human type II alveolar epithelial cells as it expresses cytokines and possesses cytochrome activity for biotransformation. A549 cells express the wild type of p53 and *epidermal growth factor receptor (EGFR)* gene and are therefore suitable for use in *in vitro* studies.

Cisplatin is an anticancer agent used for treatment of lung cancer [152]. Cisplatin induces its anticancer effects by forming DNA adducts and subsequently activating apoptotic pathways via p53 [153]. Current first-line lung cancer therapy utilises cisplatin and gemcitabine [152]. Patients undergo a three week treatment regime. In addition, pemetrexed is also used in combination with cisplatin for first-line therapy. However there is resistance to cisplatin therapy as cancer cells reduce drug uptake, inactivate the drug and increase DNA repair [153]. In addition, cell survival pathways (phosphoinositide-3-kinase/Akt), anti-apoptotic molecules (Bcl-2) are increased with a decrease in p53 expression which culminates in cisplatin resistance. Therefore effective alternative treatments are being investigated.

1.10.2. Oesophageal cancer

Oesophageal cancer (OC) is the most commonly diagnosed cancer in black men in SA. The increased prevalence is due to the presence of mycotoxins such as Fumonisin B_1 in staple foods such as maize [154]. The risk factors associated to the development of OC includes ethnicity, diet and lifestyle. Family history, tobacco smoking and alcohol consumption also contributes to the aetiology of OC. Dietary deficiencies of magnesium, zinc, nicotinic acid and riboflavin have been seen to contribute to the development of the cancer [155]. The SNO cell line is an oesophageal cancer cell line derived from human oesophageal squamous carcinoma [156]. The cells were explanted from a Zulu 62 year old male. It also retains biochemical activities and is therefore suitable for use in *in vitro* studies.

Paclitaxel and 5-Fu are the first-line drugs used for oesophageal cancer therapy [157]. They are used in combination due to their synergistic effects. However there were many side-effects

including alopecia, fatigue, and bone marrow suppression. Therefore alternate therapies are being investigated to inhibit cancer progression, improve drug efficacy, quality of life and increase positive outcome.

1.11. Cancer progression

Cancer cells evade the apoptotic cascade [53]. Mutation in genes that control important checkpoints and repair mechanisms results in the development of cancer [130]. Apoptosis plays an important role in homeostasis by removal of cells that have activated oncogenes or damaged DNA [129]. However in cancer, there is an increase in oncogene expression and loss of p53 function thus cell cycle arrest does not occur further facilitating the progression of malignant cells into tumours. Lymphoma cancer cells over-express the anti-apoptotic molecule Bcl-2 and inhibit apoptosis. Cancer cells are able to synthesise decoy receptors of which CD95 (Fas) and TRIAL ligands bind to but are unable to signal the required apoptotic cascade. Chaperone proteins Hsp27 and Hsp70 are also elevated [109]. Exposure to cigarette smoke contains many compounds such as aromatic amines, N-nitroso compounds and polycyclic aromatic hydrocarbons which when in contact with the cytochrome P_{450} system becomes activated to its carcinogenic form [145]. This results in the formation of cancer and inhibition of the apoptotic cascade. Therefore targeting apoptosis in cancer cells prevents cancer progression and can be beneficial in therapy.

1.12. Cancer therapy - targeting apoptotic pathways

The apoptotic mechanism is a therapeutic target in cancer therapies [129]. In chemotherapy, the p53 response and the induction of apoptosis affects normal cells in addition to cancer cells thus resulting in alopecia (hair loss). Therefore an anticancer agent that specifically target and induce apoptosis in cancer cells with minimal effect on normal healthy cells is imperative. Cancer therapies such as cisplatin and paclitaxel target the mitochondria of cells and cause an increase in expression of Bax with a concomitant decrease of Bcl-2. This result in caspase activation and the execution of the apoptotic cascade. Research into chemotherapeutics has designed and developed mechanism based therapy to target various aspects of cancer cell survival and the induction of apoptosis [143]. However there are many limitations that are seen.

1.13. Current limitations of cancer therapy - complementary and alternative medicine as a possible solution

Cancer patients on anticancer therapies primarily experience several side effects. These include hair loss, nausea, anaemia, skin irritation, nephrotoxicity and infertility [50]. Cancer treatment

involves surgical removal, irradiation and chemotherapy [158]. In addition, the costs of current chemotherapies are rapidly increasing. Chemotherapy is non-specific with high toxicity levels and at times drug-resistant. Chemotherapy is toxic as there is limited aqueous solubility due to the diluent used to make up the treatment. It also lacks selectivity as current anticancer drug kills rapidly dividing cells which includes not only cancer cells but also normal healthy cells namely bone marrow and immune cells [75]. Also, multidrug resistance is a limiting factor as p-glycoprotein transports anticancer drugs out of the cell preventing their activation and mode of action.

Traditional medicine has benefitted many people by offering complementary and alternative treatment, providing relief from a plethora of ailments. Apoptosis is a useful marker for determining the potential of plants as an anticancer drug [159]. Medicinal plants have high biocompatibility, low toxicity and potent biological activity [50]. Therefore investigations into the anticancer activity of medicinal plants will be beneficial as they often display cytotoxic effects.

1.14. MO and cancer - Therapeutic interventions

Lung and oesophageal cancer still remains incurable therefore cost-effective alternate plant based therapies are actively being investigated [93]. MOE possess anticancer properties by increasing glutathione-S-transferase (GST) levels which can detoxify carcinogens [16]. MOE induced apoptosis in KB carcinoma cells [52]. Aqueous crude extracts of MOE possess anticancer properties in HeLa cancer cell line [160]. Although MOE and AuNP's possess potent biological activities, there is no information with regards to its effects against lung and oesophageal cancer. Therefore scientific evidence pertaining to the effectiveness and mechanistic action of this medicinal plant and its synthesised AuNP's requires investigation.

1.15. Future prospects

MOE and its synthesised AuNP's show therapeutic potential in cancer. The synthesised AuNP's further facilitate its uptake in cancer cells. South Africa has one of the highest HIV infection burdens globally and patients on antiretroviral therapy are prone to develop metabolic syndrome (dyslipidaemia, lipodystrophy and insulin resistance). MOE can be utilised in such patients since it has high nutritional, anticancer and immune-boosting activity. HIV also increase risk of secondary infections e.g., TB [7]. MOE also possess anti-bacterial properties and can therefore be used as a therapeutic control for HIV and TB. Treatment with MOE and its synthesised

AuNP's can be the next step in advance therapy thus SA's traditional plant, MO, potentially has a positive impact on human health.

References

1. Mendis, S., Armstrong, T., Bettcher, D., Branca, F., Lauer, J., Mace, C., Poznyak, V., Riley, L., Da Costa E Silva, V., Stevens, G. Global status report on noncommunicable diseases. World Health Organization, 2014, 1-280.
2. Globocan. *Estimated cancer Incidence, Mortality, Prevalence and Disability-adjusted life years (DALYs) Worldwide in 2012 [http://globocan.iarc.fr/]*. 2012.
3. Jemal, A., Bray, F., Center, M.M., Ferlay, J., Ward, E., Forman, D. Global cancer statistics. CA Cancer J Clin, 2011, 61:69-90.
4. Pacella-Norman, R., Urban, M.I., Sitas, F., Carrara, H., Sur, R., Hale, M., Ruff, P., Patel, M., Newton, R., Bull, D., Beral, V. Risk factors for oesophageal, lung, oral and laryngeal cancers in black South Africans. Br J Cancer, 2002, 86:1751-1756.
5. Sheridan, J., Collins, A.M. Adult lung cancer in Southern Africa: epidemiology and aetiology. Afr J Respir Med, 2013, 8:10-12.
6. Mayosi, B.M., Flisher, A.J., Lalloo, U.G., Sitas, F., Tollman, S.M., Bradshaw, D. The burden of non-communicable diseases in South Africa. Lancet, 2009, 374:934-947.
7. Munoz-Fernandez, M.A., Navarro, J., Garcia, A., Punzon, C., Fernandez-Cruz, E., Fresno, M. Replication of human immunodeficiency virus-1 in primary human T cells is dependent on the autocrine secretion of tumor necrosis factor through the control of nuclear factor-KB activation. J Allergy Clin Immunol, 1997, 100:838-845.
8. Bello, B., Fadahun, O., Kielkowski, D., Nelson, G. Trends in lung cancer mortality in South Africa: 1995-2006. BMC Public Health, 2011, 11:1-5.
9. Circu, M.L., Aw, T.Y. Glutathione and modulation of cell apoptosis. Biochim Biophys Acta, 2012, 1823:1767-1777.
10. Fan, T., Han, L., Cong, R., Liang, J. Caspase family proteases and apoptosis. Acta Bioch Bioph Sin, 2005, 37:719-727.
11. Hengartner, M.O. The biochemistry of apoptosis. Nature, 2000, 407:770-776.
12. Chen, X., Bai, Y., Zhong, Y., Xie, X., Long, H., Yang, Y., Wu, S., Jia, Q., Wang, X. Wogonin has multiple anti-cancer effects by regulating c-Myc/SKP2/Fbw7α and HDAC1/HDAC2 pathways and inducing apoptosis in human lung adenocarcinoma cell line A549. PLoS One, 2013, 8:1-7.

13. Massiello, A., Chalfant, C.E. SRp30a (ASF/SF2) regulates the alternative splicing of caspase-9 pre-mRNA and is required for ceramide-responsiveness. J Lipid Res, 2006, 47:892-897.
14. Shultz, J.C., Goehe, R.W., Wijesinghe, D.S., Murudkar, C., Hawkins, A.J., Shay, J.W., Minna, J.D., Chalfant, C.E. Alternative splicing of caspase 9 is modulated by the phosphoinositide 3-kinase/Akt pathway via phosphorylation of SRp30a. Cancer Res, 2010, 70:9185-9196.
15. Shultz, J.C., Goehe, R.W., Murudkar, C.S., Wijesinghe, D.S., Mayton, E.K., Massiello, A., Hawkins, A.J., Mukerjee, P., Pinkerman, R.L., Park, M.A., Chalfant, C.E. SRSF1 regulates the alternative splicing of caspase 9 via a novel intronic splicing enhancer affecting the chemotherapeutic sensitivity of non-small cell lung cancer cells. Mol Cancer Res, 2011, 9:889-900.
16. Goyal, B.R., Agrawal, B.B., Goyal, R.K., Mahta, A.A. Phyto-pharmacology of *Moringa oleifera* Lam an overview. Nat Prod Radiance, 2007, 6:347-353.
17. Djakalia, B., Guichard, B.L., Soumaila, D. Effect of *Moringa oleifera* on growth performance and health status of young post-weaning rabbits. Res J Poultry Sci, 2011, 4:7-13.
18. Sreelatha, S., Jeyachitra, A., Padma, P.R. Antiproliferation and induction of apoptosis by *Moringa oleifera* leaf extract on human cancer cells. Food Chem Toxicol, 2011, 49:1270-1275.
19. Sanchez-Machado, D.I, Nunez-Gastelum, J.A., Reyes-Moreno, C., Ramirez-Wong, B., Lopez-Cervantes, J. Nutritional quality of edible parts of *Moringa oleifera.* Food Anal Method, 2010, 3:175-180.
20. Fahey, J.W. *Moringa oleifera*: A review of the medical evidence for its nutritional, therapeutic, and prophylactic properties. part 1. Trees for Life J, 2005, 1-5.
21. Mishra, G., Singh, P., Verma, R., Kumar, S., Srivastav, S., Jha, K.K., Khosa, R.L. Traditional uses, phytochemistry and pharmacological properties of *Moringa oleifera* plant: An overview. Der Pharmacia Lettre, 2011, 3:141-164.
22. Prasad, T.N.V.K.V., Elumalai, E.K. Biofabrication of Ag nanoparticles using *Moringa oleifera* leaf extract and their antimicrobial activity. Asian Pac J Trop Biomed, 2011, 439-442.
23. Giridhari, V.V.A., Malathi, D., Geetha, K. Anti-diabetic property of drumstick (*Moringa oleifera*) leaf tablets. Int J Health Nutr, 2011, 2:1-5.
24. Varmani, S.G., Garg, M. Health benefits of *Moringa oleifera:* A miracle tree. Int J Food Nutr Sci, 2014, 3:111-117.

25. Ali, E.N. *Moringa oleifera* leaves possible uses as environmentally friendly material: A review. Int J Chem, Environ Biol Sci, 2014, 2:141-145.
26. Kasolo, J.N., Bimenya, G.S., Ojok, L., Ogwal-okeng, J.W. Phytochemicals and acute toxicity of *Moringa oleifera* roots in mice. J Pharmacognosy Phytother, 2011, 3:38-42.
27. Nxumaloa, N., Alabab, O., Harrisa, B., Chersicha, M., Goudge, J. Utilization of traditional healers in South Africa and costs to patients: Findings from a national household survey. J Public Health Policy, 2011, 32:S124-S136.
28. World Health Organization. World Health Organization, Factsheet 134: Traditional Medicine. Geneva: WHO. 2003.
29. Ramachandran, C., Peter, K.V., Gopalakrishnan, P.K. Drumstick (*Moringa oleifera*): a multipurpose Indian vegetable. Econ Bot, 1980, 34:276-283.
30. Cajuday, L.A., Pocsidio, G.L. Effects of *Moringa oleifera Lam*. (Moringaceae) on the reproduction of male mice (*Mus musculus*). J Med Plants Res, 2010, 4:1115-1121.
31. Limaye, D.A., Nimbkar, A.Y., Jain, R., Ahmed, M. Cardiovascular effects of the aqueous extract of *Moringa pterygosperma.* Phytother Res, 1995, 9:37-40.
32. Rao, K.S. Misra, S.H. Anti-inflammatory and anti-hepatotoxic activities of the roots of *Moringa pterygosperma Geaertn.* Indian J Pharm Sci, 1998, 60:12-16.
33. Asare, G.A., Gyan, B., Bugyei, K., Adjei, S., Mahama, R., Addo, P., Otu-Nyarko, L., Wiredu, E.K., Nyarko, A. Toxicity potentials of the nutraceutical *Moringa oleifera* at supra-supplementation levels. J Ethnopharmacol, 2012, 139**:**265-272.
34. Makkar, H.P.S., Becker, K. Nutrients and antiquality factors in different morphological parts of the *Moringa oleifera* tree. J Agric Sci, 1997, 128:311-322.
35. Siddhuraju, P., Becker. K. Antioxidant properties of various solvent extracts of total phenolic constituents from three different agroclimatic origins of drumstick tree (*Moringa oleifera Lam*.) leaves. J Agric Food Chem, 2003, 51:2144-2155.
36. Schuck, A.G., Weisburg, J.H., Esan, H., Robin, E.F., Bersson, A.R., Weitschner, J.R., Lahasky, T., Zuckerbraun, H.L., Babich, H. Cytotoxic and proapoptotic activities of gallic acid to human oral cancer HSC-2 cells. Oxid Antioxid Med Sci, 2013, 2:265-274.
37. Moss, L.A.S., Jensen-Taubman, S., Rubinstein, D., Viole, G., Stetler-Stevenson, W.G. Dietary intake of a plant phospholipid/lipid conjugate reduces lung cancer growth and tumor angiogenesis. Carcinogenesis, 2014, 35:1556-1563.
38. Mbikay, M. Therapeutic potential of *Moringa oleifera* leaves in chronic hyperglycemia and dyslipidemia: a review. Front Pharmacol, 2012, 3:1-12.

39. Waterman, C., Cheng, D.M., Rojas-Silva, P., Poulev, A., Dreifus, J., Lila, M.A., Raskin, I. Stable, water extractable isothiocyanates from *Moringa oleifera* leaves attenuate inflammation *in vitro.* Phytochemistry, 2014, 103:114-122.

40. Guevara, A.P., Vargas, C., Sakurai, H., Fujiwara, Y., Hashimoto, K., Maoka, T., Kozuka, M., Ito, Y., Tokuda, H., Nishino, H. An antitumor promoter from *Moringa oleifera Lam.* Mutat Res, 1999, 440:181-188.

41. Anwar, F., Latif, S., Ashraf, M., Gilani, A.H. *Moringa oleifera*: A food plant with multiple medicinal uses. Phytother Res, 2007, 21:17-25.

42. Divi, S.M., Bellamkonda, R., Dasireddy, S.K. Evaluation of antidiabetic and antihyperlipedemic potential of aqueous extract of *Moringa oleifera* in fructose fed insulin resistant and STZ induced diabetic wistar rats: A comparative study. Asian J Pharm Clin Res, 2011, 5:67-72.

43. Farooq, F., Rai, M., Tiwari, A., Khan, A.A., Farooq, S. Medicinal properties of *Moringa oleifera*: An overview of promising healer. J Med Plants Res, 2012, 6:4368-4374.

44. Marrufo, T.J., Encarnacao, S., Silva, O.M.D., Duarte, A., Neto, F.F., Barbosa, F.M., Agostinho, A.B. Chemical characterization and determination of antioxidant and antimicrobial activities of the leaves of *Moringa oleifera.* International Network Environmental Management Conflicts, Santa Catarina - Brasil, 2013, 2:1-15.

45. Shanker, K., Gupta, M.M., Srivastava, S.K., Bawankule, D.U., Pal, A., Khanuja, S.P.S. Determination of bioactive nitrile glycoside(s) in drumstick (*Moringa oleifera*) by reverse phase HPLC. Food Chem, 2007, 105:376-382.

46. Sultana, B., Anwar, F., Ashraf, M. Effect of extraction solvent/technique on the antioxidant activity of selected medicinal plant extracts. Molecules, 2009, 14: 2167-2180.

47. Khalafalla, M.M., Abdellatef, E., Dafalla, H.M., Nassrallah, A.A., Aboul-Enein, K.M., Lightfoot, D.A., El-Deeb, F.E., El-Shemy, H.A. Active principle from *Moringa oleifera Lam* leaves effective against two leukemias and a hepatocarcinoma. Afr J Biotechnol, 2010, 9:8467-8471.

48. Budda, S., Butryee, C., Tuntipopipat, S., Rungsipipat, A., Wangnaithum, S., Lee, J., Kupradinun, P. Suppressive effects of *Moringa oleifera* Lam pod against mouse colon carcinogenesis induced by azoxymethane and dextran sodium sulfate. Asian Pac J Cancer Prev, 2011, 12:3221-3228.

49. Kumar, V., Pandey, N., Mohan, V., Singh, R.P. Antibacterial and antioxidant activity of extract of *Moringa oleifera* leaves - An *in vitro* study. Int J Pharm Sci Rev Res, 2012, 12:89-94.
50. Jung, I.L. Soluble extract from *Moringa oleifera* leaves with a new anticancer activity. PLoS One, 2014, 9:1-10.
51. Lipinski, C.A. Drug-like properties and the causes of poor solubility and poor permeability. J Pharmacol Toxicol Methods, 2000, 44:235-249.
52. Sreelatha, S., Padma, P.R. Modulatory effects of *Moringa oleifera* extracts against hydrogen peroxide-induced cytotoxicity and oxidative damage. Hum Exp Toxicol, 2011, 1-11.
53. Sharma, H., Parihar, L., Parihar, P. Review on cancer and anticancerous properties of some medicinal plants. J Med Plants Res, 2011. 5:1818-1835.
54. Awodele, O., Oreagba, I.A., Odoma, S., da Silva, J.A.T., Osunkalu, V.O. Toxicological evaluation of the aqueous leaf extract of *Moringa oleifera* Lam. (Moringaceae). J Ethnopharmacol, 2012, 139:330-336.
55. Eshak, M.G., Osman, H.F. Role of *Moringa oleifera* leaves on biochemical and genetical alterations in irradiated male rats. Middle East J Sci Res, 2013, 16:1303-1315.
56. Jafarain, A., Asghari, G., Ghassami, E. Evaluation of cytotoxicity of *Moringa oleifera* Lam. callus and leaf extracts on Hela cells. Adv Biomed Res, 2014, 3:1-5.
57. Luqman, S., Srivastava, S., Kumar, R., Maurya, A.K., Chanda, D. Experimental assessment of *Moringa oleifera* leaf and fruit for its antistress, antioxidant, and scavenging potential using *in vitro* and *in vivo* assays. Evid Based Complement Alternat Med, 2011, 2012:1-12.
58. Kooltheat, N., Sranujit, R.P., Chumark, P., Potup, P., Laytragoon-Lewin, N., Usuwanthim, K. An ethyl acetate fraction of *Moringa oleifera* Lam. inhibits human macrophage cytokine production induced by cigarette smoke. Nutrients, 2014, 6:697-710.
59. Rakshit, S., Mandal, L., Pal, B.C., Bagchi, J., Biswas, N., Chaudhuri, J., Chowdhury, A.A., Manna, A., Chaudhuri, U., Konar, A., Mukherjee, T., Jaisankar, P., Bandyopadhyay, S. Involvement of ROS in chlorogenic acid-induced apoptosis of Bcr-Abl+ CML cells. Biochem Pharmacol, 2010, 80:1662-1675.
60. Luo, H., Daddysman, M.K., Rankin, G.O., Jiang, B., Chen, Y.C. Kaempferol enhances cisplatin's effect on ovarian cancer cells through promoting apoptosis caused by down regulation of cMyc. Cancer Cell Int, 2010, 10:1-9.

61. Mekapothula, S. Gold nanoparticle-biomolecule conjugates: synthesis, properties, cellular interactions and cytotoxicity studies in Faculty of Graduate School 2008, University of Missouri.
62. Kang, B., Mackey, M.A., El-Sayed, M. Nuclear targeting of gold nanoparticles in cancer cells induces DNA damage, causing cytokinesis arrest and apoptosis. J Am Chem Soc, 2010, 132:1517-1519.
63. Boisselier, E., Astruc, D. Gold nanoparticles in nanomedicine: preparations, imaging, diagnostics, therapies and toxicity. Chem Soc Rev, 2009, 38:1759-1782.
64. Cai, W., Gao, T., Hong, H., Sun, J. Applications of gold nanoparticles in cancer nanotechnology. Nanotechnol Sci Appl, 2008, 1:17-32.
65. Anand, K., Gengan, R.M., Phulukdaree, A., Chuturgoon, A. Agroforestry waste *Moringa oleifera* petals mediated green synthesis of gold nanoparticles and their anti-cancer and catalytic activity. J Ind Eng Chem, 2014, 21:1105-1111.
66. Gengan, R.M., Anand, K., Phulukdaree, A., Chuturgoon, A. A549 lung cell line activity of biosynthesized silver nanoparticles using *Albizia adianthifolia* leaf. Colloids Surf B Biointerfaces, 2013, 105:87-91.
67. Makarov, V.V., Love, A.J., Sinitsyna, O.V., Makarova, S.S., Yaminsky, I.V., Taliansky, M.E., Kalinina, N.O. "Green" nanotechnologies: synthesis of metal nanoparticles using plants. Acta naturae, 2014, 6:35-44.
68. Shankar, S.S., Rai, A., Ahmad, A., Sastry, M. Rapid synthesis of Au, Ag, and bimetallic Au core - Ag shell nanoparticles using Neem (*Azadirachta indica*) leaf broth. J Colloid Interface Sci, 2004, 275:496-502.
69. Belliraj, T.S., Nanda, A., Ragunathan, R. *In-vitro* hepatoprotective activity of *Moringa oleifera* mediated synthesis of gold nanoparticles. J Chem Pharm Res, 2015, 7:781-788.
70. Philip, D. Green synthesis of gold and silver nanoparticles using *Hibiscus rosa sinensis.* Physica E, 2010, 42:1417-1424.
71. Philip, D., Unni, C. Extracellular biosynthesis of gold and silver nanoparticles using Krishna tulsi (*Ocimum sanctum*) leaf. Physica E, 2011, 43:1318-1322.
72. Govender, R., Phulukdaree, A., Gengan, R.M., Anand, K., Chuturgoon, A.A. Silver nanoparticles of *Albizia adianthifolia*: the induction of apoptosis in human lung carcinoma cell line. J Nanobiotechnology, 2013, 11:1-9.
73. Malathi, S., Balakumaran, M.D., Kalaichelvan, P.T., Balasubramanian, S. Green synthesis of gold nanoparticles for controlled delivery. Adv Mat Lett, 2013, 4:933-940.
74. Kumar, A., Boruah, B.M., Liang, X. Gold nanoparticles: promising nanomaterials for the diagnosis of cancer and HIV/AIDS. J Nanomaterials, 2011, 1-17.

75. Lim, Z.J., Li, J.J., Ng, C., Yung, L.L., Bay, B. Gold nanoparticles in cancer therapy. Acta Pharmacol Sin, 2011, 32:983-990.

76. Parveen, A., Rao, S. Cytotoxicity and genotoxicity of biosynthesized gold and silver nanoparticles on human cancer cell lines. J Clust Sci, 2014:1-14.

77. Tedescoa, S., Doyle, H., Blasco, J., Redmond, G., Sheehan, D. Oxidative stress and toxicity of gold nanoparticles in *Mytilus edulis.* Aquat Toxicol, 2010, 100:178-186.

78. Baptista, P., Pereira, E., Eaton, P., Doria, G., Miranda, A., Gomes, I., Quaresma, P., Franco, R. Gold nanoparticles for the development of clinical diagnosis methods. Anal Bioanal Chem, 2008, 391:943-950.

79. Chakraborty, A., Das, D., Sinha, M., Dey, S., Bhattacharjee, S. *Moringa oleifera* leaf extract mediated green synthesis of stabilized gold nanoparticles. J Bionanosci, 2013, 7:1-5.

80. Patra, H.K., Turner, A.P.F. The potential legacy of cancer nanotechnology: cellular selection. Cell Press, 2014, 32:21-31

81. Patra, H.K., Banerjee, S., Chaudhuri, U., Lahiri, P., Dasgupta, A.K. Cell selective response to gold nanoparticles. Nanomed Nanotech Biol Med, 2007, 3:111-119.

82. Fraga, S., Faria, H., Soares, M.E., Duarte, J.A., Soares, L., Pereira, E., Costa-Pereira, C., Teixeira, J.P., de Lourdes Bastos, M., Carmo, H. Influence of the surface coating on the cytotoxicity, genotoxicity and uptake of gold nanoparticles in human $HepG_2$ cells. J Appl Toxicol, 2013, 33:1111-1119.

83. Schlinkert, P., Casals, E., Boyles, M., Tischler, U., Hornig, E., Tran, N., Zhao, J., Himly, M., Riediker, M., Oostingh, G.J., Puntes, V., Duschl, A. The oxidative potential of differently charged silver and gold nanoparticles on three human lung epithelial cell types. J Nanobiotechnology, 2015, 13:1-18.

84. De Jong, W., Hagens, W., Krystek, P., Burger, M., Sips, A., Geertsma, R. Particle size-dependent organ distribution of gold nanoparticles after intravenous administration. Biomaterials, 2008, 29:1912-1919.

85. Chen, S., Yang, D., Lin, T., Shaw, F., Liou, C., Chuang, Y. Roles of oxidative stress, apoptosis, PGC-1α and mitochondrial biogenesis in cerebral ischemia. Int J Mol Sci, 2011, 12:7199-7215.

86. Scarpulla, R.C. Metabolic control of mitochondrial biogenesis through the PGC-1 family regulatory network. Biochim Biophys Acta, 2011, 1813:1269-1278.

87. Rahman, I. Oxidative stress, chromatin remodeling and gene transcription in inflammation and chronic lung diseases. J Biochem Mol Biol, 2003, 36:95-109.

88. Bartosz, G. Reactive oxygen species: destroyers or messengers? Biochem Pharmacol, 2009, 77:1303-1215.

89. Bratic, A., Larsson, N. The role of mitochondria in aging. J Clin Invest, 2013, 123:951-957.

90. Bentz, B.G., Hammer, N.D., Radosevich, J.A., Haines III, G.K. Nitrosative stress induces DNA strand breaks but not caspase mediated apoptosis in a lung cancer cell line. J Carcinog, 2004, 3:1-13.

91. Radi, R., Beckman, J.S., Bush, K.M., Freeman, B.A. Peroxynitrite oxidation of sulfhydryls. The cytotoxic potential of superoxide and nitric oxide. J Biol Chem, 1991, 266:4244-4250.

92. Halliwell, B., Chirico, S. Lipid peroxidation: its mechanism, measurement and significance. Am J Clin Nutr, 1993, 57:715S-725S.

93. Chen, Q., Wang, Y., Xu, K., Lu, G., Ying, Z., Wu, L., Zhan, J., Fang, R., Wu, Y., Zhou, J. Curcumin induces apoptosis in human lung adenocarcinoma A549 cells through a reactive oxygen species-dependent mitochondrial signaling pathway. Oncol Rep, 2010, 23:397-403.

94. Carlberg, I., Mannervik, B. Glutathione reductase. Methods Enzymol, 1985, 113:484-490.

95. Cindrova-Davies, T. Gabor than award lecture 2008: Pre-eclampsia - from placental oxidative stress to maternal endothelial dysfunction. Placenta, 2009, 23:S55-S65.

96. Harvey, C.J., Thimmulappa, R.K., Singh, A., Blake, D.J., Ling, G., Wakabayashi, N., Fujii, J., Myers, A., Biswal, S. Nrf2-regulated glutathione recycling independent of biosynthesis is critical for cell survival during oxidative stress. Free Radic Biol Med, 2009, 46:443-453.

97. Rangasamy, T., Cho, C.Y., Thimmulappa, R.K., Zhen, L., Srisuma, S.S., Kensler, T.W., Yamamoto, M., Petrache, I., Tuder, R.M., Biswal, S. Genetic ablation of Nrf2 enhances susceptibility to cigarette smoke induced emphysema in mice. J Clin Invest, 2004, 114:1248-1259.

98. Singh, A., Misra, V., Thimmulappa, R.K., Lee, H., Ames, S., Hoque, M.O., Herman, J.G., Baylin, S.B., Sidransky, D., Gabrielson, E., Brock, M.V., Biswal, S. Dysfunctional KEAP1-NRF2 interaction in non-small-cell lung cancer. PLoS Med, 2006, 3:1865-1876.

99. Hanada, N., Takahata, T., Zhou, Q., Ye, X., Sun, R., Itoh, J., Ishiguro, A., Kijima, H., Mimura, J., Itoh, K., Fukuda, S., Saijo, Y. Methylation of the KEAP1 gene promoter region in human colorectal cancer. BMC Cancer, 2012, 12:1-11.

100. Vazquez, F., Lim, J., Chim, H., Bhalla, K., Girnun, G., Pierce, K., Clish, C.B., Granter, S.R., Widlund, H.R., Spiegelman, B.M., Puigserver, P. PGC1α expression defines a subset of human melanoma tumors with increased mitochondrial capacity and resistance to oxidative stress. Cancer Cell, 2013, 23:287-301.

101. Kerr, J.F.R., Wyllie, A.H., Currie, A.R. Apoptosis: A basic biological phenomenon with wideranging implications in tissue kinectics. Br J Cancer, 1972, 26:239-257.

102. Thompson, C.B. Apoptosis in the pathogenesis and treatment of disease. Science, 1995, 267:1456-1462.

103. Hotchkiss, R.S., Strasser, A., McDunn, J.E., Swanson, P.E. Mechanism of disease cell death. N Engl J Med, 2009, 361:1570-1583.

104. Rao, L., Perez, D., White, E. Lamin proteolysis facilitates nuclear events during apoptosis. J Cell Biol, 1996, 135:1441-1455.

105. Schlegel, R.A., Williamson, P. Phosphatidylserine, a death knell. Cell Death Differ, 2001, 8:551-563.

106. Fadok, V.A., Voelker, D.R., Campbell, P.A., Cohen, J.J., Bratton, D.L., Henson, P.M. Exposure of phosphatidylserine on the surface of apoptotic lymphocytes triggers specific recognition and removal by macrophages. J Immunol, 1992, 148:2207-2216.

107. Wang, X. The expanding role of mitochondria in apoptosis. Genes Dev, 2001, 15:2922-2933.

108. Shimizu, S., Narita, M., Tsujimoto, Y. Bcl-2 family proteins regulate the release of apoptogenic cytochrome c by the mitochondrial channel VDAC. Nature, 1999, 399:483-487.

109. Garrido, C., Brunet, M., Didelot, C., Zermati, Y., Schmitt, E., Kroemer, G. Heat shock proteins 27 and 70 anti-apoptotic proteins with tumorigenic properties. Cell Cycle, 2006, 5:2592-2601.

110. Costantini, P., Bruey, J.M., Castedo, M., Metivier, D., Loeffler, M., Susin, S.A., Ravagnan, L., Zamzami, N., Garrido, C., Kroemer, G. Pre-processed caspase-9 contained in mitochondria participates in apoptosis. Cell Death Differ, 2002, 9:82-88.

111. Hockenbery, D., Nunez, G., Milliman, C., Schreiber, R.D., Korsmeyer, S.J. Bcl-2 is an inner mitochondrial membrane protein that blocks programmed cell death. Nature, 1993, 348:334-336.

112. Shyu, A., Wilkinson, M.F., van Hoof, A. Messenger RNA regulation: to translate or to degrade. EMBO J, 2008, 27:471-481.

113. Cooper, G.M., The Cell. A molecular approach, 2000, Sunderland: Sinauer Associates: Boston, USA.

114. Pajares, M.J., Ezponda, T., Catena, R., Calvo, A., Pio, R., Montuenga, L.M. Alternate splicing: an emerging topic in molecular and clinical oncology. Lancet Oncol, 2007, 8:349-357.
115. Shankarling, G., Lynch, K.W. Living or dying by RNA processing: caspase expression in NSCLC. J Clin Invest, 2010, 120:3798-3801.
116. Srinivasula, S.M., Ahmad, M., Fernandes-Alnemri, T., Alnemri, E.S. Autoactivation of procaspase-9 by Apaf-1-mediated oligomerization. Mol Cell, 1998, 1: 949-957.
117. Hajra, K.M., Liu, J.R. Apoptosome dysfunction in human cancer. Apoptosis, 2004, 9:691-704.
118. Nagata, S. Apoptosis by death factor. Cell, 1997, 88:355-365.
119. Radhakrishna Pillai, G., Srivastava, A.S., Hassanein, T., Chauhan, D.P., Carrier, E. Induction of apoptosis in human lung cancer cells by curcumin. Cancer Lett, 2004, 208:163-170.
120. Kaufmann, S.H., Desnoyers, S., Ottaviano, Y., Davidson, N.E., Poirier, G.G. Specific proteolytic cleavage of poly (ADP-ribose) polymerase: an early marker of chemotherapy-induced apoptosis. Cancer Res, 1993, 53:3976-3985.
121. Casiano, C.A., Martin, S.J., Green, D.R., Tan, E.M. Selective cleavage of nuclear autoantigens during CD95 (Fas/APO-1)-mediated T cell apoptosis. J Exp Med, 1996, 184:765-770.
122. D'Amours, D., Sallmann, F.R., Dixit, V.M., Poirier, G.G. Gain-of-function of poly (ADP-ribose) polymerase-1 upon cleavage by apoptotic proteases: implications for apoptosis. J Cell Sci, 2001, 114:3771-3778.
123. Sodhi, R.K., Singh, N., Jaggi, A.S. Poly (ADP ribose) polymerase-1 (PARP-1) and its therapeutic implications. Vascul Pharmacol, 2010, 53:77-87.
124. Halappanavar, S.S., Le Rhun, Y., Mounir, S., Martins, L.M., Huoti, J., Earnshaw, W.C., Shah, G.M. Survival and proliferation of cells expressing caspase-uncleavable poly (ADP-ribose) polymerase in response to death-inducing DNA damage by an alkylating agent. J Biol Chem, 1999, 274:37097-37104.
125. Eustermann, S., Videler, H., Yang, J., Cole, P.T., Gruszka, G., Veprintsev, D., Neuhaus, D. The DNA-binding domain of human PARP-1 interacts with DNA single-strand breaks as a monomer through its second zinc finger. J Mol Biol, 2011, 407:149-170.
126. Woodhouse, B.C., Dianov, G.L. Poly ADP-ribose polymerase-1: an international molecule of mystery. DNA Repair, 2008, 7:1077-1086.

127. Yung, T.M.C., Satoh, M.S. Functional competition between poly (ADP-ribose) polymerase and its 24-kDa apoptotic fragment in DNA repair and transcription. J Biol Chem, 2001, 276:11279-11286.
128. Nithipongvanitch, R., Ittarat, W., Velez, J.M., Zhao, R., St. Clair, D.K., Oberley, T.D. Evidence for p53 as guardian of the cardiomyocyte mitochondrial genome following acute adriamycin treatment. J Histochem Cytochem, 2007, 55:629-639.
129. Bertram, J.S. The molecular biology of cancer. Mol Aspects Med, 2001, 21:167-223.
130. Srivastava, R., Apoptosis, cell signalling and human disease: molecular mechansims, 2007, Human Press Inc: New Jersey.
131. Mihara, M., Erster, S., Zaika, A., Petrenko, O., Chittenden, T., Pancoska, P., Moll, U.M. p53 has a direct apoptogenic role at the mitochondria. Mol Cell, 2003, 11:577-590.
132. Vicente-Duenas, C., Romero-Camarero, I., Cobaleda, C., Sanchez-Garcia, I. Function of oncogenes in cancer development: a changing paradigm. EMBO J, 2013, 32**:**1502-1513.
133. Shortt, J., Johnstone, R.W. Oncogenes in cell survival and cell death. Cold Spring Harb Perspect Biol, 2012, 4:1-11.
134. Dang, C.V. c-Myc target genes involved in cell growth, apoptosis, and metabolism. Mol Cell Biol, 1999, 19:1-11.
135. Liao, J., Lu, H. Autoregulatory suppression of c-Myc by miR-185-3p. J Biol Chem, 2011, 286:33901-33909.
136. Nesbit, C.E., Tersak, J.M., Prochownik, E.V. MYC oncogenes and human neoplastic disease. Oncogene, 1999, 18:3004-3016.
137. Fields, W.R., Desiderio, J.G., Putnam, K.P., Bombick, D.W., Doolittle, D.J. Quantification of changes in c-myc mRNA levels in normal human bronchial epithelial (NHBE) and lung adenocarcinoma (A549) cells following chemical treatment. Toxicol Sci, 2001, 63:107-114.
138. Kim, T., Kang, J.M., Hyun, J., Lee, B., Kim, S.J., Yang, E., Hong, S., Lee, H., Fujii, M., Niederhuber, J.E., Kim, S. The Smad7-Skp2 complex orchestrates Myc stability, impacting on the cytostatic effect of TGF-β. J Cell Sci, 2014, 127:411-421.
139. Wade, M., Wahl, G.M. c-Myc, genome instability, and tumorigenesis: the devil is in the details. CTMI, 2006, 302:169-203.
140. Liu, J., Shaik, S., Dai, X., Wu, Q., Zhou, X., Wang, Z., Wei, W. Targeting the ubiquitin pathway for cancer treatment. Biochim Biophys Acta, 2015, 1855:50-60.

141. Bretones, G., Acosta, J.C., Caraballo, J.M., Ferrandiz, N., Gomez-Casares, M.T., Albajar, M., Blanco, R., Ruiz, P., Hung, W., Albero, M.P., Perez-Roger, I., Leon, J. Skp2 oncogene is a direct myc target gene and myc down-regulates $p27^{Kip1}$ through Skp2 in human leukemia cells. J Biol Chem, 2011, 286:9815-9825.

142. Huang, H., Weng, H., Wang, L., Yu, C., Huang, Q., Zhao, P., Wen, J., Zhou, H., Qu, L. Triggering Fbw7-mediated proteasomal degradation of c-Myc by Oridonin induces cell growth inhibition and apoptosis. Mol Cancer Ther, 2012, 11:1155-1165.

143. Hanahan, D., Weinberg, R.A. Hallmarks of cancer: the next generation. Cell, 2011, 144:646-674.

144. Gogvadze, V., Orrenius, S., Zhivotovsky, B. Mitochondria as targets for cancer chemotherapy. Semin Cancer Biol, 2009, 19:57-66.

145. Kiyohara, C., Otsub, A., Shirakawa, T., Fukuda, S., Hopkin, J.M. Genetic polymorphisms and lung cancer susceptibility: a review. Lung Cancer, 2002, 37:241-256.

146. Malhotra, A., Nair, P., Dhawan, D.K. Modulatory effects of curcumin and resveratrol on lung carcinogenesis in mice. Phytother Res, 2010, 24:1271-1277.

147. Aisner, J., Belani, C.P. Lung cancer: recent changes and expectations of improvements. Semin Oncol, 1993, 20:383-389.

148. Montazeri, A., Milroy, R., Hole, D., McEwen, J., Gillis, C.R. Quality of life in lung cancer patients as an important prognostic factor. Lung Cancer, 2001, 31:233-240.

149. Durham, A.L. and I.M. Adcock. The relationship between COPD and lung cancer. Lung Cancer, 2015, 90:121-127.

150. Lieber, M., Smith, B., Szakal, A., Nelson-Rees, W., Todaro, G. A continuous tumor cell-line from a human lung carcinoma with properties of Type II alveolar epithelial cells. Int J Cancer, 1976, 7:62-70.

151. Speit, G., Bonzheim, I. Genotoxic and protective effects of hyperbaric oxygen in A549 lung cells. Mutagenesis, 2003, 18:545-548.

152. Scagliotti, G.V., Parikh, P., von Pawel, J., Biesma, B., Vansteenkiste, J., Manegold, C., Serwatowski, P., Gatzemeier, U., Digumarti, R., Zukin, M., Lee, J.S., Mellemgaard, A., Park, K., Patil, S., Rolski, J., Goksel, T., de Marinis, F., Simms, L., Sugarman, K.P., Gandara, D. Phase III study comparing cisplatin plus gemcitabine with cisplatin plus pemetrexed in chemotherapy-naive patients with advanced-stage non-small-cell lung cancer. J Clin Oncology, 2008, 26:3543-3551.

153. Siddik, Z.H. Cisplatin: mode of cytotoxic action and molecular basis of resistance. Oncogene, 2003, 22:7265-7279.

154. Dlamini, Z., Bhoola, K. Esophageal cancer in african blacks of KwaZulu Natal, South Africa: an epidemiological brief. Ethnic Dis, 2005, 15:786-789.
155. Segal, I., Reinach, S.G., De Beer, M. Factors associated with oesophageal cancer in Soweto, South Africa. Br J Cancer, 1988, 58:681-686.
156. Bey, E., Alexander, J., Whitcutt, J.M., Hunt, J.A., Gear, J.H.S. Carcinoma of the esophagus in Africans: establishment of a continuously growing cell line from a tumor specimen. In Vitro, 1976, 12:107-114.
157. Gu, M., Li, S., Huang, X., Lin, Y., Cheng, H., Liu, L. A phase II study on continuous infusional paclitaxel and 5-Fu as first-line chemotherapy for patients with advanced esophageal cancer. Asian Pac J Cancer Prev, 2012, 13:5587-5591.
158. Moorthi, C., Manavalan, R., Kathiresan, K. Nanotherapeutics to overcome conventional cancer chemotherapy limitations. J Pharm Pharmaceut Sci, 2011, 14:67- 77.
159. Watson, R.R., Preedy, V.R., Bioactive foods and extracts cancer treatment and prevention, 2011, CRC press.
160. Nair, S., Varalokshmi, K.N. Anticancer, cytotoxic potential of *Moringa oleifera* extracts on HeLa cell line. J Nat Pharm, 2011, 2:138-142.

CHAPTER 2

The antiproliferative effect of *Moringa oleifera* crude aqueous leaf extract on cancerous human alveolar epithelial cells

Charlette Tiloke[1], Alisa Phulukdaree[1] and Anil A. Chuturgoon[1]*

[1]*Discipline of Medical Biochemistry, School of Laboratory Medicine and Medical Sciences, College of Health Sciences, University of KwaZulu-Natal, Durban, South Africa*

Charlette Tiloke[1] email: 208501101@stu.ukzn.ac.za

Alisa Phulukdaree[1] email: 204504283@stu.ukzn.ac.za

Professor Anil A. Chuturgoon[1]* - Corresponding author email: chutur@ukzn.ac.za

Tel: +27 31 260 4404
Fax: +27 31 260 4785

Postal address: Discipline of Medical Biochemistry, Nelson R Mandela School of Medicine, University of KwaZulu-Natal, Private Bag 7, Congella, 4013, Durban, South Africa

BMC Complementary and Alternative Medicine, 2013, 13, 226: 1-8
DOI: 10.1186/1472-6882-13-226
(Top 100 publication in journal, highly accessed, 21 citations)

Abstract

Background: The incidence of lung cancer is expected to increase due to increases in exposure to airborne pollutants and cigarette smoke. *Moringa oleifera* (MO), a medicinal plant found mainly in Asia and South Africa is used in the traditional treatment of various ailments including cancer. This study investigated the antiproliferative effect of MO leaf extract (MOE) in cancerous A549 lung cells.

Methods: A crude aqueous leaf extract was prepared and the cells were treated with 166.7µg/ml MOE (IC_{50}) for 24h and assayed for oxidative stress (TBARS and Glutathione assays), DNA fragmentation (comet assay) and caspase (3/7 and 9) activity. In addition, the expression of Nrf2, p53, Smac/DIABLO and PARP-1 was determined by Western blotting. The mRNA expression of *Nrf2* and *p53* was assessed using qPCR.

Results: A significant increase in reactive oxygen species with a concomitant decrease in intracellular glutathione levels ($p < 0.001$) in MOE treated A549 cells was observed. MOE showed a significant reduction in Nrf2 protein expression (1.89-fold, $p < 0.05$) and mRNA expression (1.44-fold). A higher level of DNA fragmentation ($p < 0.0001$) was seen in the MOE treated cells. MOE's pro-apoptotic action was confirmed by the significant increase in p53 protein expression (1.02-fold, $p < 0.05$), *p53* mRNA expression (1.59-fold), caspase-9 (1.28-fold, $p < 0.05$), caspase-3/7 (1.52-fold) activities and an enhanced expression of Smac/DIABLO. MOE also caused the cleavage and activation of PARP-1 into 89 KDa and 24 KDa fragments ($p < 0.0001$).

Conclusion: MOE exerts antiproliferative effects in A549 lung cells by increasing oxidative stress, DNA fragmentation and inducing apoptosis.

Keywords: *Moringa oleifera*, Drumstick tree, Lung cancer, Oxidative stress, Nrf2, Apoptosis

Background

Lung cancer is a leading cause of morbidity and mortality in many countries [1]. Inhalation of airborne pollutants, exposure to toxins present in grain dusts and fungal spores and cigarette smoking causes lung damage and increases the risk of carcinogenesis [2]. South Africa (SA) has the highest human immunodeficiency virus (HIV) infection burden globally and Bello et al. (2011) showed that surviving HIV positive individuals have a high risk of cancer such as lung cancer. Cancer deaths accounted for 63% in developing countries across the world [3]. Cancer is characterised by uncontrolled cell growth as cells proliferate and evade apoptosis [4]. Apoptosis is regulated by caspases through two pathways, viz., death receptor-mediated procaspase-activation pathway (extrinsic pathway) and mitochondrion-mediated procaspase-activation

pathway (intrinsic pathway) [4, 5]. To maintain cellular homeostasis, these cells follow a process of growth, division and cell death. When this process is affected, it can result in the initiation of cancer.

There are many regulators of apoptosis. The p53 tumor suppressor protein and transcription factor is up-regulated when DNA is damaged by causing G1 arrest and DNA repair; if the repair is unsuccessful then it signals for apoptosis and ultimately cell death [6, 7]. During apoptosis cellular proteins are proteolysed by caspases. These proteins also include poly (ADP ribose) polymerase-1 (PARP-1) [8].

Lung cancer still remains incurable and current drug therapies have many side-effects and alternate therapy is actively being sought [9]. If traditional medicine can provide an alternate source for treatment, the number of lung cancer deaths can be reduced. Some traditional medicines possess antiproliferative effects such as *Sutherlandia frutescens,* commonly referred to as cancer bush, is used by traditional healers in SA to treat cancer [10]. *Moringa oleifera* (MO), an indigenous tree to India, is found widely in SA [11]. It belongs to the family Moringaceae and is cultivated for medicinal and industrial purposes [12]. It is commonly referred to as the 'tree of life' or Drumstick tree [12, 13]. All parts of the MO plant possess medicinal properties, but the leaves have high nutritional value (high levels of vitamins C and A, potassium, proteins, calcium and iron) [14, 15]. In addition the leaves possess phytochemicals like carotenoids, alkaloids and flavonoids [11] and is rich in amino acids such as cystine, lysine, methionine and tryptophan [16]. MO is used in traditional treatment of diabetes mellitus, cardiovascular and liver disease.

Phytochemical properties of MO play an important role in its mode of action against diseases [11]. It contains a rich source of rhamnose, glucosinolates and isothiocyanates. A study conducted by Manguro and Lemmen (2007) into the phenolics of MOE had characterised five flavonol glycosides using spectroscopic methods [17]. The anticancer property can be attributed to specific components of MOE such as 4-(α-L-rhamnopyranosyloxy) benzyl glucosinolate, 4-(α-L-rhamnopyranosyloxy) benzyl isothiocyanate, benzyl isothiocyanate and niazimicin. The leaves contain quercetin-3-O-glucoside and kaempferol-3-O-glucoside which plays a role in antioxidant defence as it scavengers for free radicals thus reducing oxidative stress [12]. Thiocarbamates such as niazimicin are found in the leaves and can be used as a chemopreventive agent [18, 19]. Studies have suggested that the anticancer and chemopreventive property of MOE can be attributed to niazimicin [20, 21].

MO leaf extracts have been shown to disrupt proliferation of cancer cells. In a study on Swiss mice, MO leaf extracts increased glutathione-S-transferase (GST) [12]. The MO leaf extracts induced apoptosis in KB carcinoma cells [22]. Sreelatha and Padma (2011) had shown that the extracts inhibited lipid peroxidation as it scavenged free radicals and reduced oxidative stress [22]. It also protected against oxidative DNA damage. To date there is no study assessing the effects of MO leaf extracts on lung carcinogenesis. The present study investigated the antiproliferative effects of a crude aqueous extract of MO leaves in A549 (human lung carcinoma) cells. It was hypothesised that MO leaf extracts induces cell death as a result of oxidative stress in the cancerous cells.

Methods

Materials

MO leaves were collected from the KwaZulu-Natal region (Durban, South Africa) and verified by the KwaZulu-Natal herbarium (Batch no. CT/1/2012, Genus no. 3128). A549 cells were purchased from Highveld Biologicals (Johannesburg, South Africa). Cell culture reagents were purchased from Whitehead Scientific (Johannesburg, South Africa). ECL-LumiGlo® chemiluminescent substrate kit was purchased from Gaithersburg (USA) and western blot reagents were purchased from Bio-Rad (USA). All other reagents were purchased from Merck (South Africa).

Cell culture

A549 lung cells were cultured (37°C, 5% CO_2) in 25cm^3 culture flasks in complete culture media (CCM) [23] comprising of Eagle's minimum essential medium supplemented with 10% foetal calf serum, 1% L-glutamine and 1% penicillin-streptomycin-fungizone until confluent [24]. Cell growth was monitored and CCM was changed as necessary. Confluent flasks were trypsinized using 1ml trypsin. Cell numbers were enumerated using trypan blue.

Leaf extract

The MO leaf extract (MOE) was prepared by crushing 10g of air-dried leaves in a pestle and mortar and the subsequent addition of 100ml de-ionised water [24, 25]. The resultant extract was boiled with continuous stirring for 20min, transferred to 50ml conical tubes and centrifuged [720xg, 10min, room temperature (RT)]. The upper aqueous layer (MOE) was removed, lyophilised and stored at 4°C. MOE stock solution was prepared by dissolving 1mg of MOE in 1ml of CCM and filter sterilised [0.22µM filter (Millipore)].

Cell viability assay

The cytotoxicity of MOE in A549 cells was determined using the Methyl thiazol tetrazolium (MTT) assay [26]. A549 cells (15,000 cells/well) were seeded into a 96-well microtitre plate. The cells were incubated with varying MOE dilutions (0, 1, 10, 50, 100, 150, 200, 250, 500µg/ml) in six replicates (300µl/well) and incubated (37°C, 5% CO_2) for 24h. A control of cells incubated with CCM only was used. A CCM/MTT salt solution (5mg/ml) was added (120µl/well) and the plate was incubated (37°C, 4h). Thereafter, supernatants were removed; dimethyl sulphoxide (DMSO) 100µl/well was added and incubated (1h). The optical density of the formazan product was measured at 570nm and reference wavelength of 690nm using a spectrophotometer (Bio Tek µQuant). The percentage cell viability was determined and a concentration-response curve was plotted using GraphPad Prism V5.0 software relative to the control. This experiment was repeated on two separate occasions before the concentration of half the maximum inhibition (IC_{50}) was calculated.

For subsequent assays, A549 cells at inoculation density of 20,000 cells per well were treated (24h) with the IC_{50} determined on viability assay.

Lipid peroxidation - quantification of malondialdehyde (MDA)

To investigate MOE generation of reactive oxygen species (ROS), Thiobarbituric acid assay (TBARS) was used. TBARS measures MDA which is the end product of lipid peroxidation and an indicator of oxidative stress [27]. Following treatment, cells lysed in 0.2% H_3PO_4 (100µl) by passing the cell solution through a 25 gauge needle at least 25 times from each sample was transferred to test tubes with the addition of 2% H_3PO_4 (200µl), 7% H_3PO_4 (400µl) and TBA/BHT solution (400µl). A positive control of MDA and a negative control of CCM were prepared. All samples were adjusted to pH 1.5 and heated (100°C, 15min). After cooling, butanol (1.5ml) was added to each test tube, vortexed and allowed to separate into distinct phases. The upper butanol phase (800µl) was transferred into eppendorfs and centrifuged (17,949xg, 6min, RT). 100µl from each sample was aliquoted into a 96-well microtitre plate in six replicates. The optical density was measured on a spectrophotometer at 532nm with reference wavelength of 600nm. The mean optical density for each sample was calculated and divided by the absorption coefficient (156 mM^{-1}). The results were expressed in µM.

Antioxidant potential - quantification of glutathione

Glutathione-Glo™ Assay (Promega) was used according to manufacturer's guidelines to quantify glutathione (GSH) levels. 50µl from each sample (MOE treated and untreated control)

was added in six replicates to the wells of an opaque polystyrene 96-well microtitre plate. GSH standards (0-50µM) were prepared from a 5mM stock diluted in de-ionised water. 50µl of each GSH standards and 50µl of the GSH-Glo™ Reagent 2X was added per well and incubated in the dark (30min, RT). Reconstituted Luciferin Detection Reagent (50µl) was added per well and incubated (15min, RT). The luminescence was measured on a Modulus™ microplate luminometer (Turner Biosystems, Sunnyvale, USA). The data was analysed and expressed as relative light units (RLU).

DNA damage

DNA damage was determined using the Comet assay [28]. Following treatment of cells (20,000 cells/well) in a 6-well plate, supernatants were removed and cells were trypsinized. Three slides per sample were prepared as the first layer of 1% low melting point agarose (LMPA, 37°C), second layer of 25µl of cells (20,000) from the samples with 175µl of 0.5% LMPA (37°C) and third layer of 0.5% LMPA (37°C) covered the slides. After solidification, the slides were then submerged in cold lysing solution [2.5M NaCl, 100mM EDTA, 1% Triton X-100, 10mM Tris (pH 10), 10% DMSO] and incubated (4°C, 1h). Following incubation the slides were placed in electrophoresis buffer [300mM NaOH, 1mM Na_2EDTA (pH 13)] for 20min and thereafter subjected to electrophoresis (25V, 35min, RT) using Bio-Rad compact power supply. The slides were then washed 3 times with neutralisation buffer [0.4M Tris (pH 7.4)] for 5min each. The slides were stained overnight (4°C) with 40µl ethidium bromide (EtBr) and viewed with a fluorescent microscope (Olympus IXSI inverted microscope with 510-560nm excitation and 590nm emission filters). Images of 50 cells and comets were captured per treatment and the comet tail lengths were measured using Soft imaging system (Life Science - ©Olympus Soft Imaging Solutions v5) and expressed in µm.

Caspase-3/7 and 9 activities

Caspase-Glo® 3/7 and Caspase-Glo® 9 Assays (Promega) were used to assess apoptosis. For each assay the same procedure was followed: A549 cells were seeded into an opaque polystyrene 96-well microtitre plate in six replicates. Following treatment, the Caspase-Glo® 3/7 and Caspase-Glo® 9 reagents were prepared according to manufacturer's guidelines. 100µl of the reagent was added per well and incubated in the dark (30min, RT). Following incubation, the luminescence was measured on a Modulus™ microplate luminometer. The data was expressed as RLU and fold change.

Western blotting

Western Blots were performed to determine the expression of Nrf2, p53, Smac/DIABLO and PARP-1. Briefly, total protein was isolated using Cytobuster™ reagent supplemented with protease inhibitor (Roche, cat. no. 05892791001) and phosphatase inhibitor (Roche, cat. no. 04906837001). The bicinchoninic acid assay (Sigma, Germany) was used to quantify the protein and was standardised to 2.042mg/ml [29]. The samples were prepared in Laemmli buffer [30], boiled (100°C, 5min) and electrophoresed (150V, 1h) in 7.5% sodium dodecyl sulfate polyacrylamide gels using a Bio-Rad compact power supply. The separated proteins were electro-transferred to nitrocellulose membrane using the Trans-Blot® Turbo Transfer system (Bio-Rad) (20V, 45min). The membranes were blocked (1h) using 3% BSA in Tris-buffered saline containing 0.5% Tween20 (TTBS - NaCl, KCL, Tris, Tween 20, dH_2O, pH 7.4). Thereafter, the membranes were immune-probed with primary antibody [Nrf2 (ab89443), p53 (ab26), PARP-1 (ab110915), 1:1,000; Smac/DIABLO (ab68352), 1:200] at 4°C overnight. The membranes were then washed 4x with TTBS (10min each) and incubated with the secondary antibody (ab97046; 1:2,000) at RT for 1h. The membranes were finally washed 4x with TTBS (10min each). To correct for loading error and to normalise the expression of the proteins, β-actin was assessed (ab8226; 1:5,000). Horse radish peroxidase (HRP) chemiluminescence detector and enhancer solution was used for the antigen-antibody complex and the signal was detected with the Alliance 2.7 image documentation system (UViTech). The expression of the proteins were analysed with UViBand Advanced Image Analysis software v12.14 (UViTech). The data was expressed as relative band density (RBD) and fold change.

Quantification of mRNA

To determine *p53* and *Nrf2* mRNA expression, RNA was first isolated from control and MOE treatment by adding 500µl Tri reagent (Am9738) as per manufacturer's guidelines. Thereafter, RNA was quantified (Nanodrop 2000) and standardised to 100ng/µl. RNA was reverse transcribed by reverse transcriptase into copy DNA (cDNA) using the RT^2 First Strand Kit (SABiosciences, C-03) as per manufacturer's instructions. Briefly, a 20µl reaction was prepared by adding 10µl genomic DNA elimination mixture (Total RNA, 5x gDNA elimination buffer, H_2O) to 10µl of RT cocktail (5x RT buffer 3, primer and external control mix, RT enzyme mix, H_2O). The reaction was then subjected to 42°C (15min) and 95°C (5min) (GeneAmp® PCR System 9700, Applied Biosystems) to obtain cDNA. Quantitative PCR (qPCR) was used to determine mRNA expression using RT^2 SYBR® Green qPCR Master Mix (SABiosciences). A 25µl reaction consisting of 12.5µl IQ™ SYBR® green supermix (cat. no. 170-8880), 8.5µl nuclease-free water, 2µl cDNA, and 1µl sense and anti-sense primer (10mM, inqaba biotec™,

Table 1) were used. The mRNA expression was compared and normalised to a housekeeping gene, *GAPDH*.

Table 1 Primer sequences used in qPCR assay

	Primer sequence	
	Sense Primer	**Anti-sense Primer**
Nrf2	5′AGTGGATCTGCCAACTACTC 3′	5′CATCTACAAACGGGAATGTCTG 3′
p53	5′CCACCATCCACTACAACTACAT3′	5′CAAACACGGACAGGACCC3′
GAPDH	5′TCCACCACCCTGTTGCTGTA3′	5′ACCACAGTCCATGCCATCAC3′

The reaction was subjected to an initial denaturation (95°C, 10min). It was followed by 40 cycles of denaturation (95°C, 15s), annealing (*Nrf2*: 57°C, 40s; *p53*: 56°C, 40s) and extension (72°C, 30s) (Chromo 4 Real-Time PCR detector, Biorad). The data was analysed using MJ opticon monitor analysis software V3.1, Biorad. The mRNA expression was determined using the Livak method and expressed as fold changes [31].

Statistical analysis

Statistical analyses were performed using GraphPad Prism v5.0 software (GraphPad Software Inc., La Jolla, USA). The results were expressed as means with standard deviation (SD). The concentration-response-inhibition equation was used to determine IC_{50} for MTT assay. The statistical significances were determined by unpaired *t*-test and a 95% confidence interval. The data were considered statistically significant with a value of $p < 0.05$.

Results

Cell viability assay

The MTT assay measures cell viability based on the generation of reducing equivalents in metabolic active cells. The A549 cell viability (%) data is presented in Table 2.

Table 2 Viability of A549 cells treated with MOE for 24h

Concentration (µg/ml)	Mean OD ± SD	Cell Viability (%)
0 (Control)	1.469 ± 0.008	100
1	1.177 ± 0.058	80.123
10	1.120 ± 0.132	76.242
50	1.001 ± 0.118	68.108
100	1.201 ± 0.082	81.756
150	1.170 ± 0.110	79.646
200	0.966 ± 0.158	65.725
250	0.922 ± 0.177	62.730
500	0.984 ± 0.350	66.950

OD: optical density, *SD*: standard deviation.

Using GraphPad prism, an IC_{50} value of 166.7µg/ml was calculated. This concentration of MOE was used in all subsequent assays.

Assessment of oxidative stress

Reactive oxygen species (ROS) induce oxidative stress. Lipid peroxidation, caused by ROS, was assayed by quantifying MDA presented in Figure 1A.

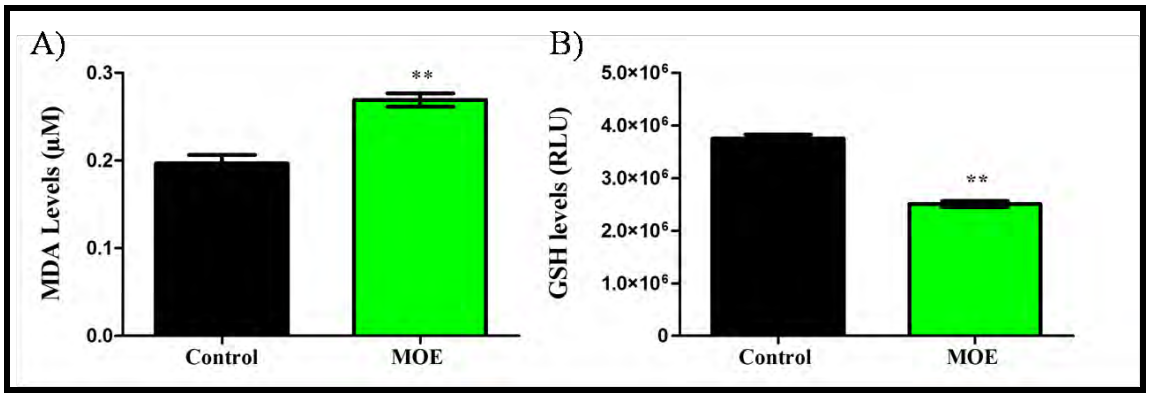

Figure 1 Oxidative stress induced by MOE on A549 cells.

An increase in MDA levels (lipid peroxidation) **(A)** and decreased intracellular GSH levels **(B)** in MOE treated cells (**$p < 0.001$).

There was a significant increase in MDA levels in MOE treatment as compared to the untreated cells (0.269 ± 0.013µM vs 0.197 ± 0.016µM, $p < 0.001$). GSH levels were significantly

decreased in the MOE treatment compared to the control [Figure 1B ($2.507 \times 10^6 \pm 0.081 \times 10^6$ RLU vs $3.751 \times 10^6 \pm 0.110 \times 10^6$ RLU, $p < 0.001$): Additional file 1].

DNA damage

The comet assay assessed DNA damage and the comet tail lengths were measured in MOE treated and untreated A549 cells (Figure 2).

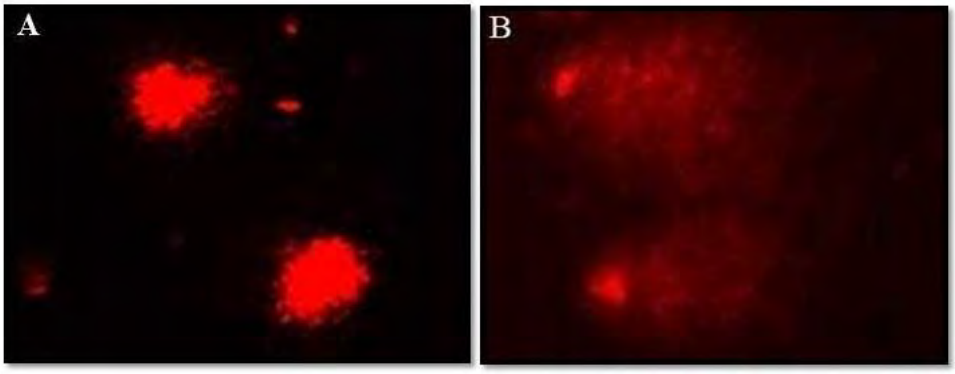

Figure 2 Comet assay images of control and MOE treatments for 24h.

DNA damage was higher in cells exposed to MOE **(B)** then control cells **(A)** (100x, ***$p < 0.0001$).

There was a significant increase in comet tail length in MOE treatment compared to the control ($18.52 \pm 4.90\mu m$ vs $5.15 \pm 1.18\mu m$, $p < 0.0001$).

Assessment of caspase-3/7 and 9 activities

Intracellular activity of caspases-3/7 and caspase-9 was measured. Table 3 presents the apoptotic induction in A549 cells.

Table 3 Apoptotic markers of A549 cells following treatment for 24h

	Mean ± SD (RLU x 10^5)		Fold change	*p*-value
	Control	MOE		
Caspase-3/7	2.097 ± 0.489	3.196 ± 0.261	1.52	0.107
Caspase-9	12.630 ± 0.020	16.160 ± 0.702	1.28	< 0.05*

*$p < 0.05$: statistically significant compared to the control, *SD*: standard deviation, *RLU*: relative light units.

There was an increase (non-significant) in caspase-3/7 activity and a significant increase in caspase-9 activity in MOE treatment compared to the control (Table 3).

Western blotting

To determine the effect of MOE on protein expression we assessed the levels of Nrf2, p53, Smac/DIABLO and PARP-1 using western blot (Figure 3).

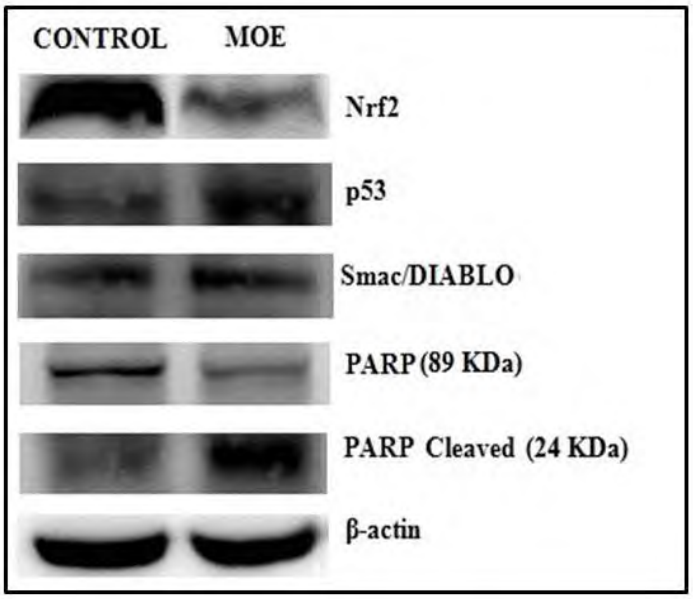

Figure 3 MOE regulating protein expression in A549 cells.

Differential expression of Nrf2, p53, Smac/DIABLO, PARP-89 KDa and 24 KDa fragment in A549 cells after treatment with MOE for 24h.

MOE induced a significant 1.89-fold decrease in Nrf2 expression [Figure 3 (0.069 ± 0.007 RBD vs control: 0.129 ± 0.022 RBD, $p < 0.05$)]; a 1.02-fold increase in p53 expression [Figure 3 (0.567 ± 0.002 RBD vs control: 0.558 ± 0.002 RBD, $p < 0.05$)] and a 1.06-fold increase in Smac/DIABLO expression [Figure 3 (1.509 ± 0.055 RBD vs control: 1.425 ± 0.007 RBD, $p = 0.162$)]. During apoptosis, PARP-1 is proteolysed by caspases to an 89 KDa and 24 KDa fragment. There was a significant 1.27-fold decrease in the expression of PARP 89 KDa fragment in the MOE treatment compared to the control [Figure 3 (0.234 ± 0.005 RBD vs 0.297 ± 0.005 RBD, $p < 0.0001$)] and a 1.46-fold increase in the level of PARP 24 KDa fragment [Figure 3 (0.419 ± 0.014 RBD vs 0.286 ± 0.016 RBD, $p < 0.0001$); Additional file 1].

Quantification of mRNA

The mRNA expression of *Nrf2* and *p53* in A549 cells was determined using qPCR relative to the control (Figure 4).

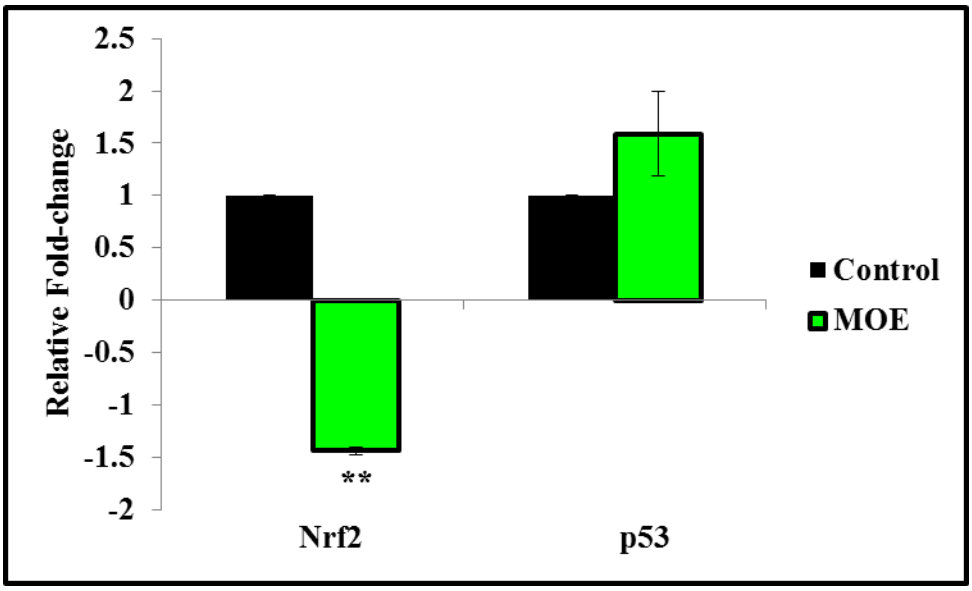

Figure 4 The effect of MOE on mRNA expression.

MOE regulated the *Nrf2* and *p53* mRNA expression in A549 cells after treatment for 24h (**$p <$ 0.001).

The *Nrf2* mRNA expression was decreased 1.44 ± 0.03-fold ($p < 0.001$) in MOE treatment (Figure 4). A 1.59 ± 0.41-fold ($p = 0.168$) increase in *p53* mRNA expression was observed in MOE treated cells.

Discussion

MO, a widely consumed traditional plant, is used to treat various ailments such as cancer [13]. Cancer is listed as the fourth leading cause of death in SA [3], with lung cancer expected to increase. This is a first study to show a possible biochemical mechanism of action of MOE on cancerous A549 cells.

Reactive oxygen species are known to induce many diseases [32]. These oxidants damage membrane phospholipids and results in lipid peroxidation [2, 27]. This study showed that MOE significantly increased lipid peroxidation as measured by elevated levels of MDA. This lipid peroxidation compromises cell membranes and their function. In addition, the mitochondrial membranes may become dysfunctional and lead to uncoupling of oxidative phosphorylation and

increased electron leak from the respiratory chain. These oxidants also react with proteins and DNA in the cell [33].

Hydrogen peroxide (H_2O_2) oxidises cysteine in GSH to produce glutathione disulphide (GSSG), thereby decreasing the antioxidant capacity of GSH. GSH levels were significantly decreased in MOE-treated A549 cells with a corresponding significant increase in lipid peroxidation (Figure 1).

The mRNA plays a pivotal role in protein synthesis as it is used as a template and thus translated into protein [34]. The transcription factor nuclear factor-erythroid 2 p45-related factor 2 (Nrf2) is important in antioxidant defence as it protects the cell from oxidative stress. Nrf2 dissociates from Kelch-like epichlorohydrin-associated protein 1 (Keap1) and translocates to the nucleus and binds to the antioxidant-response elements in promoter regions of antioxidant genes thus increasing transcription [35, 36]. Nrf2 regulates the synthesis of GSH and MOE reduced mRNA expression by 1.44-fold (Figure 4) [34]. This resulted in a significant decrease in Nrf2 protein expression in A549 cells, (Figure 3) which leads to decreased transcription of important antioxidant genes and increased oxidative damage [37]. The suppression of Nrf2 expression may explain the antiproliferative effect of MOE in this cell line. A consequence is that the endogenous antioxidant GSH is not replenished adequately and will result in increased oxidants and ultimately to cell death.

The increase in oxidative stress is genotoxic to the cell. H_2O_2 can react with metal ions such as iron and produce highly reactive hydroxyl radicals that target DNA [22]. ROS-mediated DNA damage can be a therapeutic target in cancer cells as it signals nucleases to cause DNA strand breaks. The MOE induced significant DNA strand breaks and fragmentation in the alveolar epithelial cells (Figure 2). Again this finding shows that MOE possess pro-apoptotic and antiproliferative properties.

To further confirm the pro-apoptotic action of MOE, we investigated its effect on *p53* mRNA and protein expression. MOE increased *p53* mRNA expression (Figure 4) with a significant increase in the expression of p53 protein in A549 treated cells (Figure 3). It is known that an increase in oxidative stress and DNA damage results in apoptosis [38, 39]. DNA damage up-regulates signals for repair and apoptosis. The increased expression of p53 correlates well with the increased DNA damage by MOE. This signals for apoptosis via Bax activation, a pro-apoptotic protein, which causes mitochondrial depolarisation and cytochrome c release from the

mitochondria into the cytoplasm. Cytochrome c, together with Apaf-1 and ATP forms an apoptosome resulting in pro-caspase-9 cleavage and activation of caspase-9. MOE significantly increased (1.28-fold) caspase-9 activity, which in turn activates the executioner caspases-3/7 (1.52-fold increase) (Table 3). Caspase-3/7 activity can be inhibited by inhibitor of apoptosis (IAP) proteins [40, 41]. The protein, Smac/DIABLO is concurrently released from the mitochondria with cytochrome c and inhibits IAP proteins thus ensuring execution of apoptosis. MOE afforded a slight increase on Smac/DIABLO expression (1.06-fold) [Figure 3 (1.509 ± 0.055 RBD vs control: 1.425 ± 0.007 RBD, $p = 0.162$)] that could contribute to the apoptotic pathway.

In addition PARP-1 cleavage was investigated. During apoptosis, caspases are activated resulting in the cleavage of PARP-1 [6]. PARP-1, a nuclear enzyme, is proteolysed to an 89 KDa C-terminal catalytic fragment and a 24 KDa N-terminal DNA-binding domain fragment [42]. PARP-1 (important in DNA base excision repair) maintains the integrity of the genome [43]. MOE increased caspase-3/7 activity in A549 cells which resulted in cleavage of PARP-1 into 2 fragments [44]. There was a significant (1.46-fold) increase in the expression of the 24 KDa fragment (Figure 3) in MOE treated cells. This increased cleavage of the smaller PARP-1 fragment correlates well with the increased DNA damage by MOE ($p < 0.0001$).

The phytoconstituents of MOE were shown to possess antiproliferative effects on various cell lines [20]. The leaves contain glucosinolates, isothiocyanates, niazimicin, niaziminin and quercetin which attributes to the anticancer effect [11, 20, 21]. In addition the leaves also contain other thiocarbamate, carbamates and nitrile glycosides [20].

A recent study showed the significance of MO phytochemicals in prostate cancer therapy [21]. Niazimicin and 4-(4’-O-acetyl-α-L-rhamnopyranosyloxy) benzyl isothiocyanate were identified as natural anticancer agents and compared favourably with the recommended chemotherapeutic drug, Estramustine. These phytochemicals enhanced the activity of cellular prostatic acid phosphatase and possessed less toxicity, thus showing potential as a potent and safe natural agent in prostate cancer therapy and drug design [21]. Similarly these active compounds in MOE can act as anticancer agents in lung cancer by inducing cellular apoptosis and subsequent cell death.

An *in vivo* study on the anticancer activity of MOE on B16 F10 melanoma tumors in mice, revealed that treatment at 500mg/kg-bw could delay tumor growth and increase lifespan [20].

The anticancer activity was attributed to the phytochemicals quercetin, niazimicin and niaziminin. The therapeutic and nutritional use of MOE is safe at doses below 2g/kg-bw [45]. Similarly the antiproliferative effect of MOE observed in the A549 cancerous cells may be due to the phytochemicals (e.g., isothiocyanates, niazimicin, niaziminin and quercetin) in the plant leaves.

Conclusion

The MO leaves possess antiproliferative properties as evidenced by an increase in oxidative stress leading to apoptosis of lung cancer cells. The results from the study provide a biochemical mechanism underlying the usage of MOE as a therapeutic agent in lung cancer therapy. It shows a promising complementary and alternative treatment for lung cancer. Furthermore, phytochemical analysis (Appendix 3) and the effect of MOE on other cancerous cell lines need to be assessed.

Abbreviations

BSA	Bovine serum albumin
CCM	Complete culture media
cDNA	Copy DNA
DMSO	Dimethyl sulphoxide
EtBr	Ethidium bromide
GST	Glutathione-S-transferase
GSH	Glutathione
GSSG	Glutathione disulphide
HIV	Human immunodeficiency virus
HRP	Horse radish peroxidase
H_2O_2	Hydrogen peroxide
IAP	Inhibitor of apoptosis
Keap1	Kelch-like epichlorohydrin-associated protein 1
LMPA	Low melting point agarose
MDA	Malondialdehyde
mRNA	Messenger RNA
MO	*Moringa oleifera*
MOE	MO leaf extract
MTT	Methyl thiazol tetrazolium
Nrf2	Nuclear factor-erythroid 2 p45-related factor 2

OD	Optical density
PARP-1	Poly (ADP ribose) polymerase-1
ROS	Reactive oxygen species
RT	Room temperature
RLU	Relative light units
RBD	Relative band density
SA	South Africa
SD	Standard deviation
TBARS	Thiobarbituric acid assay
TBA/BHT	Thiobarbituric acid (1%)/0.1 mM butylated hydroxytoluene solution
qPCR	Quantitative polymerase chain reaction

Competing interest

The authors declare that they have no competing interests.

Authors' contributions

CT conceived the study, designed and conducted all laboratory experiments; analysed and interpreted experimental results and prepared the draft manuscript. AP participated in laboratory experiments. AP and AC participated in the study design, data analysis and manuscript preparations. All authors read and approved the final manuscript.

Acknowledgements

Miss C. Tiloke acknowledges the prestigious Masters scholarship from the National Research Foundation, South Africa. The study was also supported by the funds from College of Health Sciences (UKZN).

Author details

Discipline of Medical Biochemistry, School of Laboratory Medicine and Medical Sciences, College of Health Sciences, University of KwaZulu-Natal, Durban, South Africa

References

1. *GLOBOCAN 2008 estimated cancer incidence, mortality, prevalence and disability-adjusted life years (DALYs) worldwide in 2008.* http://globocan.iarc.fr/.

2. Rahman I: **Oxidative stress, chromatin remodeling and gene transcription in inflammation and chronic lung diseases.** *J Biochem Mol Biol* 2003, **36:**95-109.

3. Bello B, Fadahun O, Kielkowski D, Nelson G: **Trends in lung cancer mortality in South Africa: 1995-2006.** *BMC Public Health* 2011, **11:**1-5.

4. Sharma H, Parihar L, Parihar P: **Review on cancer and anticancerous properties of some medicinal plants.** *J Med Plant Res* 2011, **5:**1818-1835.

5. Fan TJ, Han LH, Cong RS, Liang J: **Caspase family proteases and apoptosis.** *Acta Biochim Biophys Sin (Shanghai)* 2005, **37:**719-727.

6. Radhakrishna Pillai G, Srivastava AS, Hassanein TI, Chauhan DP, Carrier E: **Induction of apoptosis in human lung cancer cells by curcumin.** *Cancer Lett* 2004, **208:**163-170.

7. Nithipongvanitch R, Ittarat W, Velez JM, Zhao R, St Clair DK, Oberley TD: **Evidence for p53 as guardian of the cardiomyocyte mitochondrial genome following acute adriamycin treatment.** *J Histochem Cytochem* 2007, **55:**629-639.

8. Halappanavar SS, Le Rhun Y, Mounir S, Martins LM, Huot J, Earnshaw WC, Shah GM: **Survival and proliferation of cells expressing caspase-uncleavable poly (ADP-ribose) polymerase in response to death-inducing DNA damage by an alkylating agent.** *J Biol Chem* 1999, **274:**37097-37104.

9. Frunze P, Hamed D, Abdo H, Timothy S: **Targeted therapy for lung cancer.** *Anti-Cancer Drugs* 2012, **23:**1016-1021.

10. Gericke N, Albrecht CF, Van Wyke B, Mayeng B, Mutwa C, Hutchings A: ***Sutherlandia frutescens.*** *Am J Men's Health* 2001, **13:**9-15.

11. Fahey JW: ***Moringa oleifera:*** **a review of the medical evidence for its nutritional, therapeutic, and prophylactic properties.** Part 1. *Trees Life J* 2005:1-5.

12. Goyal BR, Agrawal BB, Goyal RK, Mehta AA: **Phyto-pharmacology of*Moringa oleifera Lam.*** An overview. *Nat Prod Rad* 2007, **6:**347-353.

13. Djakalia B, Guichard BL, Soumaila D: **Effect of *Moringa oleifera* on growth performance and health status of young post-weaning rabbits.** *Res J Poultry Sci* 2011, **4:**7-13.

14. Sreelatha S, Jeyachitra A, Padma PR: **Antiproliferation and induction of apoptosis by *Moringa oleifera* leaf extract on human cancer cells.** *Food Chem Toxicol* 2011, **49:**1270-1275.

15. Cajuday LA, Pocsidio GL: **Effects of *Moringa oleifera Lam*. (Moringaceae) on the reproduction of male mice (*Musmusculus*).** *J Med Plants Res* 2010, **4:**1115-1121.

16. Siddhuraju P, Becker K: **Antioxidant properties of various solvent extracts of total phenolic constituents from three different agroclimatic origins of drumstick tree (*Moringa oleifera Lam.*) leaves.** *J Agric Food Chem* 2003, **51:**2144-2155.

17. Manguro LOA, Lemmen P: **Phenolics of *Moringa oleifera* leaves.** *Nat Prod Res* 2007, **21:**56-68.

18. Guevara AP, Vargas C, Sakurai H, Fujiwara Y, Hashimoto K, Maoka T, Kozuka M, Ito Y, Tokuda H, Nishino H: **An antitumor promoter from *Moringa oleifera Lam*.** *Mutat Res* 1999, **440:**181-188.

19. Anwar F, Latif S, Ashraf M, Gilani AH: ***Moringa oleifera*: a food plant with multiple medicinal uses.** *Phytother Res* 2007, **21:**17-25.

20. Purwal L, Pathak AK, Jain UK: ***In vivo* anticancer activity of the leaves and fruits of *Moringa oleifera* on mouse melanoma.** *Pharmacology online* 2010, **1:**655-665.

21. Inbathamizh L, Padmini E: **Insilico studies on the enhancing effect of anti-cancer phytochemicals of *Moringa oleifera* on cellular prostatic acid phosphatase activity.** *Drug Invent Today* 2011, **3:**186-192.

22. Sreelatha S, Padma PR: **Modulatory effects of *Moringa oleifera* extracts against hydrogen peroxide-induced cytotoxicity and oxidative damage.** *Hum Exp Toxicol* 2011, **30:**1359-1368.

23. Wilson K, Walker J: *Principles and techniques of biochemistry and molecular biology.* Cambridge, England: Cambridge University Press; 2005.

24. Phulukdaree A, Moodley D, Chuturgoon AA: **The effects of *Sutherlandia frutescens* extracts in cultured renal proximal and distal tubule epithelail cells.** *S Afri J Sci* 2010, **106:**1-5.

25. Prasad TNVKV, Elumalai EK: **Biofabrication of Ag nanoparticles using *Moringa oleifera* leaf extract and their antimicrobial activity.** *Asian Pacific J Trop Biomed* 2011:439-442.

26. Mossman T: **Rapid colorimetric assay for cellular growth and survival: application to proliferation and cytotoxicity assay.** *J Immunol Methods* 1983, **65:**55-63.

27. Halliwell B, Chirico S: **Lipid peroxidation: its mechanism, measurement and significance.** *Am J Clin Nutrit* 1993, **57:**715S-725S.

28. Singh NP, McCoy MT, Tice RR, Schneider EL: **A simple technique for quantitation of low levels of DNA damage in individual cells.** *Exp Cell Res* 1988, **1751:**184-191.

29. Bainor A, Chang L, McQuade TJ, Webb B, Gestwicki JE: **Bicinchoninic acid (BCA) assay in low volume.** *Anal Biochem* 2011, **410:**310-312.

30. Yang Y, Ma H: **Western blotting and ELISA techniques.** *Research* 2009, **1:**67-86.

31. Livak KJ, Schmittgen TD: **Analysis of relative gene expression data using real-time quantitative PCR and the $2^{-\Delta\Delta CT}$ method.** *Methods* 2001, **25:**402-408.

32. Ashok Kumar N, Pari L: **Antioxidant action of *Moringa oleifera Lam*. (drumstick) against antitubercular drugs induced lipid peroxidation in rats.** *J Med Food* 2003, **6:**255-259.

33. Bartosz G: **Reactive oxygen species: destroyers or messengers?** *Biochem Pharmacol* 2009, **77:**1303-1315.

34. Cooper GM: *The cell. A molecular approach.* Boston, USA: Sunderland: Sinauer Associates; 2000.

35. Harvey CJ, Thimmulappa RK, Singh A, Blake DJ, Ling G, Wakabayashi N, Fujii J, Myers A, Biswal S: **Nrf2-regulated glutathione recycling independent of biosynthesis is critical for cell survival during oxidative stress.** *Free Radic Biol Med* 2009, **46:**443-453.

36. Singh A, Misra V, Thimmulappa RK, Lee H, Ames S, Hoque MO, Herman JG, Baylin SB, Sidransky D, Gabrielson E, Brock MV, Biswal S: **Dysfunctional KEAP1-NRF2 interaction in non-small-cell lung cancer.** *PLoS Med* 2006, **3:**1865-1876.

37. Lewis KN, Mele J, Hayes JD, Buffenstein R: **Nrf2, a guardian of healthspan and gatekeeper of species longevity.** *Integr Comp Biol* 2010, **50:**829-843.

38. Bertram JS: **The molecular biology of cancer.** *Mol Aspects Med* 2001, **21:**167-223.

39. Thompson CB: **Apoptosis in the pathogenesis and treatment of disease.** *Science* 1995, **267:**1456-1462.

40. Hengartner MO: **The biochemistry of apoptosis.** *Nature* 2000, **407:**770-776.

41. Wang X: **The expanding role of mitochondria in apoptosis.** *Genes Dev* 2001, **15:**2922-2933.

42. D'Amours D, Sallmann FR, Dixit VM, Poirier GG: **Gain-of-function of poly (ADP-ribose) polymerase-1 upon cleavage by apoptotic proteases: implications for apoptosis.** *J Cell Sci* 2001, **114:**3771-3778.

43. Eustermann S, Videler H, Yang J, Cole PT, Gruszka D, Veprintsev D, Neuhaus D: **The DNA-binding domain of human PARP-1 interacts with DNA single-strand breaks as a monomer through its second zinc finger.** *J Mol Biol* 2011, **407:**149-170.

44. Pagano A, Pitteloud C, Reverdin C, Metrailler-Ruchonnet I, Donati Y, Argiroffo CB: **Poly (ADP-ribose) polymerase activation mediates lung epithelial cell death *in vitro* but is not essential in hyperoxia-induced lung injury.** *Am J Respir Cell Mol Biol* 2005, **33:**555-564.

45. Adedapo AA, Mogbojuri OM, Emikpe BO: **Safety evaluations of the aqueous extract of the leaves of *Moringa oleifera* in rats.** *J Med Plants Res* 2009, **3:**585-591.

Chapter 3

The antiproliferative effect of *Moringa oleifera* crude aqueous leaf extract on human oesophageal cancer cells

Charlette Tiloke[1], Alisa Phulukdaree[2] and Anil A. Chuturgoon[1]*

[1]*Discipline of Medical Biochemistry and Chemical Pathology, School of Laboratory Medicine and Medical Sciences, College of Health Sciences, University of KwaZulu-Natal, Private Bag 7, Congella, Durban 4013, South Africa*

[2]*Department of Physiology, School of Medicine, Faculty of Health Sciences, University of Pretoria, Pretoria, South Africa*

Charlette Tiloke[1] e-mail: 208501101@stu.ukzn.ac.za

Dr Alisa Phulukdaree[2] e-mail: alisa.phulukdaree@up.ac.za

Professor Anil A. Chuturgoon[1]* - Corresponding author e-mail: chutur@ukzn.ac.za

Tel: +27 31 260 4404
Fax: +27 31 260 4785

Running title: *Moringa oleifera* induce cancer cell death

Journal of Medicinal Food, 2015. *In press*. (Manuscript number JMF-2015-0113)

Abstract

Oesophageal cancer (OC) is commonly diagnosed in South Africa (SA) with high incidences occurring in SA's black population. *Moringa oleifera* (MO), a multipurpose tree, is used traditionally for its nutritional and medicinal properties. It has been used for the treatment of a variety of ailments including cancer.

Aim: We investigated the antiproliferative effect of MO crude aqueous leaf extract (MOE) in a cancerous oesophageal cell line (SNO).

Methods: SNO cells and normal peripheral blood mononuclear cells (PBMCs) were exposed to a range of MOE dilutions to evaluate cytotoxicity (MTT assay). Oxidative stress and DNA fragmentation was determined using TBARS, GSH and comet assay respectively. Apoptosis was then determined by measuring phosphatidylserine (PS) externalisation (flow cytometry), caspase-3/7, -9 activity and ATP levels (luminometry). Protein expression of Nrf2, p53, Smac/DIABLO and PARP-1 was determined by western blotting, whilst *Nrf2* and *catalase* mRNA levels were assessed by qPCR.

Results: MOE was only cytotoxic in SNO cancer cells (IC_{50}: 389.2µg/ml, 24h) causing a significant increase in lipid peroxidation, DNA fragmentation and significantly decreasing GSH levels. Both *catalase* and *Nrf2* protein and mRNA levels were significantly decreased. The induction of apoptosis was confirmed by the significant increase in PS externalisation, caspase-9, caspase-3/7 (p = 0.22) activities and significant decrease in ATP levels. Further, MOE significantly increased the expression of p53, Smac/DIABLO and cleavage of PARP-1, resulting in an increase in the 24kDa fragment.

Conclusion: MOE possesses antiproliferative effects in SNO cancer cells by increasing oxidative stress, DNA fragmentation and inducing apoptosis.

Keywords: Apoptosis, DNA fragmentation, Oxidative stress, Nrf2, SNO cancer cells

Introduction

Cancer is one of the leading causes of global mortality with oesophageal cancer (OC) being ranked the sixth most common cause of death[1]. Cancer cells do not undergo apoptosis as they continue to divide and proliferate[2]. The apoptotic machinery maintains homeostasis and is composed of the intrinsic and extrinsic pathways regulated by caspases[3]. Disruptions to this machinery is the hallmark of cancer pathogenesis[3]. In developing countries such as South Africa (SA), the burden of cancer continues to increase[4]. Oesophageal cancer is most common in black men in SA and the increased prevalence may be due to presence of mycotoxins such as Fumonisin B1 in staple foods such as maize[5, 6]. The increased risk in the ethnic population may

be attributed to diet and lifestyle such as excessive consumption of home-made beer (brewed from fungal contaminated maize) and maize products. Family history, tobacco smoking, dietary deficiencies and chronic alcohol consumption contributes to the aetiology of OC[1, 7].

The incidence of OC in black South Africans are suggested to be associated with high intake of linoleic acid via maize consumption[6]. Sammon and Alderson., 1998 showed that linoleic acid increases prostaglandin E_2 (PGE_2) levels which inhibits gastric acid secretion and affects pyloric and oesophageal sphincters[8]. This causes hypochlorhydric duodenogastro-oesophageal reflux altering pH levels rendering inhibition of protease activity and function and non-breakdown of growth factors. This may contribute to carcinogenesis as cell signal transduction increases causing cell proliferation and tumour progression.

Studies on high OC risk populations have shown that individuals from the rural areas in Transkei and KwaZulu-Natal (SA) have poorer diets and lack basic health care[9]. They often rely on traditional plants which are readily available as food sources and treatment of various ailments including cancer. *Moringa oleifera* (MO; Family: Moringaceae) commonly known as the Drumstick tree is indigenous to India and also found throughout SA[10-12]. Almost all parts of the tree possess nutritional and medicinal properties however the leaves are suggested to be the highest containing vitamins, minerals, iron, essential amino acids and proteins. Several studies have shown that MO leaves possess antioxidant, anticancer properties and used in treatment of diabetes mellitus and liver diseases[10, 12, 13]. Phytochemical analysis showed the presence of bioactive compounds such as flavonoids, glucosinolates, isothiocyanates, niazimicin and gallic acid which possess anticancer effects[10-12, 14]. Current cancer therapies are expensive and often lead to drug resistance; therefore alternative, cost effective, traditional based treatment is being investigated. This study investigated the antiproliferative effect of MO crude aqueous leaf extract in cancerous oesophageal SNO cells.

Materials and Methods

Materials

Moringa oleifera leaves were collected from the KwaZulu-Natal region (Durban, SA) and verified by the herbarium (Batch no. CT/1/2012, Genus no. 3128). SNO cells were purchased from Highveld Biologicals (Johannesburg, SA). Cell culture reagents were purchased from Whitehead Scientific (Johannesburg, SA). ECL-LumiGlo® chemiluminescent substrate kit was purchased from Gaithersburg (USA) and western blot reagents were purchased from Bio-Rad (USA). All other reagents were purchased from Merck (SA).

Leaf extract

The MO leaf extract (MOE) was prepared by crushing 10g of air-dried leaves in a pestle and mortar with subsequent addition of 100ml de-ionised water[15-17]. The resultant extract was boiled with continuous stirring (20min), transferred to 50ml conical tubes and centrifuged [720xg, 10min, room temperature (RT)]. The upper aqueous layer (MOE) was removed, lyophilised and stored (4°C). MOE stock solution was prepared (1mg MOE in 1ml CCM) and filter sterilised [0.22µM filter (Millipore)].

Peripheral blood mononuclear cell extraction

Whole blood was obtained from a healthy male donor on three independent occasions and the peripheral blood mononuclear cells (PBMCs) were isolated from heparinised whole blood by differential centrifugation [Ethical approval from the University of KwaZulu-Natal Biomedical Research Ethics Committee (Reference number: BE057/15) and informed consent was obtained]. Briefly, 5ml of whole blood was layered onto equivolume Histopaque 1077 (Sigma, Germany) in 15ml conical tubes and centrifuged (400xg, 30min, RT). The buffy coat layer containing PBMCs were aspirated into sterile 15ml conical tubes and washed twice in 0.1M phosphate buffered saline (PBS) (400xg, 10min). Cell numbers were then enumerated using trypan blue.

Cell culture and exposure protocol

SNO cells were cultured in $25cm^3$ culture flasks (37ºC, 5% CO_2) in complete culture media (CCM) comprising of Eagle's minimum essential medium supplemented with 10% foetal calf serum, 1% L-glutamine and 1% penicillin-streptomycin-fungizone[18]. Isolated PBMCs were cultured at 37ºC with 5% CO_2 in Roswell park memorial institute (RPMI) medium 1640 supplemented with 10% foetal calf serum, 1% L-glutamine and 1% penicillin-streptomycin-fungizone[18]. SNO cells were grown to 90% confluency and treated with MOE; 20,000 cells per sample in all luminometric and colorimetric assays, 1,000,000 cells for flow cytometric analysis and 2,500,000 cells for western blot and qPCR analysis were used. Three experiments were conducted per assay.

Cell viability assay

SNO and PBMCs cell viability was determined using the 3-(4, 5-Dimethyl-2-thiazolyl)-2, 5-diphenyl-2H-tetrazolium bromide (MTT) assay[19]. Cells (20,000cells/well) were seeded into a 96-well microtitre plate. The cells were incubated with varying MOE dilutions (0.1-10mg/ml) in six replicates (300µl/well) and incubated (37ºC, 5% CO_2) for 24h. Control cells were incubated

with CCM only. A CCM/MTT salt solution (5mg/ml) was added (120µl/well) and the plate was incubated (37ºC, 4h). Thereafter, supernatants were removed; dimethyl sulphoxide (DMSO) 100µl/well was added and incubated (1h). The optical density of the formazan product was measured (570/690nm) using a spectrophotometer (Bio Tek µQuant). The results were expressed as percentage cell viability relative to the control. This experiment was repeated on three separate occasions before the concentration of half the maximum inhibition (IC_{50}) of MOE for the cells (SNO and PBMCs) were determined. Due to minimal toxicity observed in PBMCs, all other experiments were conducted on SNO cells to determine the mechanism of cell death.

Lipid peroxidation - quantification of malondialdehyde (MDA)

Thiobarbituric acid (TBARS) assay was used to assess reactive oxygen species (ROS) by measuring MDA, end product of lipid peroxidation[20]. Following treatment, cells were lysed in 0.2% H_3PO_4 (100µl) by passing the cell solution through a 25 gauge needle at least 25x and was transferred to test tubes with addition of 2% H_3PO_4 (200µl), 7% H_3PO_4 (400µl) and TBA/BHT solution (400µl). A positive control of MDA and a negative control of CCM were prepared. All samples were adjusted to pH 1.5 and heated (100°C, 15min). After cooling, butanol (1.5ml) was added, vortexed and allowed to separate into distinct phases. The upper butanol phase (800µl) was transferred into eppendorfs and centrifuged (17,949xg, 6min, RT). 100µl from each sample was added to a 96-well microtitre plate in six replicates. The optical density was measured on a spectrophotometer (532/600nm). The mean optical density was calculated, divided by the absorption coefficient (156mM-1) and expressed in µM.

Glutathione (GSH) quantification

Glutathione-Glo™ Assay (Promega) was used according to manufacturer's guidelines to quantify reduced GSH levels. 50µl from each sample (MOE treated and untreated control) was added in six replicates to the wells of an opaque polystyrene 96-well microtitre plate. GSH standards (0-50µM) were prepared from a 5mM stock diluted in de-ionised water. 50µl of each GSH standards and 50µl of the GSH-Glo™ Reagent 2X was added per well and incubated in the dark (30min, RT). Reconstituted Luciferin Detection Reagent (50µl) was added per well and incubated (15min, RT). The luminescence was measured on a Modulus™ microplate luminometer (Turner Biosystems, Sunnyvale, USA). The data was analysed and expressed in µM from the linear equation generated from the standard curve.

DNA damage

DNA damage was determined using the Comet assay[21]. Three slides per sample were prepared as the first layer of 1% low melting point agarose (LMPA, 37°C), second layer of 25µl of cells (20,000) from the samples with 175µl of 0.5% LMPA (37°C) and third layer of 0.5% LMPA (37°C) covered the slides. After solidification, the slides were then submerged in cold lysing solution [2.5M NaCl, 100mM EDTA, 1% Triton X-100, 10mM Tris (pH 10), 10% DMSO] and incubated (4°C, 1h). Following incubation the slides were placed in electrophoresis buffer [300mM NaOH, 1mM Na2EDTA (pH 13)] for 20min and thereafter subjected to electrophoresis (25V, 35min, RT) using Bio-Rad compact power supply. The slides were washed 3x with neutralisation buffer [0.4M Tris (pH 7.4)] (5min each). The slides were stained overnight (4°C) [40µl ethidium bromide (EtBr)] and viewed with a fluorescent microscope (Olympus IXSI inverted microscope with 510-560nm excitation and 590nm emission filters). Images of 50 cells and comets were captured per treatment and the comet tail lengths were measured using Soft imaging system (Life Science - ©Olympus Soft Imaging Solutions v5) and expressed in µm.

Assessment of phosphatidylserine (PS) externalisation

The Annexin-V-Fluos assay (Roche) was used to detect PS externalisation, an early marker of apoptosis. 100µl of each sample (1,000,000cells/tube) were transferred to polystyrene flow cytometry tubes, stained with 100µl annexin-V-Fluos labelling solution and incubated in the dark (15min, RT). 400µl of Annexin-V Binding buffer (1x) was added and the labelled cells were detected by fluorescence-activated cell sorting (FACS) Calibur flow cytometer (BD Biosciences, SA). The cells were gated to exclude cellular debris using FlowJo v7.1 software (Tree Star Inc., Ashland, USA). Approximately 50,000 events were obtained and the data was analysed using CellQuest PRO v4.02 software (BD Biosciences, SA). The data was expressed as relative fold change.

ATP quantification

The CellTitre-Glo® assay (Promega) was used to quantify ATP levels. SNO cells (20,000cells/well) were seeded into an opaque polystyrene 96-well microtitre plate in six replicates. Following treatment, the CellTiter-Glo® Reagent 2X was prepared according to manufacturer's guidelines and 100µl of the reagent was added per well. The plate was then incubated in the dark (30min, RT). Following incubation, the plate was read on the ModulusTM microplate luminometer. The data was expressed as RLU and fold change.

Caspase-9 and 3/7 activities

Caspase-Glo® 9 and Caspase-Glo® 3/7 Assays (Promega) were used to assess apoptosis. For each assay the same procedure was followed: SNO cells were seeded into an opaque polystyrene 96-well microtitre plate in six replicates. Following treatment, the Caspase-Glo® 9 and Caspase-Glo® 3/7 reagents were prepared according to manufacturer's guidelines. 100µl of the reagent was added per well and incubated in the dark (30min, RT). Following incubation, the luminescence was measured on a Modulus™ microplate luminometer. The data was expressed as RLU and fold change.

Western blotting

Western Blotting assessed Nrf2, p53, Smac/DIABLO and PARP-1 protein expression. Briefly, total protein was isolated using Cytobuster™ reagent supplemented with protease inhibitor (Roche, cat. no. 05892791001) and phosphatase inhibitor (Roche, cat. no. 04906837001). The bicinchoninic acid assay (Sigma, Germany) was used for protein quantification and was standardised to 1mg/ml[22]. The samples were prepared in Laemmli buffer[23], boiled (100ºC, 5min) and electrophoresed (150V, 1h) in 7.5% sodium dodecyl sulfate polyacrylamide gels using Bio-Rad compact power supply. The separated proteins were electro-transferred to nitrocellulose membrane using the Trans-Blot® Turbo Transfer system (Bio-Rad) (20V, 45min). The membranes were blocked (1h) using 3% bovine serum albumin (BSA) in Tris-buffered saline containing 0.5% Tween20 (TTBS - NaCl, KCL, Tris, Tween 20, dH2O, pH 7.4). Thereafter, the membranes were immune-probed with primary antibody [Nrf2 (ab89443), p53 (ab26), PARP-1 (ab110915), 1:1000; Smac/DIABLO (ab68352), 1:200] at 4ºC overnight. The membranes were washed 4x (TTBS, 10min each) and incubated with secondary antibody (ab97046; 1:2,000) at RT (1h). The membranes were washed 4x (TTBS, 10min each). To correct for loading error and normalise protein expression, β-actin was assessed (ab8226; 1:2,000). Horseradish peroxidase chemiluminescence detector and enhancer solution was used and the signal was detected with Alliance 2.7 image documentation system (UViTech). Protein expression were analysed with UViBand Advanced Image Analysis software (UViTech, v12.14). The data expressed as relative band density (RBD) and fold change.

Quantification of mRNA

To determine *Nrf2* and *catalase* mRNA levels in SNO cells, RNA was first isolated from the control and MOE treatment by adding 500µl Tri reagent (Life technologies Am9738) as per manufacturer's guidelines. Thereafter, RNA was quantified (Nanodrop 2000) and standardised to 1000ng/µl. RNA was reverse transcribed by reverse transcriptase into copy DNA (cDNA)

using the iScript™ cDNA synthesis kit (Bio-Rad, SA, cat. no. 1708891) as per manufacturer's instructions. Briefly, a 20µl reaction was prepared by adding 4µl 5x iScript reaction mix, 1µl iScript reverse transcriptase, 12µl nuclease free water, 3µl RNA template. The reaction was then subjected to 25°C (5min), 42°C (30min), 85°C (5min) and a final hold at 4°C [CFX96 Real Time thermal cycler (Bio-Rad, SA)] to obtain cDNA.

Quantitative PCR (qPCR) was used to determine mRNA levels using iQ Superscript reagent (Bio-Rad, SA). A 25µl reaction consisting of 12.5µl IQ™ SYBR® green supermix (Bio-Rad, SA, cat. no. 170-8880), 8.5µl nuclease free water, 2µl cDNA, and 1µl sense and anti-sense primer (10µM, Inqaba Biotec, SA, Table 1) were used. The mRNA levels was compared and normalised to a housekeeping gene, *GAPDH*. The reaction was subjected to an initial denaturation (95°C, 8min). It was followed by 40 cycles of denaturation (95°C, 15s), annealing (*Nrf2*, *catalase*: 58°C, 40s) and extension (72°C, 30s) [CFX96 Real Time thermal cycler (Bio-Rad, SA)]. The data was analysed using CFX Manager™ software V3.0 (Bio-Rad, SA). The mRNA levels were determined using the Livak method and expressed as fold changes[24].

Table 1: Primer sequences used in qPCR assay

	Primer sequence	
	Sense Primer	**Anti-sense Primer**
Nrf2	5′ AGTGGATCTGCCAACTACTC 3′	5′ CATCTACAAACGGGAATGTCTG 3′
Catalase	5′ TAAGACTGACCAGGGCATC 3′	5′ CAAACCTTGGTGAGATCGAA 3′
GAPDH	5′ TCCACCACCCTGTTGCTGTA 3′	5′ ACCACAGTCCATGCCATCAC 3′

Statistical analysis

Statistical analyses were performed using GraphPad Prism v5.0 software (GraphPad Software Inc., La Jolla, USA). The results were expressed as means with standard error of the mean (SEM). The statistical significances were determined by student *t*-test with 95% confidence interval. The data were considered statistically significant with a value of $p < 0.05$.

Results

Cell viability assay

MOE induced a dose-dependent decline in SNO cell viability and an IC_{50} value of 389.2µg/ml was obtained and used in all subsequent assays (Figure 1). MOE showed a proliferative effect in normal healthy PBMCs (Figure 1) and an IC_{50} was not determined.

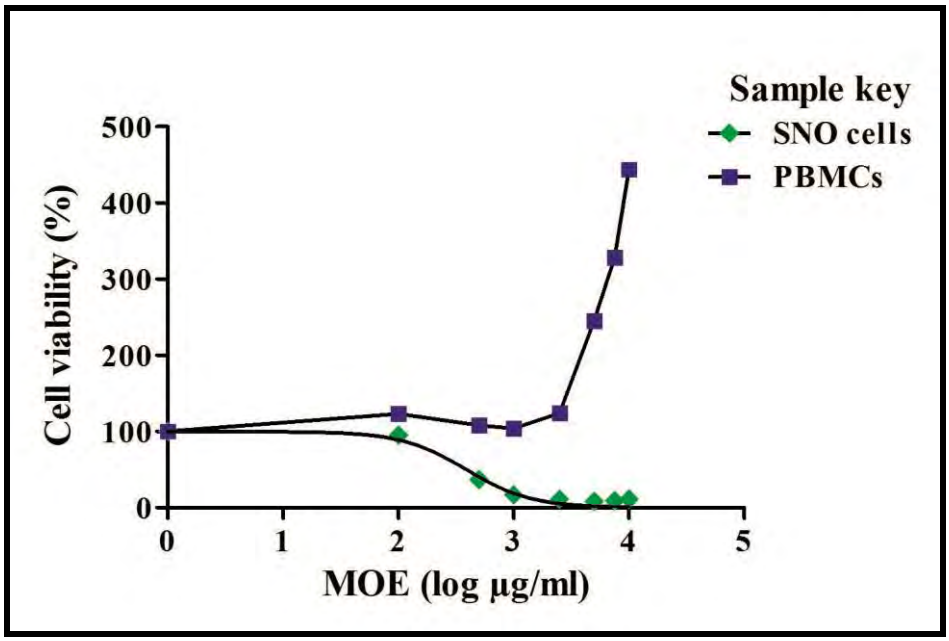

Figure 1: % SNO and normal PBMCs cell viability after exposure to MOE for 24h

Oxidative stress

The TBARS assay was used to measure MDA levels (a measure of lipid peroxidation). A significant increase in MDA levels was seen in the MOE treatment (0.09 ± 0.01µM vs control: 0.07 ± 0.00µM; *$p < 0.05$) (Figure 2A).

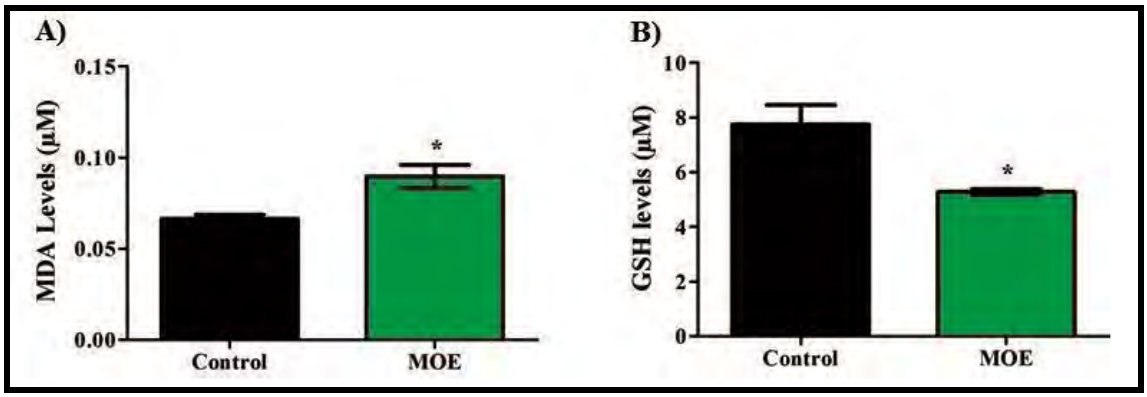

Figure 2: Oxidative stress in SNO cells after exposure to MOE for 24h (*$p < 0.05$)

Further the antioxidant, GSH, was significantly decreased as compared to the untreated control (5.28 ± 0.12µM vs 7.75 ± 0.71µM; *$p < 0.05$) (Figure 2B).

DNA Damage

The comet assay showed MOE was genotoxic as observed by the significantly increased DNA fragmentation in SNO cells compared to the untreated control (Figure 3; 46.09 ± 0.77 vs 21.44 ± 0.36; ***$p < 0.0001$).

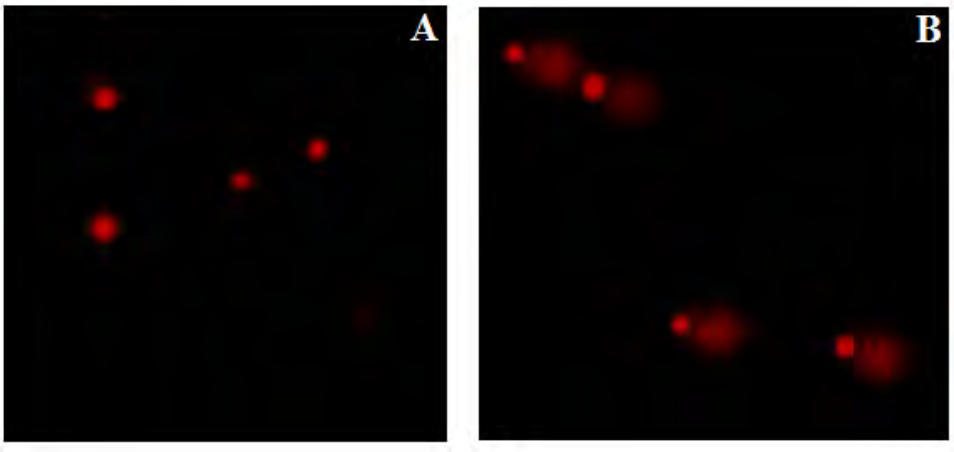

Figure 3: Comet assay images of control (A) and MOE treated (B) SNO cells for 24h (***$p <$ 0.0001, 100x)

Assessment of apoptosis

The effect of MOE on apoptotic markers i.e. PS externalisation, caspase activity and ATP levels was determined (Table 2).

Table 2: Apoptotic markers in SNO cells after treatment with MOE for 24h

	Mean ± SEM		
	Control	MOE	*p*-value
PS externalisation (relative fold change)	1	2.52	<0.0001***
ATP (x10^5 RLU)	69.82 ± 1.43	50.29 ± 0.53	<0.0001***
Caspase-9 (x10^5 RLU)	29.19 ± 0.57	32.72 ± 0.80	<0.05*
Caspase-3/7 (x10^5 RLU)	2.31 ± 0.03	2.51 ± 0.11	0.22

***$p < 0.0001$, *$p < 0.05$: significantly different compared to the control, SEM: standard error of the mean, RLU: relative light units, PS: phosphatidylserine

A significant increase in PS externalisation was seen in the MOE treated cells. In addition, an increase in caspase-9 (1.12-fold) and caspase-3/7 (1.09-fold) activity was noted. There was a

significant 1.39-fold decrease in cellular ATP levels in the MOE treatment compared to the untreated control.

Western Blotting

The protein levels of Nrf2, p53, Smac/DIABLO and PARP-1 was assessed using western blotting (Figure 4).

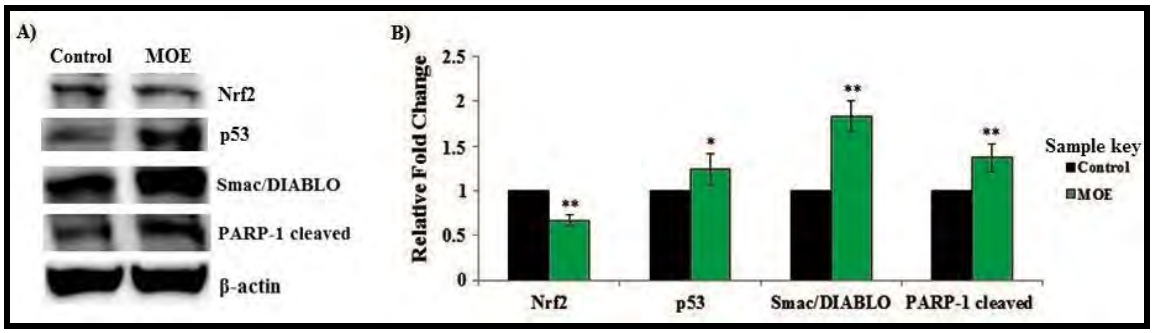

Figure 4: Protein levels (A) and the relative fold change (B) in SNO cells after exposure to MOE for 24h (**$p < 0.001$, *$p < 0.05$)

Exposure to MOE caused a significant 1.49-fold decrease in Nrf2 levels (0.18 ± 0.02 RBD vs control: 0.27 ± 0.01 RBD, **$p < 0.001$) (Figure 4). There was a 1.24-fold increase in p53 levels compared to the control (0.16 ± 0.00 RBD vs 0.13 ± 0.01, *$p < 0.05$). A 1.82-fold increase in Smac/DIABLO levels in the MOE treated SNO cells was seen (0.45 ± 0.03 RBD vs control: 0.25 ± 0.02 RBD, **$p < 0.001$) (Figure 4). Also, there was a 1.37-fold increase in the levels of cleaved PARP-1 (24kDa fragment) (0.17 ± 0.01 vs control: 0.13 ± 0.00, **$p < 0.001$) (Figure 4).

Quantification of mRNA

The effect of MOE on *Nrf2* and *catalase* mRNA expression was determined using qPCR (Figure 5).

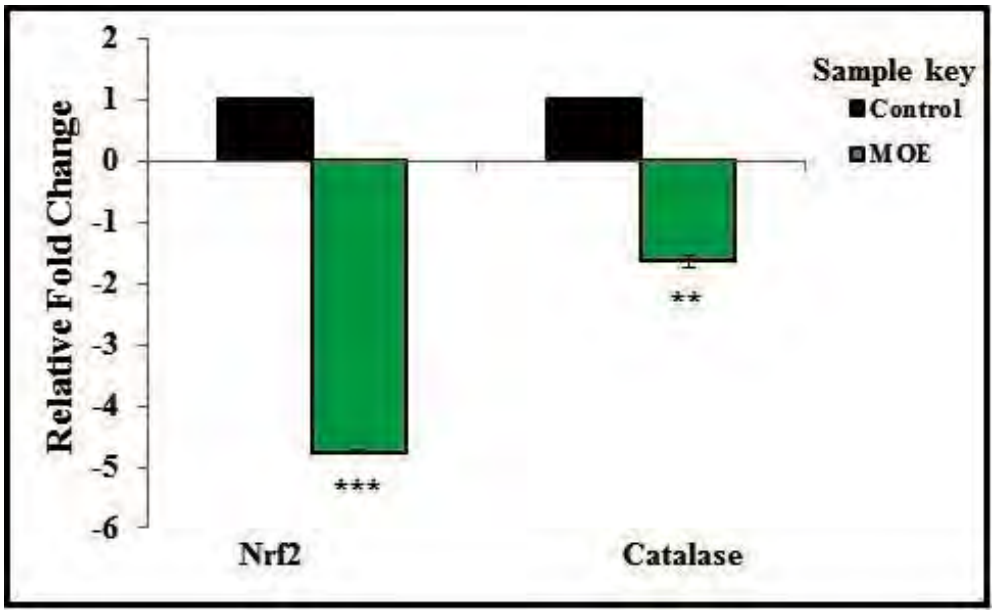

Figure 5: mRNA expression in SNO cells after exposure to MOE for 24h (***$p < 0.0001$, **$p < 0.001$)

A significant 4.76 ± 0.03-fold (***$p < 0.0001$) decrease in *Nrf2* mRNA expression was seen in the MOE treated SNO cells (Figure 5). In addition, *catalase* expression was also decreased by 1.64 ± 0.09-fold (**$p < 0.001$).

Discussion

The balance between cell proliferation and apoptosis is critical for cellular homeostasis[25]. Often in disease states, there is aberration in apoptosis potentially leading to carcinogenesis. Oesophageal cancer is one of the leading causes of cancer mortality[1] in SA. MOE is used traditionally throughout SA for the treatment of various ailments including cancer[10]. MOE caused a dose-dependent decline in SNO cell viability with no cytotoxicity in normal healthy PBMCs (Figure 1). MOE is rich in nutrients with high levels of amino acids and proteins[26, 27]. MOE contains glutamine which can be utilised as an energy source by lymphocytes[28]. The increased rate of the normal PBMCs metabolism/viability may be due to the abundant supply of glutamine. We then investigated the antiproliferative effect of MO crude aqueous leaf extract in SNO oesophageal cancer cells.

Reactive oxygen species (ROS) are countered in cells by the production of antioxidants, however ROS overproduction results in oxidative stress[29]. A chronic increase in oxidative stress has been implicated in damage to proteins, lipids and DNA. Free radicals react with polyunsaturated fatty acids causing lipid peroxidation and damage to cellular membranes. MOE

significantly increased ROS levels evidenced by lipid peroxidation in SNO cells (Figure 2A). Cancer cells have higher metabolic activity[30] therefore exposure to compounds such as MOE which contain polyphenols may increase levels of ROS. Polyphenols present in MOE such as gallic acid possess pro-oxidant properties and induced apoptosis in cancer cell lines[31]. Chlorogenic acid, also a polyphenol present in MOE caused ROS induced apoptosis in K562 leukaemia cells and human oral squamous cell carcinoma[32]. MOE also affected the antioxidant response in SNO cells by significantly decreasing GSH levels (Figure 2B). The transcription factor, nuclear factor-erythroid 2 p45-related factor 2 (Nrf2), regulates cellular antioxidant enzymes by binding to the antioxidant response element (ARE) in the promoter region and increases the transcription of antioxidant and cytoprotective genes[33]. GSH homeostasis is maintained via Nrf2 transcription. MOE significantly decreased both *Nrf2* mRNA (Figure 5) and protein (Figure 4) expression in SNO cancer cells. A consequence of decreased Nrf2 levels will result in inadequately replenished GSH and antioxidant response. *Catalase* mRNA levels were also significantly reduced (Figure 5). An imbalance between ROS and antioxidants in SNO cells resulted in oxidative stress. In addition, highly reactive hydroxyl radicals target DNA and induce damage[34]. A significant increase in DNA fragmentation was observed in MOE treated cells (Figure 3).

The mitochondrion is a source of ROS production[35]. High levels of ROS and oxidative DNA damage signals for p53 induction of apoptosis via the mitochondria (intrinsic apoptotic pathway). MOE significantly increased p53 protein levels (Figure 4) which signals for activation of a pro-apoptotic molecule Bax[36]. Bax activation leads to mitochondrial release of cytochrome c (cyt c) into the cytoplasm, forms an apoptosome with ATP and Apaf-1, causing the cleavage and activation of caspase-9[37]. MOE increased caspase-9 and caspase-3/7 activity (Table 2) suggesting intrinsic pathway of apoptosis. Studies have shown that MOE possess anticancer properties and induced apoptosis in various cancer cell lines[12, 13]. MOE's phytochemical composition showed that it abundantly contains glucosinolates, flavonoids, and phenolic acids[38]. In addition, it also contains niazimicin, 4-(α-L-rhamnopyranosyloxy) benzyl glucosinolate, 4-(α-L-rhamnopyranosyloxy) benzyl isothiocyanate[39], quercetin and kaempferol contributing to the antiproliferative effect we observed in SNO cells[40]. The bioactive compound, gallic acid, have induced apoptosis in 3T3-L1 pre-adipocytes by caspase-9 and -3/7 activation[31]. Gallic acid subsequently caused the cleavage of poly (ADP-ribose) polymerase (PARP-1).

PARP-1 is a DNA repair-associated enzyme that maintains genome integrity[41]. When apoptosis occurs the effector caspase-3/7, is responsible for cleavage of PARP-1 into an 89kDa and

24kDa fragment inhibiting its repair mechanism and cell survival function[41, 42]. MOE caused cleavage of PARP-1 with a significant increase in the 24kDa fragment (Figure 4). This again shows MOE's apoptosis inducing effect in SNO cells. The 24kDa fragment (DNA binding domain) irreversibly binds to DNA stand breaks, preventing repair, ultimately committing to cell death.

Furthermore Smac/DIABLO is concurrently released from the mitochondria which prevents inhibitor of apoptosis proteins (IAP's) from halting the apoptotic machinery. Smac/DIABLO proteins levels were significantly increased (Figure 4) thus allowing the execution of apoptosis. Chlorogenic acid induced ROS production with subsequent release of cyt c and Smac/DIABLO from the mitochondria in K562 leukaemia cells leading to apoptosis[32]. Similarly in SNO cells, the significant increase in expression may be attributed to chlorogenic acid that is present in the crude extract. In addition, MOE increased PS externalisation (2.52-fold) from the inner leaflet to the outer plasma membrane[43].

Charoensin, 2014 showed that MOE possess antiproliferative properties in HepG2, MCF-7, fibroblast cells and induced quinone reductase activity, an anticarcinogenic phase II enzyme[40]. In addition, MOE decreased NFkB signalling and synergistically acted with cisplatin to cause cytotoxicity in pancreatic cancer cells[44]. Studies suggest that the intake of MOE is safe below 2g/kg-bw[45]. Further analysis conducted on the SNO cells treated with MOE over longer time period, 48h and 72h, also showed a dose-dependent decline in cell viability (data not shown) (Appendix 4). Therefore MOE's antiproliferative effect in SNO cells can be attributed to its phytochemical composition.

MOE exerts an antiproliferative effect in SNO cells by inducing the intrinsic apoptotic pathway. The study shows a possible use of MOE in the treatment of oesophageal cancer. However phytochemical analysis (Appendix 3) to identify bioactive compounds will ascertain the antiproliferative effect.

Acknowledgements

Miss C. Tiloke acknowledges the prestigious Doctoral scholarship from the National Research Foundation, SA. The study was also supported by the funds from College of Health Sciences (UKZN).

Author Disclosure Statement

No competing financial interests exist.

References

1. Bravi F, Edefonti V, Randi G, Garavello W, La Vecchia C, Ferraroni M, Talamini R, Franceschi S, Decarli A: Dietary patterns and the risk of esophageal cancer. *Ann Oncol* 2012;23:765-770.
2. Sharma H, Parihar L, Parihar P: Review on cancer and anticancerous properties of some medicinal plants. *J Med Plant Res* 2011;5:1818-1835.
3. Hanahan D, Weinberg RA: Hallmarks of cancer: the next generation. *Cell* 2011;144: 646-674.
4. Jemal A, Bray F, Center MM, Ferlay J, Ward E, Forman D: Global Cancer Statistics. *CA Cancer J Clin* 2011;61:69-90.
5. Dlamini Z, Bhoola K: Esophageal cancer in african blacks of KwaZulu Natal, South Africa: an epidemiological brief. *Ethnic Dis* 2005;15:786-789.
6. Pink RC, Bailey TA, Iputo JE, Sammon AM, Woodman AC, Carter DRF: Molecular basis for maize as a risk factor for esophageal cancer in a South African population via a prostaglandin E2 positive feedback mechanism. *Nutrition and Cancer* 2011;63: 714-721.
7. Segal I, Reinach SG, De Beer M: Factors associated with oesophageal cancer in Soweto, South Africa. *Br J Cancer* 1988;58:681-686.
8. Sammon A, Alderson D: Diet, reflux and the development of squamous cell carcinoma of the oesophagus in Africa. *Br J Surg* 1998;85:891-896.
9. Sewram V, Sitas F, O'Connell D, Myers J: Diet and esophageal cancer risk in the Eastern Cape Province of South Africa. *Nutrition and Cancer* 2014;66:791-799.
10. Dhakar RC, Maurya SD, Pooniya BK, Bairwa N, Gupta MS: Moringa: The herbal gold to combat malnutrition. *Chron young sci* 2011;2:119-125.
11. Fahey JW: *Moringa oleifera*: A review of the medical evidence for its nutritional, therapeutic, and prophylactic properties. part 1. *Trees for Life J* 2005;1-5.
12. Goyal BR, Agrawal BB, Goyal RK, Mahta AA: Phyto-pharmacology of *Moringa oleifera* Lam an overview. *Nat Prod Radiance* 2007;6:347-353.
13. Sreelatha S, Jeyachitra A, Padma PR: Antiproliferation and induction of apoptosis by *Moringa oleifera* leaf extract on human cancer cells. *Food Chem Toxicol* 2011;49;1270-1275.

14. Mishra G, Singh P, Verma R, Kumar S, Srivastav S, Jha KK, Khosa RL: Traditional uses, phytochemistry and pharmacological properties of *Moringa oleifera* plant: An overview. *Der Pharmacia Lettre* 2011;3:141-164.
15. Tiloke C, Phulukdaree A, Chuturgoon AA: The antiproliferative effect of *Moringa oleifera* crude aqueous leaf extract on cancerous human alveolar epithelial cells. *BMC Complement Altern Med* 2013;13:1-8.
16. Phulukdaree A, Moodley D, Chuturgoon AA: The effects of *Sutherlandia frutescens* extracts in cultured renal proximal and distal tubule epithelial cells. *S Afri J Sci* 2010;106,1-5.
17. Prasad TNVKV, Elumalai EK: Biofabrication of Ag nanoparticles using *Moringa oleifera* leaf extract and their antimicrobial activity. *Asian Pac J Trop Biomed 2011*;439-442.
18. Wilson K, Walker J: Principles and techniques of biochemistry and molecular biology. Cambridge University Press, 2005.
19. Mossman T: Rapid colorimetric assay for cellular growth and survival: application to proliferation and cytotoxicity assay. *J Immunol Methods* 1983;65:55-63.
20. Halliwell B, Chirico S: Lipid peroxidation: its mechanism, measurement and significance. *Am J Clin Nutr* 1993;57:715S-725S.
21. Singh NP, McCoy MT, Tice RR, Schneider EL: A simple technique for quantitation of low levels of DNA damage in individual cells. *Exp Cell Res* 1988;1751:184-191.
22. Bainor A, Chang L, McQuade TJ, Webb B, Gestwicki JE: Bicinchoninic acid (BCA) assay in low volume. *Anal Biochem* 2011;410:310-312.
23. Yang Y, Ma H: Western Blotting and ELISA techniques. Researcher 2009;1:67-86.
24. Livak KJ, Schmittgen TD: Analysis of relative gene expression data using real-time quantitative PCR and the 2-ΔΔCt method. *Methods* 2001;25:402-408.
25. Gao T, Furnari F, Newton AC: PHLPP: A phosphatase that directly dephosphorylates Akt, promotes apoptosis, and suppresses tumor growth. *Mol Cell* 2005;18:13-24.
26. Moyo B, Masika PJ, Hugo A, Muchenje V: Nutritional characterization of Moringa (*Moringa oleifera* Lam.) leaves. *Afr J Biotechnol* 2011;10:12925-12933.
27. Ndubuaku UM, Nwankwo VU, Baiyeri KP: Influence of poultry manure application on leaf amino acid profile, growth and yield of moringa (*Moringa oleifera* Lam) plants. *Int J Cur Tr Res* 2013;2:390-396.
28. Roth E, Oehler R, Manhart N, Exner R, Wessner B, Strasser E, Spittler A: Regulative potential of glutamine - relation to glutathione metabolism. *Nutrition* 2002;18:217-221.

29. Jaiswal D, Rai PK, Mehta S, Chatterji S, Shukla S, Rai DK, Sharma G, Sharma B, Khair S, Watal G: Role of *Moringa oleifera* in regulation of diabetes-induced oxidative stress. *Asian Pac J Trop Med* 2013;426-432.
30. Schuck AG, Weisburg JH, Esan H, Robin EF, Bersson AR, Weitschner JR, Lahasky T, Zuckerbraun HL, Babich H: Cytotoxic and proapoptotic activities of gallic acid to human oral cancer HSC-2 cells. *Oxid Antioxid Med Sci* 2013;2:265-274.
31. Verma S, Singh A, Mishra A: Gallic acid: molecular rival of cancer. *Environ Toxicol Pharmacol* 2013;35:473-485.
32. Rakshit S, Mandal L, Pal BC, Bagchi J, Biswas N, Chaudhuri J, Chowdhury AA, Manna A, Chaudhuri U, Konar A, Mukherjee T, Jaisankar P, Bandyopadhyay S: Involvement of ROS in chlorogenic acid-induced apoptosis of Bcr-Abl+ CML cells. *Biochem Pharmacol* 2010;80:1662-1675.
33. Yu S, Khor TO, Cheung K, Wenge L, Wu T, Huang Y, Foster BA, Kan YW, Kong A: Nrf2 expression is regulated by epigenetic mechanisms in prostate cancer of TRAMP mice. *PLoS One* 2010;5:1-9.
34. Sreelatha S, Padma PR: Modulatory effects of *Moringa oleifera* extracts against hydrogen peroxide-induced cytotoxicity and oxidative damage. *Hum Exp Toxicol* 2010;1-10.
35. Bartosz G: Reactive oxygen species: destroyers or messengers? *Biochem pharmacol* 2009;77:1303-1315.
36. Bertram JS: The molecular biology of cancer. *Mol aspects med* 2001;21:167-223.
37. Hengartner MO: The biochemistry of apoptosis. *Nature* 2000;407:770-776.
38. Mbikay M: Therapeutic potential of *Moringa oleifera* leaves in chronic hyperglycemia and dyslipidemia: a review. *Front Phamacol* 2012;3:1-12.
39. Manguro LOA, Lemmen P: Phenolics of *Moringa oleifera* leaves. *Nat Prod Res* 2007;21:56-68.
40. Charoensin C: Antioxidant and anticancer activities of *Moringa oleifera* leaves. *J Med Plants Res* 2014;8:318-325.
41. Halappanavar SS, Le Rhun Y, Mounir S, Martins LM, Huoti J, Earnshaw WC, Shah GM: Survival and proliferation of cells expressing caspase-uncleavable Poly (ADP-ribose) polymerase in response to death-inducing DNA damage by an alkylating agent. *J Biol Chem* 1999;274:37097-37104.
42. Chaitanya GV, Alexander JS, Babu PP: PARP-1 cleavage fragments: signatures of cell-death proteases in neurodegeneration. *Cell Commun Signal* 2010:8:1-11.

43. Schlegel RA, Williamson P: Phosphatidylserine, a death knell. Cell Death Differ 2001;8;551-563.
44. Berkovich L, Earon G, Ron I, Rimmon A, Vexler A, Lev-Ari S: *Moringa oleifera* aqueous leaf extract down-regulates nuclear factor-kappaB and increases cytotoxic effect of chemotherapy in pancreatic cancer cells. *BMC Complement Altern Med* 2013;13:1-7.
45. Adedapo AA, Mogbojuri OM, Emikpe BO: Safety evaluations of the aqueous extract of the leaves of *Moringa oleifera* in rats. *J Med Plants Res* 2009;3:585-591.

Corresponding author: Professor Anil A. Chuturgoon

- Discipline of Medical Biochemistry and Chemical Pathology, School of Laboratory Medicine and Medical Sciences, College of Health Sciences, University of KwaZulu-Natal, Private Bag 7, Congella, Durban 4013, South Africa
- E-mail: chutur@ukzn.ac.za
- Tel: +27 31 260 4404
- Fax: +27 31 260 4785

CHAPTER 4

Moringa oleifera gold nanoparticles modulate oncogenes, tumor suppressor genes and *caspase-9* splice variants in A549 cells

Charlette Tiloke[1], Alisa Phulukdaree[2], Krishnan Anand[3], Robert M Gengan[3] and Anil A. Chuturgoon[1*]

[1]*Discipline of Medical Biochemistry and Chemical Pathology, School of Laboratory Medicine and Medical Sciences, College of Health Sciences, University of KwaZulu-Natal, Private Bag 7, Congella, Durban 4013, South Africa*

[2]*Department of Physiology, School of Medicine, Faculty of Health Sciences, University of Pretoria, Pretoria, South Africa*

[3]*Department of Chemistry, Faculty of Applied Sciences, Durban University of Technology, Durban, 4001, South Africa*

Professor Anil A. Chuturgoon[1*] - Corresponding author email: chutur@ukzn.ac.za

Tel: +27 31 260 4404
Fax: +27 31 260 4785

Running head: Gold nanoparticles induce cancer cell death

Journal of Cellular Biochemistry, 2015.
DOI: 10.1002/jcb.25528

Keywords:

- **Gold nanoparticles**
- ***Moringa oleifera***
- **lung cancer**
- **c-myc**
- **splice variants**
- **apoptosis**

Number of figures: 10

Number of tables: 3

Contract grant sponsor:

- Doctoral scholarship from the National Research Foundation, South Africa.
- University of KwaZulu-Natal College of Health Sciences Scholarship.

Conflict of interest

The authors declare that they have no conflict of interest.

Abstract

Gold nanoparticles (AuNP's) facilitate cancer cell recognition and can be manufactured by green synthesis using nutrient rich medicinal plants such as *Moringa oleifera* (MO). Targeting dysregulated oncogenes and tumor suppressor genes is crucial for cancer therapeutics.

Aim: We investigated the antiproliferative effects of AuNP synthesised from MO aqueous leaf extracts (ML_{AuNP}) in A549 lung and SNO oesophageal cancer cells.

Methods: A one-pot green synthesis technique was used to synthesise ML_{AuNP}. A549, SNO cancer cells and normal peripheral blood mononuclear cells (PBMCs) were exposed to ML_{AuNP} and C_{AuNP} to evaluate cytotoxicity (MTT assay); apoptosis was measured by phosphatidylserine (PS) externalisation, mitochondrial depolarisation ($\Delta\Psi m$) (flow cytometry), caspase-3/7, -9 activity and ATP levels (luminometry). The mRNA expression of *c-myc, p53, Skp2, Fbw7α* and *caspase-9* splice variants was determined using qPCR, whilst relative protein expression of c-myc, p53, SRp30a, Bax, Bcl-2, Smac/DIABLO, Hsp70 and PARP-1 were determined by western blotting.

Results: ML_{AuNP} and C_{AuNP} were not cytotoxic to PBMCs, whilst its pro-apoptotic properties were confirmed in A549 and SNO cells. ML_{AuNP} significantly increased caspase activity in SNO cells while ML_{AuNP} significantly increased PS externalisation, $\Delta\Psi m$, caspase-9, caspase-3/7 activities and decreased ATP levels in A549 cells. Also, p53 mRNA and protein levels, SRp30a (p=0.428), Bax, Smac/DIABLO and PARP-1 24kDa fragment levels were significantly increased. Conversely, ML_{AuNP} significantly decreased Bcl-2, Hsp70, Skp2, Fbw7α, c-myc mRNA and protein levels and activated alternate splicing with *caspase-9a* splice variant being significantly increased.

Conclusion: ML_{AuNP} possesses antiproliferative properties and induced apoptosis in A549 cells by activating alternate splicing of caspase-9.

Introduction

Cancer is the second leading cause of mortality worldwide following cardiovascular disease with approximately 8.2 million cancer deaths (21.7% of noncommunicable diseases) and 14.1 million new diagnoses [Globocan, 2012; Mendis et al., 2014]. Cancer mortality is projected to increase to 12.6 million by year 2030. Lung cancer alone accounts for 1.59 million deaths and is the leading cause of cancer mortality [Globocan, 2012]. Despite major advancements in cancer therapies, it remains incurable and quality of life after diagnosis is reduced [Cheng et al., 2005]. Bello et al. (2011) suggested South Africans are at higher risk of developing lung cancer due to their lifestyle changes and the high burden of infectious diseases [Bello et al., 2011].

Cancer cells are able to proliferate through activation of oncogenes (e.g. c-myc) and inactivation of tumor suppressor genes (e.g. p53) [Bonomi et al., 2013]. Oncogenes and dysregulation of tumor suppressor genes encourage tumor progression. Apoptosis maintains homeostasis and any disruption to this process leads to cancer pathogenesis. c-Myc, a transcription factor, regulates gene expression for cell growth and apoptosis [Chen et al., 2013], whilst Skp2 (S-phase kinase-associated protein 2) and Fbw7 (F-box and WD repeat domain-containing 7) mediate the posttranslational regulation of c-myc. Skp2 also acts as an oncogene and is overexpressed in human cancers [Chen et al., 2013].

Cancer cells metabolic activity are increased enabling them to rapidly divide [Eblen, 2012]. Chemotherapeutic agents are non-specific as they target these rapidly dividing cells at the expense of normal healthy cells [Eblen, 2012]. Differential expression of genes and proteins are seen in chemotherapy resistance. The cellular proteome is a key regulator in chemotherapy. Fundamental processes such as gene expression, mRNA transcription and translation into protein as well as modification and degradation of proteins influence the cellular proteome. In particular, alternate splicing of pre-mRNA also affects the cellular proteome as it determines which variant of the gene is translated, resulting in proteins with differing functional efficacy. For example, the splice variant of caspase-9 has shown that expression of *caspase-9b* inhibits apoptosis and is implicated in chemotherapy resistance [Shultz et al., 2011]. On the other hand, *caspase-9a* expression induces apoptosis and thus regulation of inclusion/exclusion of exon 3, 4, 5, 6 cassette is a determinant of cell fate. This process is often manipulated by cancer cells to ensure their survival [Eblen, 2012].

Emerging cancer therapies such as nanoparticles (NP's) are now being developed to specifically target cancer cells [Zhang et al., 2003]. Nanoparticles have characteristic properties of being very small (1-100nm) [Kumar et al., 2011] and are able to interact with biomolecules both on the cell surface and intracellularly [Cai et al., 2008]. Nanoparticles are useful in anticancer drug delivery systems however, their exact mechanism of action still remains to be elucidated [Kang et al., 2010]. Among the many nanoparticles being developed, studies show that gold nanoparticles (AuNP's) are stable and can easily enter a cell, and are useful in the treatment of rheumatoid arthritis, possess anticancer and antimicrobial properties and have good biocompatibility [Kumar et al., 2011; Siddiqi et al., 2012; Tedesco et al., 2010]. Gold nanoparticles also have therapeutic potential as an anti-HIV agent [Kumar et al., 2011]. The advantage of AuNP's is that they are biologically inert and non-toxic [Lim et al., 2011; Parveen and Roa, 2014] and their use is favoured over toxic silver and cadmium nanoparticles that are

commercially in demand. Nanoparticle properties and applications are due to their size and shape [Xie et al., 2007b; Xie et al., 2009]. Nanoparticles are synthesised chemically or via the use of medicinal plants [Prasad and Elumalai, 2011]. In addition, NP's can be synthesised using biological extracts such as green algae and bovine serum albumin [Xie et al., 2007a; Xie et al., 2007c]. The use of plant extracts to synthesise nanoparticles is recently discovered [Prasad and Elumalai, 2011] and this green chemistry is cost effective and advantageous in large scale production, especially in third world countries [Salamanca-Buentello et al., 2005].

Moringa oleifera (MO) belongs to the family Moringaceae, commonly known as Drumstick tree [Fahey, 2005; Goyal et al., 2007], is indigenous to India and is also found widely in South Africa (SA). Almost all parts of the tree possess medicinal properties however the leaves contain high nutritional source of vitamins, calcium, iron, potassium, proteins and possess antioxidant, anticancer and hepatoprotective properties [Prasad and Elumalai, 2011; Sreelatha et al., 2011]. Due to SA's socio-economic, cultural background and minimal support of basic healthcare in rural areas, MO has been widely used for the treatment and management of malnutrition, diabetes mellitus, cardiovascular and liver diseases amongst several others [Erasto et al., 2005; Goyal et al., 2007]. The leaf extract contain bioactive compounds which aid in its anticancer activity. These compounds include niazimicin, gallic acid, rhamnose, glucosinolates and isothiocyanates [Fahey, 2005; Goyal et al., 2007; Mishra et al., 2011]. Recently, AuNP's of MO flower petals were prepared and showed activity in A549 lung cancer cells [Anand et al., 2014]. Our study now is on the leaf extract which was used in an environmentally friendly synthesis of AuNP's (ML_{AuNP}). We investigated the antiproliferative and apoptosis inducing effects of a novel ML_{AuNP} in cancerous A549 lung cells. It was hypothesized that ML_{AuNP} has an antiproliferative effect by inducing apoptosis in A549 cells as a result of ML_{AuNP} selectively targeting oncogenes and tumor suppressor genes.

Materials & Methods

Materials

Moringa oleifera leaves were collected from the KwaZulu-Natal region (Durban, SA) and verified by the KwaZulu-Natal (SA) herbarium (Batch no. CT/1/2012, Genus no. 3128). Gold (III) chloride trihydrate ($HAuCl_4.3H_2O$) was purchased from Sigma-Aldrich, SA. A549 cells were purchased from Highveld Biologicals (Johannesburg, SA). Cell culture reagents were purchased from Whitehead Scientific (Johannesburg, SA). ECL-LumiGlo® chemiluminescent substrate kit was purchased from Gaithersburg [United States of America (USA)] and western

blot reagents were purchased from Bio-Rad (USA). All other reagents were purchased from Merck (SA).

Synthesis of ML_{AuNP}

A one-pot green synthesis technique was used to synthesise ML_{AuNP} [Anand et al., 2014; Li et al., 2015]. The synthesis and characterization were conducted at Durban University of Technology (Durban, SA). The MO leaf extract was prepared as per Tiloke et al. (2013) [Tiloke et al., 2013]. The resultant extract (5ml) was added to 1mM aqueous gold chloride solution (100ml) and allowed to react at room temperature (RT) for the reduction of Au^{3+} ions to Au. ML_{AuNP} were then characterized and particle size was determined using UV spectrometry and transmission electron microscopy respectively. In addition, further characterisation of the hydrodynamic size and size distribution of the ML_{AuNP} was determined using dynamic light scattering (DLS) and Image J. The Zeta potential of ML_{AuNP} was also assessed.

Synthesis of Trisodium citrate gold nanoparticles (C_{AuNP}) – chemical synthesis method

The synthesis and characterisation were conducted at Durban University of Technology (Durban, SA). A volume of 100ml Au (III) (1.4mM) was used with the addition of 2ml of 0.34M trisodium citrate. This was allowed to stir continuously for the production of C_{AuNP}.

Peripheral blood mononuclear cell extraction

Whole blood was obtained from a healthy male donor and the peripheral blood mononuclear cells (PBMCs) were isolated from heparinized whole blood by differential centrifugation [Ethical approval from the University of KwaZulu-Natal Biomedical Research Ethics Committee (Reference number: BE057/15) and informed consent was obtained]. Briefly, 5ml of whole blood was layered onto equivolume Histopaque 1077 (Sigma, Germany) in 15ml conical tubes and centrifuged (400xg, 30min, RT). The buffy coat layer containing PBMCs were aspirated into sterile 15ml conical tubes and washed twice in 0.1M phosphate buffered saline (PBS) (400xg, 10min). Cell numbers were then enumerated using trypan blue.

Cell culture and exposure protocol

A549 and SNO cells were cultured in $25cm^3$ culture flasks in complete culture media (CCM) comprising of Eagle's minimum essential medium (EMEM) supplemented with 10% foetal calf serum, 1% L-glutamine and 1% penicillin-streptomycin-fungizone [Wilson and Walker, 2005]. Cell growth was monitored and cultures were maintained at 37ºC with 5% CO_2. A549 and SNO cells were grown to 90% confluency and treated with the C_{AuNP} and $ML_{AuNP.}$ Isolated PBMCs

were cultured at 37ºC with 5% CO_2 in Roswell park memorial institute (RPMI) medium 1640 supplemented with 10% foetal calf serum, 1% L-glutamine and 1% penicillin-streptomycin-fungizone [Wilson and Walker, 2005]. Cell density at 20,000 was used per sample in all luminometric and colorimetric assays. A549 cell density at 1,000,000 cells was used for flow cytometric analysis and 2,500,000 cells for western blot and qPCR analysis.

Cell viability assay

The viability of A549, SNO cells and PBMCs after exposure to C_{AuNP} and ML_{AuNP} was determined using the 3-(4, 5-Dimethyl-2-thiazolyl)-2, 5-diphenyl-2H-tetrazolium bromide (MTT) assay [Mossman, 1983]. Cells were seeded into a 96-well microtitre plate (20,000 cells/well). The cells were incubated with varying C_{AuNP} concentrations (1.9 - 475µg/ml) and ML_{AuNP} concentrations (1.575 - 393.83µg/ml) in six replicates (300µl/well) and incubated (37ºC, 5% CO_2) for 24h. Control cells were incubated with CCM only. A CCM/MTT salt solution (5mg/ml) was added (120µl/well) and the plate was incubated (37ºC, 4h). Thereafter, supernatants were removed; dimethyl sulphoxide (DMSO) 100µl/well was added and incubated (1h). The optical density of the formazan product was measured (570/690nm) using a spectrophotometer (Bio-Tek µQuant, USA). The results were expressed as percentage cell viability relative to the control. This experiment was repeated on two separate occasions before the IC_{50} of C_{AuNP} and ML_{AuNP} for the cells (A549, SNO and PBMCs) were determined. Due to minimal toxicity observed in PBMCs, all other experiments were conducted on A549 and SNO cells to determine the mechanism of cell death.

ATP quantification

The CellTitre-Glo® assay (Promega) was used to quantify ATP in samples which is an indication of metabolically active cells. A549 and SNO cells (20,000 cells/well) were seeded into an opaque polystyrene 96-well microtitre plate in six replicates. Following treatment, the CellTiter-Glo® Reagent 2X was prepared according to manufacturer's guidelines and 100µl of the reagent was added per well. The plate was then incubated in the dark (30min, RT). Following incubation, the plate was read on the Modulus™ microplate luminometer. The luminescent signal was measured which is proportional to the amount of ATP present and the data was expressed as RLU and fold change.

Caspase-3/7 and 9 activities

Caspase-Glo® 3/7 and Caspase-Glo® 9 Assays (Promega) were used to assess apoptosis. For each assay the same procedure was followed: A549 and SNO cells (20,000 cells/well) were

seeded into an opaque polystyrene 96-well microtitre plate in six replicates. Following treatment, the Caspase-Glo® 3/7 and Caspase-Glo® 9 reagents were prepared according to manufacturer's guidelines. A volume of 100µl of the reagent was added per well and incubated in the dark (30min, RT). Following incubation, the luminescence was measured on a Modulus™ microplate luminometer. The data was expressed as RLU and fold change.

Assessment of phosphatidylserine externalisation

The Annexin-V-Fluos assay (Roche) was used to detect phosphatidylserine (PS) externalisation. PS is externalised in both apoptotic and necrotic cells and is therefore differentiated by addition of propidium iodide (PI). PI only stains DNA of necrotic cells. A volume of 100µl of each sample (1,000,000 cells/tube) were transferred to polystyrene flow cytometry tubes, stained with 100µl annexin-V-Fluos labelling solution and incubated in the dark (15min, RT). A volume of 400µl of Annexin-V Binding buffer (1x) was added to the samples and the labelled cells were detected by fluorescence-activated cell sorting (FACS) Calibur flow cytometer (BD Biosciences, SA). The cells were gated to exclude cellular debris using FlowJo v7.1 software (Tree Star Inc., Ashland, USA). Approximately 50,000 events were obtained and the data was analyzed using CellQuest PRO v4.02 software (BD Biosciences, SA). The data was expressed as a percentage of apoptotic cells.

Mitochondrial membrane potential

The JC-1 Mitoscreen assay was used to assess mitochondrial membrane potential according to manufacturers' guidelines. A volume of 100µl of each sample (1,000,000 cells/tube) was transferred to polystyrene flow cytometry tubes with the addition of 150µl JC-1 dye and incubated (37ºC, 5% CO_2, 10min). The cells were washed twice with JC-1 wash buffer (1x). Between washes cells were centrifuged (400xg, 5min). Cells were re-suspended in 200µl flow cytometry sheath fluid and labelled cells were detected on FACS Calibur flow cytometer. The cells were gated to exclude cellular debris using FlowJo v7.1 software. 50,000 events were obtained and the data was analyzed using CellQuest PRO v4.02 software. The results were expressed as a percentage of cells containing depolarised mitochondria.

Western blotting

Western Blots were performed to determine the protein levels of c-myc, p53, SRp30a, Bax, Bcl-2, Smac/DIABLO, Hsp70 and PARP-1. Briefly, total protein was isolated using Cytobuster™ reagent supplemented with protease inhibitor (Roche, SA, cat. no. 05892791001) and phosphatase inhibitor (Roche, SA, cat. no. 04906837001). The bicinchoninic acid assay

(Sigma, Germany) was used to quantify the protein and was standardized to 1.066mg/ml [Bainor et al., 2011]. The samples were prepared in Laemmli buffer [Yang and Ma, 2009], boiled (100ºC, 5min) and electrophoresed (150V, 1h) in 7.5% sodium dodecyl sulfate polyacrylamide gels using a Bio-Rad compact power supply. The separated proteins were electro-transferred to nitrocellulose membrane using the Trans-Blot® Turbo Transfer system (Bio-Rad, SA) (20V, 45min). The membranes were blocked (1h) using 3% bovine serum albumin (BSA) in Tris-buffered saline (TTBS - NaCl, KCL, Tris, Tween 20, dH_2O, pH 7.4). Thereafter, the membranes were immune-probed with primary antibody [p53 (ab26), PARP-1 (ab110915), 1:1,500; c-myc (Cell Signaling #9402), SRp30a (PA5-30220), Bax (ab5714), Bcl-2 (Cell Signaling #3869), Hsp70 (BD610607), 1:1,000; and Smac/DIABLO (ab68352), 1:200] at 4ºC overnight. The membranes were then washed 4x with TTBS (10min each) and incubated with secondary antibody [mouse (ab97046), rabbit (sc-2004), 1:2,000] at RT for 1h. The membranes were finally washed 4x with TTBS (10min each). To correct for loading error and to normalise the expression of the proteins, β-actin was assessed (ab8226; 1:2,000). Horseradish peroxidase chemiluminescence detector and enhancer solution was used for the antigen-antibody complex and the signal was detected with the Alliance 2.7 image documentation system (UViTech). The expression of the proteins was analyzed with UViBand Advanced Image Analysis software (UViTech, v12.14). The data was expressed as relative band density (RBD) and fold change.

Quantification of mRNA

To determine *c-myc, p53, skp2* and *Fbw7α* mRNA levels in A549 cells, RNA was first isolated from the control and ML_{AuNP} treatment by adding 500µl Tri reagent (Life technologies Am9738) as per manufacturer's guidelines. Thereafter, RNA was quantified (Nanodrop 2000) and standardized to 600ng/µl. RNA was reverse transcribed by reverse transcriptase into copy DNA (cDNA) using the iScript™ cDNA synthesis kit (Bio-Rad, SA, cat. no. 1708891) as per manufacturer's instructions. Briefly, a 20µl reaction was prepared by adding 4µl 5x iScript reaction mix, 1µl iScript reverse transcriptase, 12µl nuclease free water, 3µl RNA template. The reaction was then subjected to 25°C (5min), 42°C (30min), 85°C (5min) and a final hold at 4°C [CFX96 Real Time thermal cycler (Bio-Rad, SA)] to obtain cDNA.

Quantitative PCR (qPCR) was used to determine mRNA levels using iQ Superscript reagent (Bio-Rad, SA). A 25µl reaction consisting of 12.5µl IQ™ SYBR® green supermix (Bio-Rad, SA, cat. no. 170-8880), 8.5µl nuclease free water, 2µl cDNA, and 1µl sense and anti-sense primer (10mM, Inqaba Biotec, SA, Table 1) were used. The mRNA levels was compared and

normalized to a housekeeping gene, *GAPDH*. The reaction was subjected to an initial denaturation (95°C, 8 min). It was followed by 40 cycles of denaturation (95°C, 15s), annealing (*c-myc, p53, Skp2, Fbw7α:* 56°C, 40s) and extension (72°C, 30s) [CFX96 Real Time thermal cycler (Bio-Rad, SA)]. The data was analyzed using CFX Manager™ software V3.0 (Bio-Rad, SA). The mRNA levels was determined using the Livak method and expressed as fold changes [Livak and Schmittgen, 2001].

Table 1 Primer sequences used in qPCR assay

	Primer sequences	
	Sense Primer	Anti-sense Primer
c-myc	5'-AGCGACTCTGAGGAGGAACAAG-3'	5'-GTGGCACCTCTTGAGGACCA-3'
p53	5'-CCACCATCCACTACAACTACAT-3'	5'-CAAACACGGACAGGACCC-3'
Skp2	5'-TGGGAATCTTTTCCTGTCTG-3'	5'-GAACACTGAGACAGTATGCC-3'
Fbw7α	5'-AGTAGTATTGTGGACCTGCCCGTT-3'	5'-GACCTCAGAACCATGGTCCAACTT-3'
GAPDH	5'-TCCACCACCCTGTTGCTGTA-3'	5'-ACCACAGTCCATGCCATCAC-3'

Alternate splicing of *caspase-9*

To determine the expression of *caspase-9* splice variants, *caspase-9* sense primer (5'-GCTCTTCCTTTGTTCATCTCC-3') and anti-sense primer (5' CATCTGGCTCGGGGTTACTGC 3') (10mM, Inqaba Biotec, SA) were used [Massiello and Chalfant, 2006; Shultz et al., 2011; Shultz et al., 2010]. The reaction was subjected to an initial denaturation (94°C, 8 min). It was followed by 35 cycles (20% of the reverse transcriptase reaction was amplified) of denaturation (94°C, 30s), annealing (caspase-9: 58°C, 30s) and extension (72°C, 1min) [CFX96 Real Time thermal cycler (Bio-Rad, SA)]. The qPCR product was examined on 1.5% agarose gel using Alliance 2.7 image documentation system (UViTech). Densitometric analysis [UViBand Advanced Image Analysis software (UViTech, v12.14)] was conducted to assess *caspase-9a* and *caspase-9b* splice variant. The data was expressed as RBD and ratio of *caspase-9a/caspase-9b*.

Statistical analysis

Statistical analyses were performed using GraphPad Prism v5.0 software (GraphPad Software Inc., La Jolla, USA). The results were expressed as means with standard error of the mean (SEM). The comparisons and statistical significances were determined by unpaired *t*-test and a 95% confidence interval. The data were considered statistically significant with a value of $p < 0.05$.

Results

Phytochemical analysis of *Moringa oliefera* aqueous leaf extract

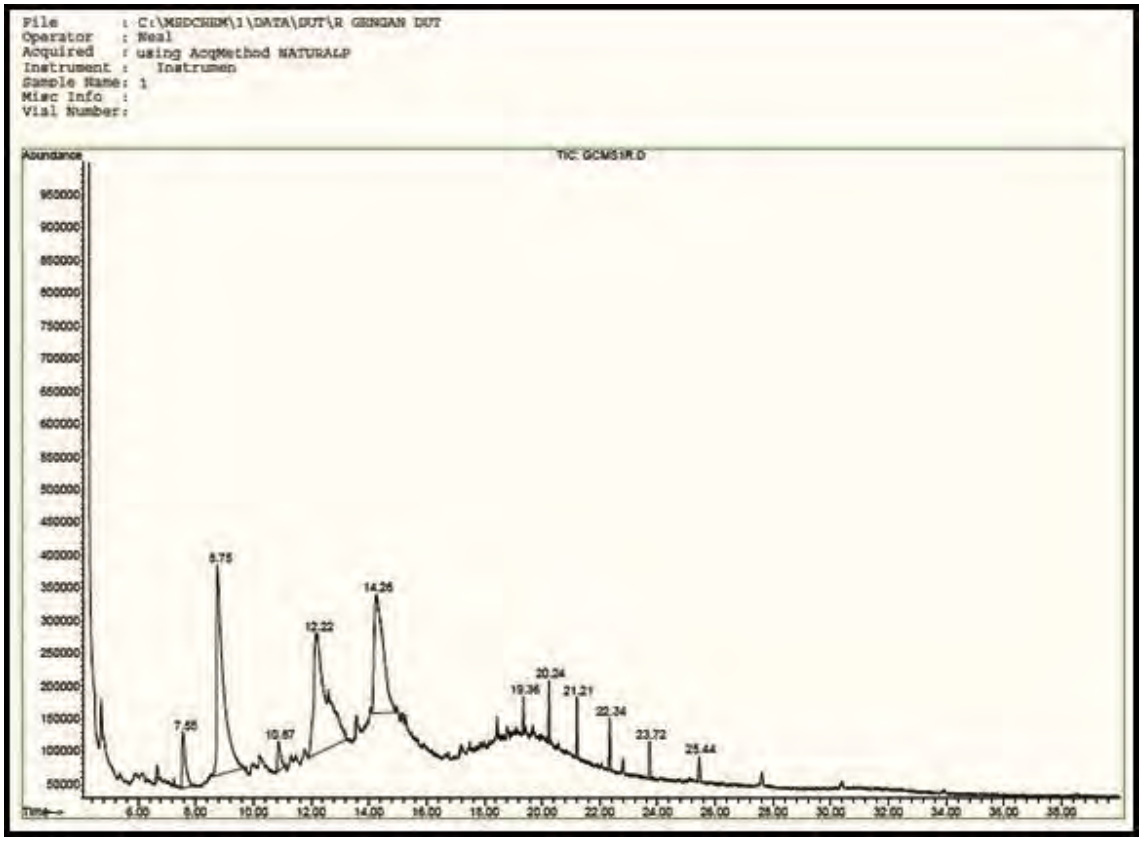

Figure 1 Chemical composition of *Moringa oleifera* aqueous leaf extract by GC-MS analysis

Moringa oleifera aqueous leaf extract showed eleven peaks in the GC-MS chromatogram (Figure 1). The compounds were separated according to their retention time on fused silica capillary column. The total ion chromatogram (TIC) indicates the presence of various organic compounds with significant abundant peaks at retention time 7.55, 8.75, 10.87, 12.22, 14.26, 19.36, 20.24, 21.21, 22.34, 23.72 and 25.44 min having molecular ions (m/z) of 144.0, 126.0,

142.0, 58.0, 60.0, 310.0, 338.0, 352.0, 279.0, 366.0 and 380.0 respectively. These compounds mainly comprised of hydrocarbons and phenolic compounds. Pyran-4-one (7.55), 2-Furancarboxaldehyde (8.75), Docosane (19.36), Tetracosane (21.21), Pentacosane (22.34), Heptacosane (23.72) identified as major chemical constituents followed by Octacosane (25.44) [Al-Owaisi et al., 2014].

Synthesis of ML_{AuNP}

The molar calculation of the crude leaf extract cannot be determined. We synthesised the ML_{AuNP}'s on the basis of weight percent ratios of leaf extract and gold chloride. In the present study - 5g of leaf in 100ml water and 0.0393g of gold chloride in 100ml of water, making the final W% ratio is 5:0.039% [Shankar et al., 2004]

A colour change to red-brown (Figure 2.1) within a few seconds of mixing the leaf extract with the $HAuCl_4$ solution supported the formation of ML_{AuNP}'s. This was attributed to the excitation of surface plasmon vibrations in gold nanoparticles. The observation validated the reduction of Au^{3+} ions to Au by the plant components. The Surface Plasmon Resonance (SPR) is visible as a broad band at λ_{max} 542nm (Figure 2.1), consistent with literature [Stuchinskaya et al., 2011]. The UV-visible absorption spectra of both aqueous leaf extract (Figure 2.2 A) as well as gold chloride solution (Figure 2.2 B) is shown below:

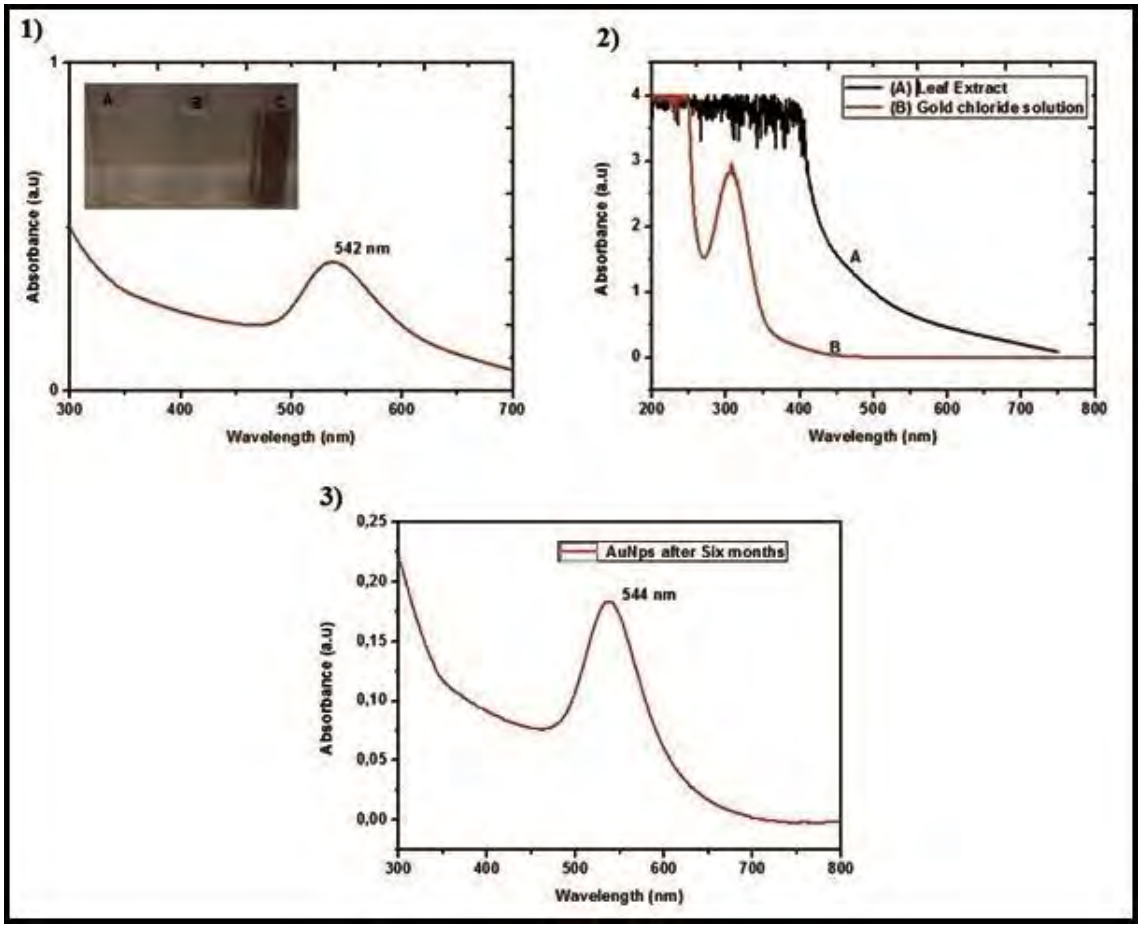

Figure 2 The UV-visible absorption spectra of 1) AuNP's biosynthesised by aqueous leaf extract of *Moringa oleifera* Insert 2.1: The colour change when ML_{AuNP}'s were formed (A) Aqueous leaf extract (B) Gold chloride solution (C) Gold nanoparticles 2) (A) Aqueous leaf extract (B) Gold chloride solution 3) Stability of ML_{AuNP}'s at 544nm UV-visible absorption spectra analysis after six months

The obtained ML_{AuNP}'s dispersion was stable for over six months at room temperature. The peak at 544nm in UV-visible absorption spectra (Figure 2.3) is attributed to the surface plasmon resonance of stable AuNPs. Also, the plasmon band has been sharp and symmetric, which indicates that the solution does not contain much of aggregated particles after six months.

The transmission electron microscopy (TEM) micrographs and size distribution of the ML_{AuNP}'s indicated that most of the particles are spherical or near spherically shaped, however, some polyhedral particles are also present. It was also observed that the ML_{AuNP}'s were highly poly-dispersed in the colloidal solution. ML_{AuNP}'s had a large size distribution (10-20nm) (Figure 3).

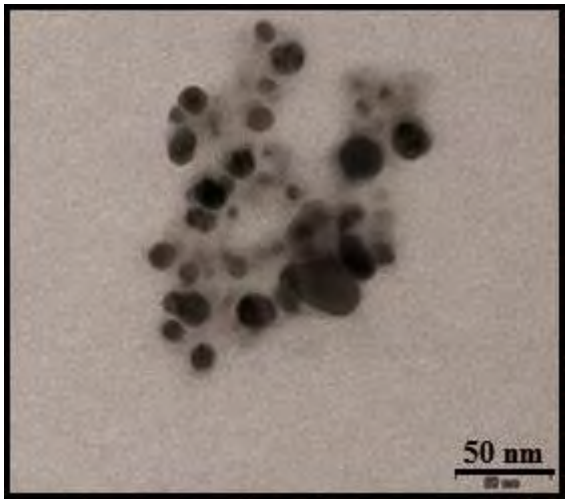

Figure 3 Representative TEM micrograph of ML_{AuNP}'s biosynthesised by aqueous leaf extract of *Moringa oleifera*

The ML_{AuNP} shape was determined to be spherical or near spherical and polyhedral with size of 10-20nm.

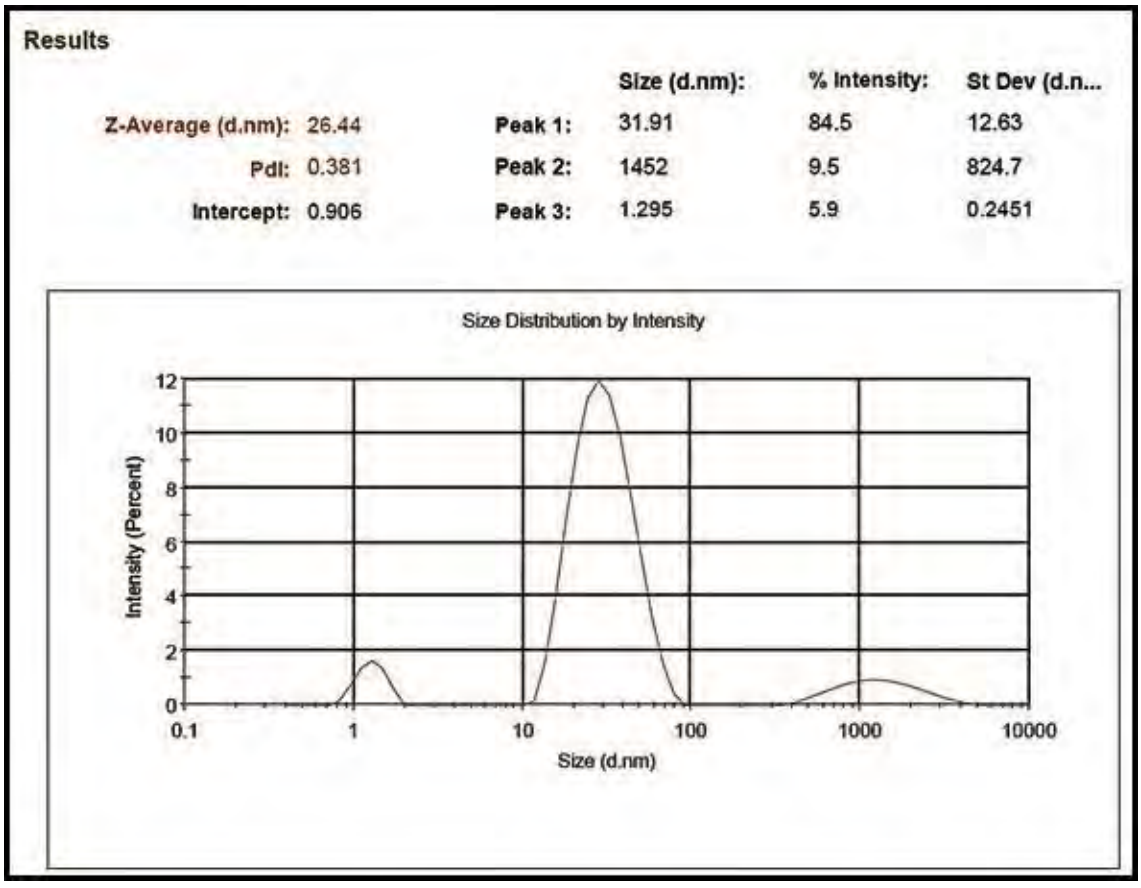

Figure 4 The hydrodynamic size of ML_{AuNP} showed a maximum intensity at 26.44nm as determined by DLS

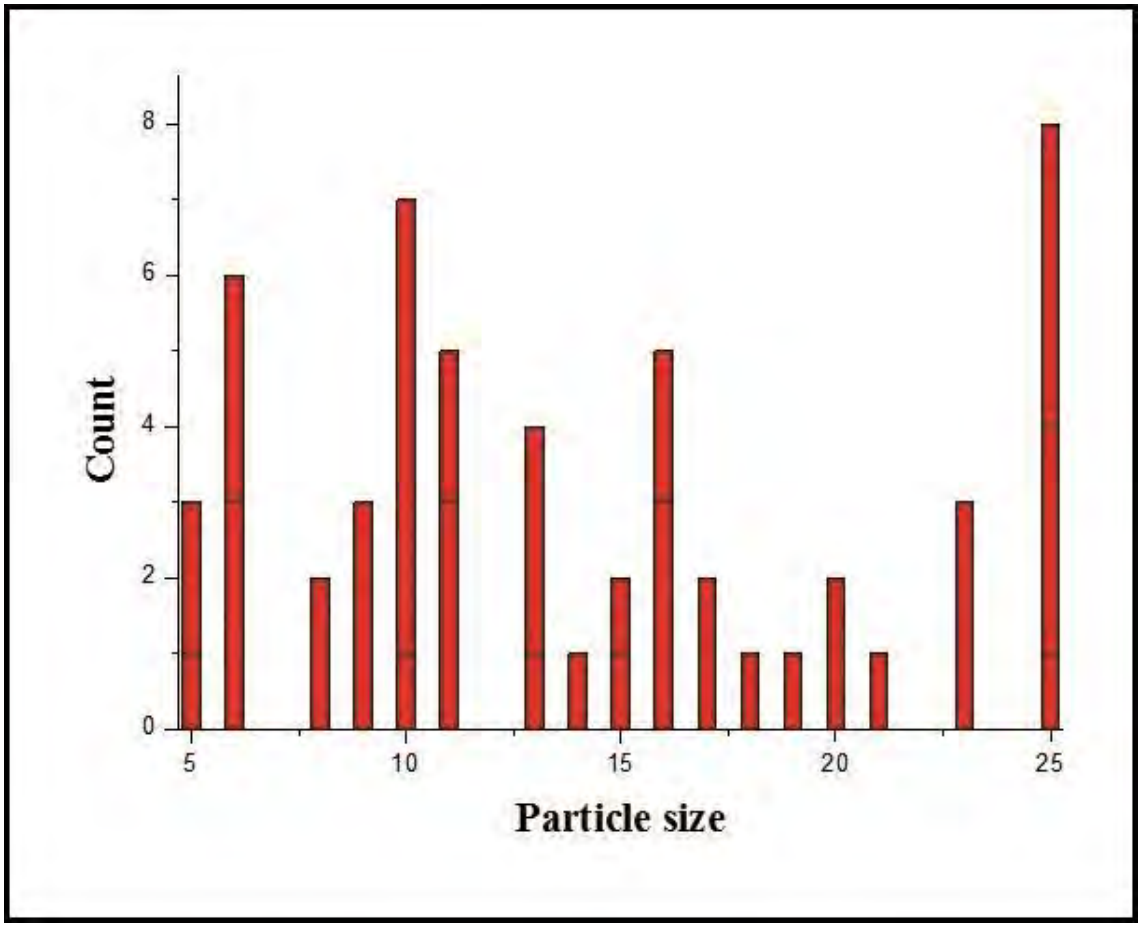

Figure 5 The size distribution of ML_{AuNP} (Image J)

The size distribution of ML_{AuNP} was determined by DLS. The average hydrodynamic size was 26.44nm (Figure 4 and Figure 5) which were similar to *Melia azedarach's* leaf extract [Sukirtha et al., 2012]. The ML_{AuNP} size obtained from TEM and DLS was different. This can be attributed to the different principles applied for determining the size distribution.

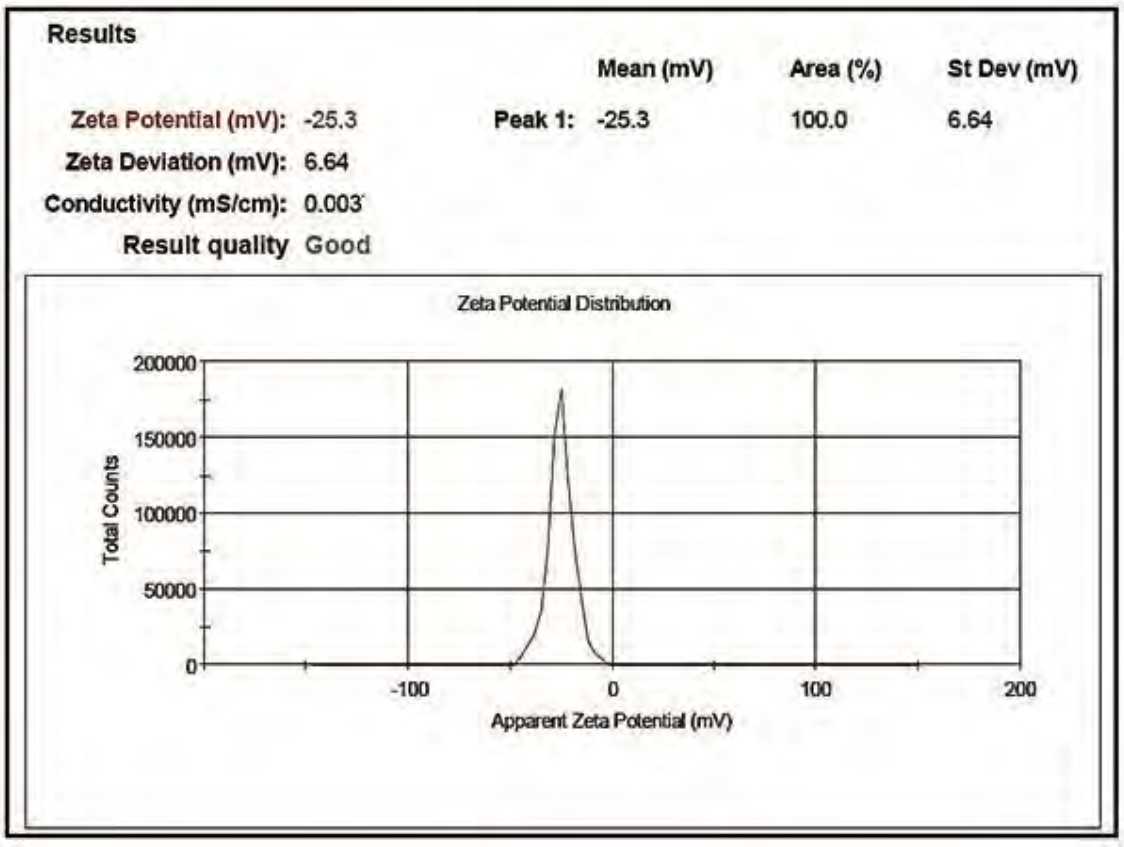

Figure 6 Stability of ML_{AuNP}'s at -25.3mV in zeta potential analysis

Many reports have proposed that surface active molecules can stabilise the nanoparticles and that the reaction of the metal ions is possibly facilitated by reducing sugars and or plant based organic molecules. However, a stable dispersion of particles was evident from the zeta potential of -25.3mV (Figure 6); a zeta potential higher than 30mV or lesser than -30mV is indicative of a stable system [Kotakadi et al., 2014].

Cell viability assay

ML_{AuNP} and trisodium citrate AuNPs (C_{AuNP}) (synthesised by conventional chemical methods) cytotoxicity in A549 lung cancer cells, SNO oesophageal cancer cells and normal healthy PBMCs was then determined using the MTT assay. C_{AuNP} and ML_{AuNP} treatment for 24h caused a dose-dependent decline in A549 and SNO cell viability. C_{AuNP} IC_{50} value was determined as 121.4µg/ml (A549) and 410.4µg/ml (SNO) (Figure 7A). An IC_{50} value of 98.46µg/ml (A549) and 92.01µg/ml (SNO) was calculated for ML_{AuNP} (Figure 7B). Furthermore, C_{AuNP} and ML_{AuNP} showed no cytotoxicity in normal healthy PBMCs (Figure 7A and B respectively) and an IC_{50} value was unable to be determined.

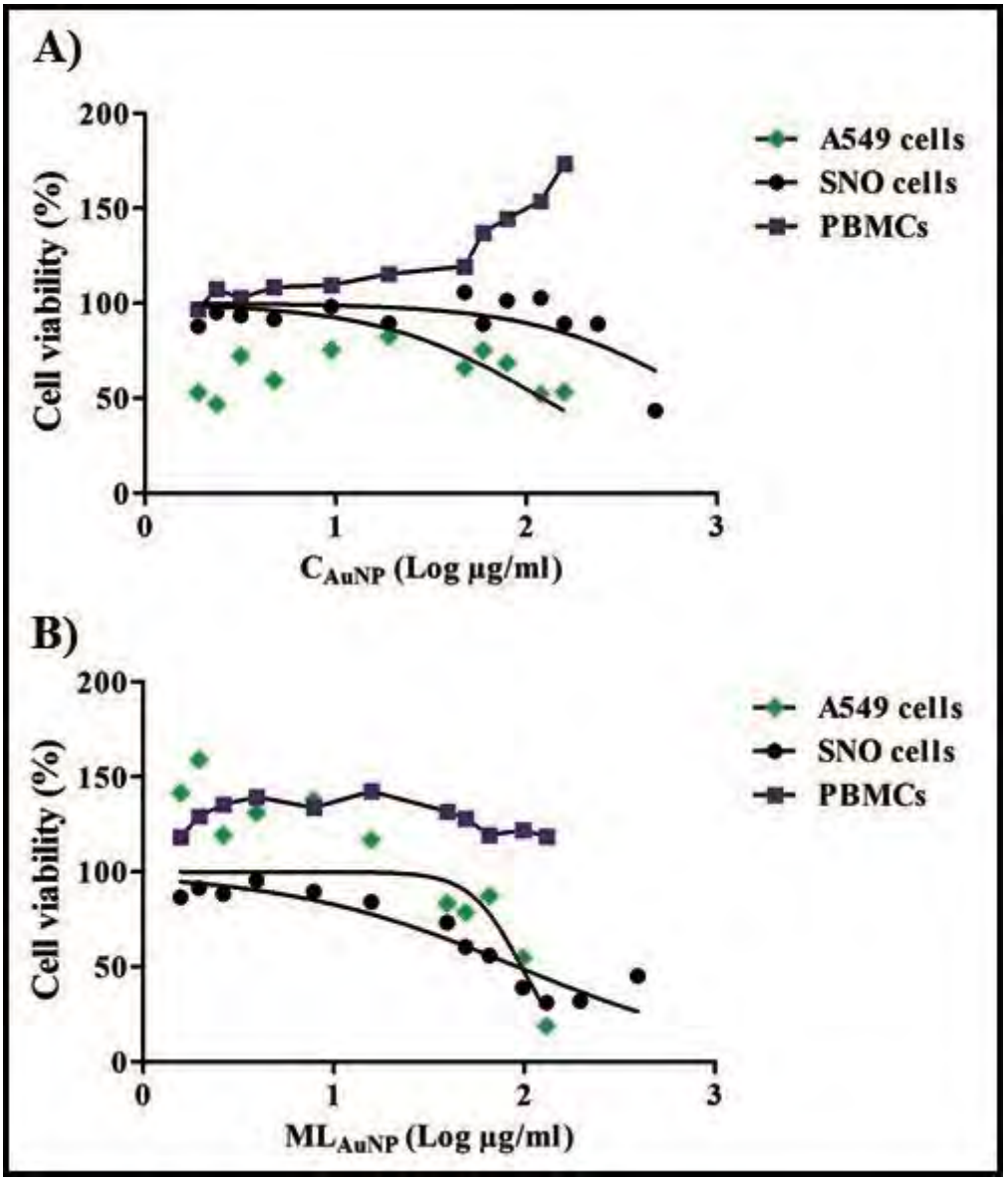

Figure 7 Percentage A549, SNO and PBMCs cell viability after exposure to C_{AuNP} and ML_{AuNP} for 24h

The MTT assay was used to determine A549, SNO and PBMCs cell viability. A dose-dependent decline in A549 and SNO cell viability was observed whereas no cytotoxicity was observed in PBMCs.

Assessment of apoptosis induction

The percentage of apoptosis induced in both A549 and SNO cells by ML_{AuNP} is presented in Table 2 and 3.

Table 2 ATP and caspase activity in A549 and SNO cells following treatment with ML_{AuNP} for 24h

	A549 cells (mean ± SEM)		SNO cells (mean ± SEM)		
	Control	ML_{AuNP}	Control	C_{AuNP}	ML_{AuNP}
ATP ($x10^5$ RLU)	20.47 ± 0.13	17.12 ± 0.33***	33.36 ± 0.44	32.96 ± 0.86	6.61 ± 0.05***
Caspase-3/7 ($x10^5$ RLU)	0.54 ± 0.02	0.73 ± 0.03**	0.02 ± 0.00	0.04 ± 0.00*	0.05 ± 0.00**
Caspase-9 ($x10^5$ RLU)	4.34 ± 0.00	4.94 ± 0.09*	1.96 ± 0.00	1.97 ± 0.04	2.20 ± 0.00*

***$p < 0.0001$, **$p < 0.001$, *$p < 0.05$ *: Significantly different compared to control, SEM: standard error of the mean, RLU: relative light unit

Table 3 Phosphatidylserine externalisation and mitochondrial depolarisation in A549 cells following treatment with ML_{AuNP} for 24h

	A549 cells (mean ± SEM)	
	Control	ML_{AuNP}
PS extenalisation (%)	1.03 ± 0.07	3.99 ± 0.04***
ΔΨm (%)	16.70 ± 0.50	23.90 ± 0.20**

***$p < 0.0001$, **$p < 0.001$, *$p < 0.05$ *: Significantly different compared to control, SEM: standard error of the mean, PS: Phosphatidylserine, ΔΨm: Mitochondrial depolarisation

An early marker of apoptosis is PS externalisation which was significantly increased in A549 cells (3.88-fold, Table 3). ML_{AuNP} altered mitochondrial function by significantly increasing ΔΨm (1.43-fold) and simultaneously decreasing ATP levels (1.20-fold) (Table 2 and 3) in A549 cells. The ATP levels in SNO cells were decreased by C_{AuNP} and ML_{AuNP} (1.01-fold and 5.05-fold respectively) (Table 2). Also, executioner caspase-3/7 (1.34-fold) and initiator caspase-9 (1.14-fold) activities were increased by ML_{AuNP} treatment in A549 cells as compared to the control (Table 2). In addition, C_{AuNP} and ML_{AuNP} increased executioner caspase-3/7 significantly in SNO cells (2-fold and 2.5-fold respectively) (Table 2). Also initiator caspase-9 increased after exposure to C_{AuNP} and ML_{AuNP} in the cancerous SNO cells (1.01-fold and 1.12-fold respectively) (Table 2).

Western Blotting

The protein levels of c-myc, p53, SRp30a, Bax, Bcl-2, Smac/DIABLO, Hsp70 and PARP-1 were assessed using western blot (Figure 8).

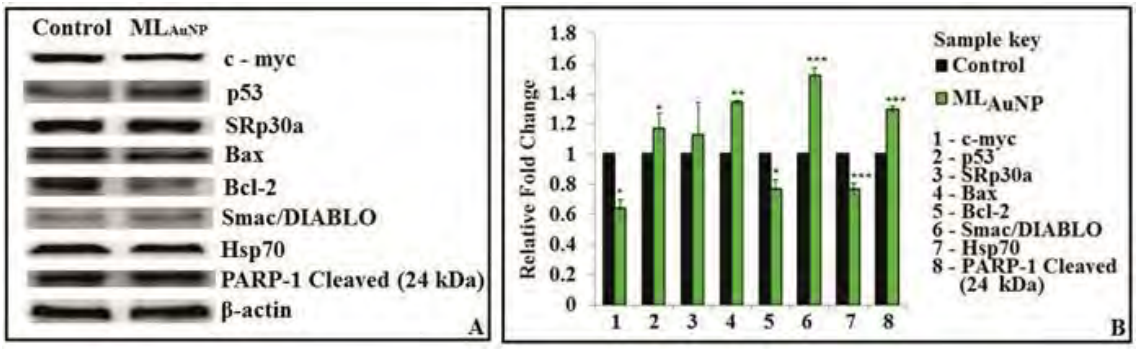

Figure 8 The effect of ML_{AuNP} on protein levels in A549 cells

Western blot analysis of protein levels (A) and the relative fold change (B) in A549 lung cancer cells after exposure to ML_{AuNP} (***$p < 0.0001$, **$p < 0.001$, *$p < 0.05$). Apoptotic proteins were significantly increased with a simultaneous decrease in anti-apoptotic proteins. Protein bands were normalised against β-actin.

Oncogenes such as c-myc are responsible for cell proliferation and tumor progression [Bonomi et al., 2013]. In A549 lung cancer cells, exposure to ML_{AuNP} caused a significant 1.56-fold decrease in c-myc levels (0.04 ± 0.00 RBD vs control: 0.07 ± 0.00 RBD, $p < 0.05$) (Figure 8). This led to the assessment of p53, a tumor suppressor gene which was significantly increased by 1.17-fold (0.13 ± 0.00 RBD vs control: 0.11 ± 0.01, $p < 0.05$) (Figure 8). ML_{AuNP} treated A549 cells further demonstrated a significant increase in pro-apoptotic proteins such as Bax (1.34-fold, 0.12 ± 0.00 RBD vs control: 0.09 ± 0.00 RBD, $p < 0.001$) and Smac/DIABLO levels (1.52-fold, 0.10 ± 0.00 RBD vs control: 0.07 ± 0.00 RBD, $p < 0.0001$) (Figure 8). During apoptosis PARP-1 is cleaved and exposure to ML_{AuNP} caused the cleavage and activation of PARP-1. A 1.30-fold increase in PARP-1 24 kDa fragment was seen (0.23 ± 0.00 RBD vs control: 0.17 ± 0.00 RBD, $p < 0.0001$) (Figure 8). Interestingly, SRp30a, an alternate splicing factor, was increased by 1.13-fold in A549 treated cells (0.05 ± 0.01 RBD vs control: 0.04 ± 0.00 RBD, $p = 0.428$) (Figure 8). In addition, anti-apoptotic Bcl-2 protein was decreased (1.30-fold) by ML_{AuNP} compared to the control (0.11 ± 0.01 RBD vs 0.14 ± 0.01 RBD, $p < 0.05$) (Figure 8). Furthermore Hsp70 was also significantly reduced (1.30-fold, 0.57 ± 0.00 RBD vs control: 0.73 ± 0.02 RBD, $p < 0.0001$) (Figure 8).

Quantification of mRNA

The mRNA levels of *c-myc, p53, skp2* and *Fbw7α* in A549 cells was determined using qPCR relative to the control (Figure 9). The *c-myc* mRNA levels were decreased 1.44 ± 0.05-fold ($p < 0.001$) in ML_{AuNP} treatment (Figure 9). A 1.77 ± 0.12-fold ($p < 0.05$) increase in *p53* mRNA levels was observed in ML_{AuNP} treated cells. *Skp2* levels decreased by 7.33-fold ± 0.01 ($p < 0.0001$) and *Fbw7α* decreased by 2.82-fold ± 0.04 ($p < 0.0001$) in ML_{AuNP} treatment (Figure 9).

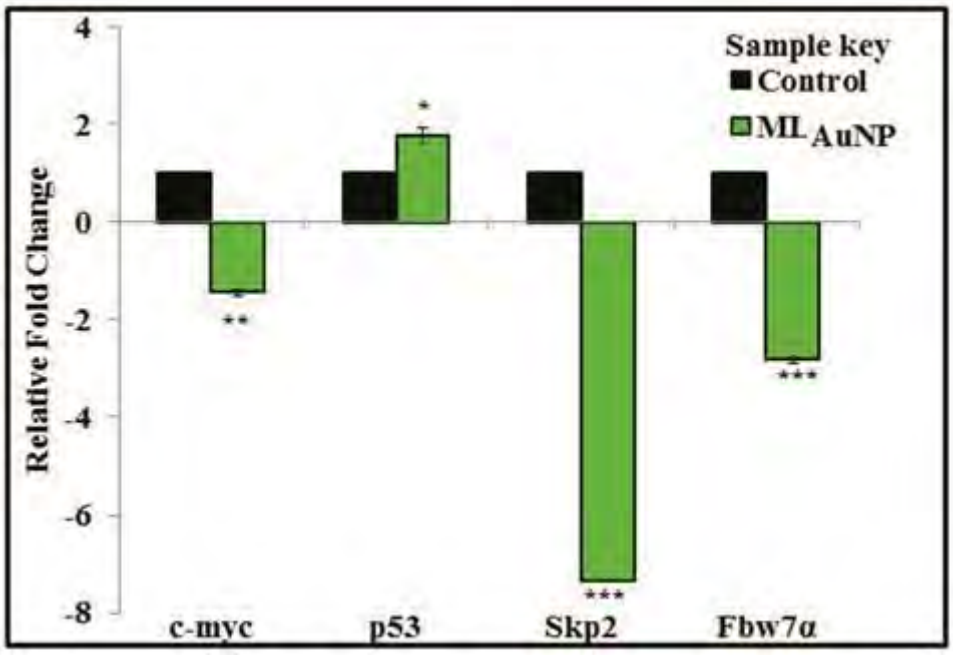

Figure 9 The mRNA levels of *c-myc, p53, skp2* and *Fbw7α* in A549 cells

mRNA levels were differential expressed in A549 cells after exposure to ML_{AuNP} for 24h (***$p < 0.0001$, **$p < 0.001$, *$p < 0.05$).

Alternate splicing of *caspase-9*

Alternate splicing pattern of *caspase-9* was determined using qPCR and presented in Figure 10.

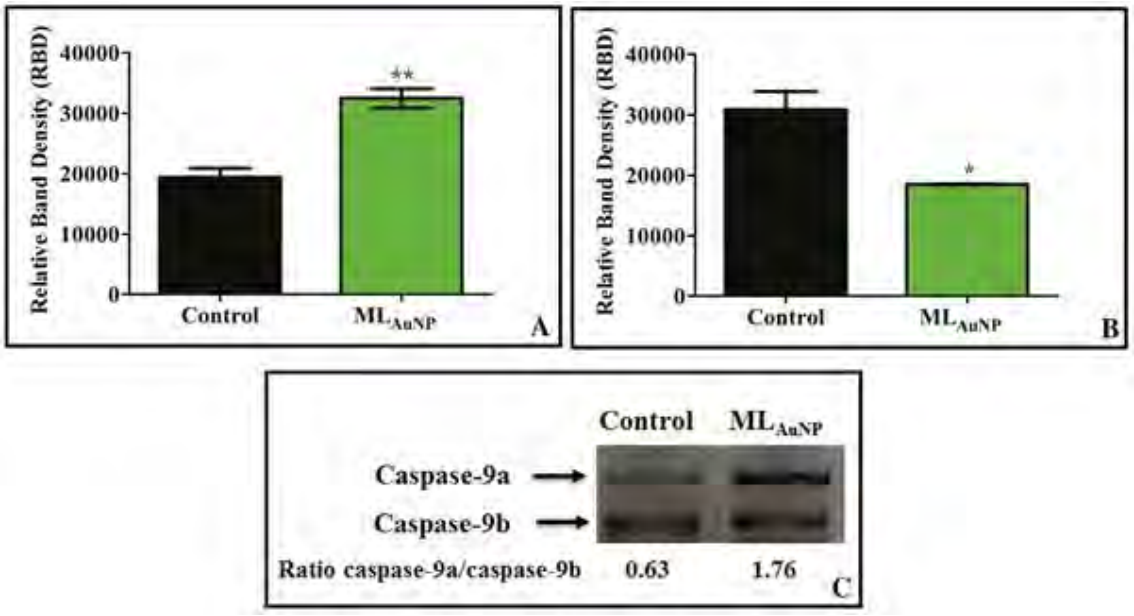

Figure 10 The effect of ML_{AuNP} on alternate splicing of *caspase-9* in A549 cells

Caspase-9a (A) and *caspase-9b* (B) levels were determined by densitometric analysis of qPCR product (C) (**$p < 0.001$, *$p < 0.05$). ML_{AuNP} activated alternate splicing with a significant increase in *caspase-9a* splice variant.

ML_{AuNP} activated alternate splicing of *capase-9* in A549 cancer cells resulting in both a significant 1.68-fold (**$p < 0.001$) increase in pro-apoptotic *caspase-9a* and a 1.67-fold (*$p < 0.05$) decrease in *caspase-9b* levels (Figure 10). Analysis of the alternate splice variants of *caspase-9* showed that ML_{AuNP} changed the *caspase-9a/caspase-9b* ratio from 0.63 ± 0.03 to 1.76 ± 0.08 in the cancer cells.

Discussion

Lung cancer is characterised by uncontrolled cell growth, loss of normal functionality and evasion of apoptosis [Ho et al., 2010]. Current anticancer therapies possess adverse effects and are becoming drug resistant and hence new and more effective agents are actively being investigated. An effective treatment regime for lung cancer will not only increase survival rates but also improve quality of life [Montazeri et al., 2001]. Nanoparticles have huge potential in the treatment of various cancers [Lim et al., 2011; Selim and Hendi, 2012]. ML_{AuNP} was synthesised using MO crude aqueous leaf extract in an environmentally friendly synthesis (Figure 2 - Figure 6). The leaf components possess reducing potential which aided in the green synthesis of the AuNP's [Anand et al., 2014]. There are many phytochemicals present in the leaf extract which includes phenolic acids and flavonoids such as gallic acid, itaconic acid and catechol [Belliraj et al., 2015; El Sohaimy et al., 2015; Luqman et al., 2012]. In addition, the

chemical composition of *Moringa oleifera* aqueous leaf extract by GC-MS analysis showed that it mainly contained hydrocarbons and phenolic compounds (Figure 1). Pyran-4-one, 2-Furancarboxaldehyde, Docosane, Tetracosane, Pentacosane, Heptacosane and Octacosane were identified as major chemical constituents. They play a role in the reduction of the metal ions to form the gold nanoparticles. Gallic acid, a bioactive compound present in the leaf extract can act as a reducing and stabilising agent [Li et al., 2015]. ML_{AuNP} and C_{AuNP} induced cytotoxicity and decreased cell viability in A549 lung and SNO oesophageal cancer cells in a dose-dependent manner (Figure 7), whilst no cytotoxicity was observed in normal healthy PBMCs (Figure 7). ML_{AuNP} as compared to C_{AuNP}, induced greater cytotoxicity and increased antiproliferative effects in both cancerous A549 and SNO cells, reducing A549 and SNO cell viability to 19% and 31% respectively. However C_{AuNP} only reduced A549 and SNO cell viability to 53% and 44% respectively. This shows the selective targeting of AuNP's to cancerous cells, with increased selectivity by the ML_{AuNP}. In addition, ML_{AuNP} was not cytotoxic to normal healthy PBMC's and the increased PBMC's cell viability may be due to the bioactive compounds present in the aqueous crude leaf extract such as glutamine [Ndubuaku et al., 2013; Roth et al., 2002]. Due to minimal toxicity observed in PBMCs, we investigated the mechanism of cell death induced by ML_{AuNP} in A549 and SNO cells.

The c-myc oncoprotein, a basic helix-loop-helix leucine-zipper transcription factor, regulates genes controlling cell growth and proliferation [An et al., 2008]. Lung cancer cells have increased c-myc expression. The ubiquitin-proteasome pathway is responsible for the proteolysis of c-myc involving the F-box protein and ubiquitin ligase components, whilst c-myc mRNA and protein stability contributes to its role in carcinogenesis [Kim et al., 2014]. Posttranslational regulation of c-myc is via Skp2 and Fbw7α [Chen et al., 2013], that are different regulation subunits of the SCF-type E3 ligase (Skp1/Cullin/F-box protein complexes) responsible for proteasomal degradation. The c-myc/Skp2/Fbw7α pathway is linked to tumor progression and is therefore a potential target for anticancer agents [Chen et al., 2013]. c-Myc increases Skp2 expression which also acts as a co-factor increasing c-myc's transcriptional activity [Kim et al., 2014]. Glycogen synthase kinase 3 (Gsk3) mediates Fbw7α degradation of c-myc. Gsk3 phosphorylates threonine 58 residue on c-myc which serves as a recognition site for Fbw7α. ML_{AuNP} significantly decreased both c-myc mRNA and protein expression in A549 cells (Figure 8 and Figure 9). Also Skp2 levels were significantly decreased (Figure 9). This influences c-myc's transcriptional function hence the inhibition of its proliferative effect. In addition, Skp2 causes the degradation of p27 (cyclin dependent kinase inhibitor) thus allowing cell proliferation and therefore loss of Skp2 function will result in p27 induced cell cycle arrest

and inhibition of cell proliferation [Dai et al., 2006; Kim et al., 2014]. Drug resistant cancers often have decreased Fbw7 expression which acts as a tumor suppressor [Chen et al., 2013; Dai et al., 2006]. ML_{AuNP} significantly decreased Fbw7α mRNA levels (Figure 9). The anticancer effect of Wogonin in A549 cells was due to decreased c-myc, Skp2 and Fbw7α levels [Chen et al., 2013]. The induction of apoptosis occurred independently of Fbw7α. Similarly, ML_{AuNP} decreased c-myc, Skp2 and Fbw7α levels suggesting a possible role in drug-resistant cancers.

The p53 tumor suppressor gene functions by regulating cell growth, proliferation and apoptosis. In cancer cells, p53 function is often dysregulated thereby allowing abnormal cells to continue to proliferate. ML_{AuNP} treatment caused a significant increase in p53 mRNA and protein expression (Figure 8 and Figure 9). A consequence of increased p53 expression resulted in increased expression of Bax, a pro-apoptotic protein and a simultaneous decrease in the anti-apoptotic Bcl-2 protein (Figure 8). Furthermore the induction of apoptosis through the activation of Bax causes it to bind to voltage-dependent anion channel (VDAC) and influences its activity [Hengartner, 2000]. The VDAC protein forms a subunit of the mitochondrial permeability transition pore (MPTP). The depolarization of the mitochondrial membrane by ML_{AuNP} opens the MPTP resulting in cytochrome c (cyt c) release from the mitochondria into the cytoplasm, together with ATP. A consequence is that Apaf-1 cleaves procaspase-9 resulting in activation of caspase-9 (Table 2).

The regulation of gene and protein expression is a determinant of cell fate. The serine/arginine-rich proteins (SR proteins) are required for alternate splicing [Manley and Krainer, 2010]. The alternate pre-mRNA processing of *caspase-9* gene produces two splice variants, the pro-apoptotic *caspase-9a* and the anti-apoptotic *caspase-9b* [Massiello and Chalfant, 2006; Shultz et al., 2011; Shultz et al., 2010]. The inclusion of exon 3, 4, 5, 6 cassette results in *caspase-9a* splice variant and the induction of apoptosis. *Caspase-9b* (exon exclusion) competes with *caspase-9a* for binding to the apoptosome. SRp30a is an important splicing factor in the alternative splicing of caspase-9 [Massiello and Chalfant, 2006] and ML_{AuNP} increased SRp30a protein expression (Figure 8) thus activating alternate splicing of pre-mRNA in A549 cells. There was a significant increase in *caspase-9a* with a concomitant decrease in *caspase-9b* mRNA levels in A549 cells (Figure 10). ML_{AuNP} increased the *caspase-9a/caspase-9b* ratio from 0.63 to 1.76. Our findings are consistent with those of Massiello and Chalfant. (2006), where ceramide treated A549 cells resulted in alternate splicing of caspase-9 with increased capase-9a and decreased *caspase-9b* splice variants [Massiello and Chalfant, 2006]. The ratio of *caspase-9a/caspase-9b* increased after ceramide treatment. Also SRp30a was identified as the RNA

trans-acting factor (regulating splicing factor) involved in the pre-mRNA processing and its downregulation favoured *caspase-9b* at the expense of *caspase-9a* [Massiello and Chalfant, 2006]. The increased expression of *caspase-9a* splice variant by ML_{AuNP} resulted in an increase in caspase-9 activity. Increased caspase-9 caused activation of the executioner caspases-3/7 leading to apoptosis (Table 2). These observations strongly suggest that ML_{AuNP} preferentially targets the mitochondria and induces apoptosis via the intrinsic pathway. Furthermore, ML_{AuNP} in SNO cells displayed a greater increase in caspase activity as compared to C_{AuNP} (Table 2). The results show that ML_{AuNP} can be used as an antiproliferative agent.

In addition, during the execution of apoptosis, poly (ADP-ribose) polymerase 1 (PARP-1), a nuclear enzyme, is cleaved into an 89 kDa C-terminal catalytic fragment and a 24 kDa N-terminal DNA-binding domain fragment [D'Amours et al., 2001]. ML_{AuNP} actively induced PARP-1 cleavage in A549 cells as evidenced by the significant increase in the 24 kDa fragment (Figure 8) confirming the execution of apoptosis. Further, PS externalization [Schlegel and Williamson, 2001] was also significantly increased by ML_{AuNP} (Table 2).

Inhibitor of apoptosis protein (IAP), contain baculoviral IAP repeat (BIR) domains, is an intracellular protein that inhibits caspase activity [Hengartner, 2000; Wang, 2001]. Smac/DIABLO which is concurrently released with cyt c from the mitochondria, binds to the BIR domain of IAP thus antagonising its action and ensures the execution of apoptosis [Fischer and Schulze-Osthoff, 2005]. ML_{AuNP} significantly increased Smac/DIABLO protein levels (Figure 8). Our data clearly shows that ML_{AuNP} induces and promotes apoptosis in A549 lung cancer cells. Hsp70, a chaperone molecule, inhibits key effectors in apoptosis [Garrido et al., 2006] and are highly expressed in cancer cells. Hsp70 inhibits apoptosome formation as it binds to Apaf-1 and prevents the recruitment of procaspase-9, thus inhibiting apoptosis and enabling the cancer cells to continue proliferation. In our study, Hsp70 expression was significantly reduced by ML_{AuNP} (Figure 8), thus ensuring the effective execution of apoptosis and the inability of the cancer cells to continue proliferation.

Selim and Hendi, (2012) showed the induction of apoptosis by chemically synthesised AuNP's in an MCF-7 (breast cancer) cell line [Selim and Hendi, 2012]. AuNP's significantly increased p53, Bax, caspase-3 and caspase-9 and decreased Bcl-2 expression. Another study showed that AuNP's decreased GSH levels, increased mitochondrial depolarisation and ultimately led to cell death in HL7702 cells [Gao et al., 2011]. Chemically synthesised AuNP's also caused A549 cell cycle arrest and accumulation in the G1 phase of the cell cycle [Chuang et al., 2013]. Green

synthesis of AuNP's using a plant extract from *Podophyllum hexandrum* showed antiproliferative properties in human cervical carcinoma cells (HeLa cells) [Jeyaraj et al., 2014]. The green synthesis of AuNP's by MO leaves shows promise as an anticancer agent by inducing increased apoptosis in lung cancer cells. The development of nanoparticles has shown potential in therapies which ultimately improve survival rates [Leong and Ng, 2014]. Synthesised AuNP's inhibited ovarian cancer cell growth in a size and concentration dependent manner [Arvizo et al., 2013]. It also inhibited MAPK-signalling with a reversal of the epithelial-mesenchymal transition in the cancer cells displaying antiproliferative and anti-metastatic properties. The physico-chemical properties of NP's depends on the size, shape, charge, hydrophobicity as well as functional groups which facilitates their interaction with biological systems however the mechanism of action is still to be fully elucidated [Davis et al., 2008; Tay et al., 2014].

ML_{AuNP} was successfully produced in a one-pot green synthesis by MO leaves. The synthesised ML_{AuNP} was not cytotoxic to normal healthy PBMCs but was cytotoxic and induced apoptosis, via the intrinsic pathway, in cancerous A549 lung cells. ML_{AuNP} targeted oncogenes, tumor suppressor genes and was able to activate alternate splicing of caspase-9 to effectively execute the apoptotic cascade in lung cancer cells. In addition, ML_{AuNP} caused a dose-dependent decrease in SNO cancer cell viability and activated caspase activity, showing that ML_{AuNP} has an affinity affect cancer cells. Further, ML_{AuNP} showed greater reduction in cell viability in A549 cells as compared to Trisodium citrate gold nanoparticles (C_{AuNP}) (chemically synthesised gold nanoparticles); ML_{AuNP} as compared to C_{AuNP} also induced higher caspase activity in cancerous SNO cells - showing it specifically targets cancer cells.

Acknowledgements

Miss C. Tiloke acknowledges the prestigious Doctoral scholarship from the National Research Foundation, SA. The study was also supported by the funds from College of Health Sciences (UKZN).

References

Al-Owaisi M, Al-Hadiwi N, Khan SA. 2014. GC-MS analysis, determination of total phenolics, flavonoid content and free radical scavenging activities of various crude extracts of *Moringa peregrina* (Forssk.) Fiori leaves. Asian Pac J Trop Biomed 4:964-970.

An J, Yang D, Xu Q, Zhang S, Huo Y, Shang Z, Wang Y, Wu D, Zhou P. 2008. DNA-dependent protein kinase catalytic subunit modulates the stability of c-Myc oncoprotein. BMC Molecular cancer 7:1-12.

Anand K, Gengan R, Phulukdaree A, Chutugoon AA. 2014. Agroforestry waste *Moringa oliefera* petals mediated green synthesis of gold nanoparticles and their anti-cancer and catalytic activity. J Industrial Engineering Chem 21:1105-1111.

Arvizo RR, Saha S, Wang E, Robertson JD, Bhattacharya R, Mukherjee P. 2013. Inhibition of tumor growth and metastasis by a self-therapeutic nanoparticle. Proc Natl Acad Sci 110:6700-6705.

Bainor A, Chang L, McQuade TJ, Webb B, Gestwicki JE. 2011. Bicinchoninic acid (BCA) assay in low volume. Anal Biochem 410 310-312.

Belliraj TS, Nanda A, Ragunathan R. 2015. *In-vitro* hepatoprotective activity of *Moringa oleifera* mediated synthesis of gold nanoparticles J Chem Pharm Res 7:781-788.

Bello B, Fadahun O, Kielkowski D, Nelson G. 2011. Trends in lung cancer mortality in South Africa: 1995-2006. BMC Public Health 11:2-5.

Bonomi S, Gallo S, Catillo M, Pignataro D, Biamonti G, Ghigna C. 2013. Oncogenic alternative splicing switches: role in cancer progression and prospects for therapy. Int J Cell Biol 1-17.

Cai W, Gao T, Hong H, Sun J. 2008. Applications of gold nanoparticles in cancer nanotechnology. Nanotechnol Sci Appl 1:17-32.

Chen X, Bai Y, Zhong Y, Xie X, Long H, Yang Y, Wu S, Jia Q, Wang X. 2013. Wogonin has multiple anti-cancer effects by regulating c-Myc/Skp2/Fbw7α and HDAC1/HDAC2 pathways and inducing apoptosis in human lung adenocarcinoma cell line A549. PLoS one 8:1-7.

Cheng Y, Lee S, Lin S, Chang W, Chen Y, Tsai N, Liu Y, Tzao C, Yu D, Harn H. 2005. Anti-proliferative activity of *Bupleurum scrozonerifolium* in A549 human lung cancer cells *in vitro* and *in vivo*. Cancer lett 222:183-193.

Chuang S, Lee Y, Liang R, Roam G, Zeng Z, Tu H, Wang S, Chueh PJ. 2013. Extensive evaluations of the cytotoxic effects of gold nanoparticles. Biochimica et Biophysica Acta 1830 4960-4973.

D'Amours D, Sallmann FR, Dixit VM, Poirier GG. 2001. Gain-of-function of poly (ADP-ribose) polymerase-1 upon cleavage by apoptotic proteases: implications for apoptosis. J Cell Sci 114:3771-3778.

Dai M, Jin Y, Gallegos JR, Lu H. 2006. Balance of yin and yang: ubiquitylation-mediated regulation of p53 and c-Myc. Neoplasia 8:630-644.

Davis ME, Chen Z, Shin DM. 2008. Nanoparticle therapeutics: an emerging treatment modality for cancer. Nat Rev Drug Discov 7:771-782.

Eblen ST. 2012. Regulation of chemoresistance via alternative messenger RNA splicing. Biochem Pharmacol 83:1063-1072.

El Sohaimy SA, Hamad GM, Mohamed SE, Amar MH, Al-Hindi RR. 2015. Biochemical and functional properties of *Moringa oleifera* leaves and their potential as a functional food. GARJAS 4:188-199.

Erasto P, Adebola PO, Grierson S, Afolayan AJ. 2005. An ethnobotanical study of plants used for the treatment of diabetes in the Eastern Cape Province, South Africa. African J Biotech 12:1458-1460.

Fahey JW. 2005. *Moringa oleifera*: A review of the medical evidence for its nutritional, therapeutic, and prophylactic properties. part 1. Trees for Life J 1-5.

Fischer U, Schulze-Osthoff K. 2005. Apoptosis-based therapies and drug targets. Cell Death Diff 12:942-961.

Gao W, Xu K, Ji L, Tang B. 2011. Effect of gold nanoparticles on glutathione depletion-induced hydrogen peroxide generation and apoptosis in HL7702 cells. Toxicol Lett 205:86-95.

Garrido C, Brunet M, Didelot C, Zermati Y, Schmitt E, Kroemer G. 2006. Heat shock proteins 27 and 70 anti-apoptotic proteins with tumorigenic properties. Cell cycle 5:2592-2601.

Globocan. 2012. Globocan 2012 Estimated cancer Incidence, Mortality, Prevalence and Disability-adjusted life years (DALYs) Worldwide in 2012 [http://globocan.iarc.fr/].

Goyal BR, Agrawal BB, Goyal RK, Mahta AA. 2007. Phyto-pharmacology of *Moringa oleifera* Lam an overview. Nat Prod Rad 6:347-353.

Hengartner MO. 2000. The biochemistry of apoptosis. Nature 407:770-776.

Ho JA, Chang H, Shih N, Wu L, Chang Y, Chen C, Chou C. 2010. Diagnostic detection of human lung cancer-associated antigen using a gold nanoparticle-based electrochemical immunosensor. Anal Chem 82:5944-5950.

Jeyaraj M, Arun R, Sathishkumar G, MubarakAli D, Rajesh M, Sivanandhan G, Kapildev G, Manickavasagam M, Thajuddin N, Ganapathi A. 2014. An evidence on G2/M arrest, DNA damage and caspase mediated apoptotic effect of biosynthesized gold nanoparticles on human cervical carcinoma cells (HeLa). Materials Res Bulletin 15-24.

Kang B, Mackey MA, El-Sayed M. 2010. Nuclear targeting of gold nanoparticles in cancer cells induces DNA damage, causing cytokinesis arrest and apoptosis. J Am Chem Soc 132:1517-1519.

Kim T, Kang JM, Hyun J, Lee B, Kim SJ, Yang E, Hong S, Lee H, Fujii M, Niederhuber JE, Kim S. 2014. The Smad7-Skp2 complex orchestrates Myc stability, impacting on the cytostatic effect of TGF-β. J Cell Sci 127:411-421.

Kotakadi VS, Gaddam SA, Rao YS, Prasad TNVKV, Reddy AV, Sai Gopal DVR. 2014. Biofabrication of silver nanoparticles using *Andrographis paniculata*. Eur J Med Chem 73:135-140.

Kumar A, Boruah B, Liang X. 2011. Gold nanoparticles: promising nanomaterials for the diagnosis of cancer and HIV/AIDS. J Nano:1-17.

Leong DT, Ng KW. 2014. Probing the relevance of 3D cancer models in nanomedicine research. Adv Drug Deliv Rev 79-80:95-106.

Li D, Liu Z, Yuan Y, Liu Y, Niu F. 2015. Green synthesis of gallic acid-coated silver nanoparticles with high antimicrobial activity and low cytotoxicity to normal cells. Process Biochem 50:357-366.

Lim ZJ, Li JJ, NG C, Yung LL, Bay B. 2011. Gold nanoparticles in cancer therapy. Acta Pharmacol Sin 32:983-990.

Livak KJ, Schmittgen TD. 2001. Analysis of relative gene expression data using real-time quantitative PCR and the $2^{-\Delta\Delta Ct}$ method. Methods 25:402-408.

Luqman S, Srivastava S, Kumar R, Maurya AK, Chanda D. 2012. Experimental assessment of *Moringa oleifera* leaf and fruit for its antistress, antioxidant, and scavenging potential using *in vitro* and *in vivo* assays. Evid Based Complement Alternat Med 2012:1-12.

Manley JL, Krainer AR. 2010. A rational nomenclature for serine/arginine-rich protein splicing factors (SR proteins). Genes Dev 24:1073-1074.

Massiello A, Chalfant CE. 2006. SRp30a (ASF/SF2) regulates the alternative splicing of caspase-9 pre-mRNA and is required for ceramide-responsiveness. J Lipid Res 47:892-897.

Mendis S, Armstrong T, Bettcher D, Branca F, Lauer J, Mace C, Poznyak V, Riley L, Da Costa E Silva V, Stevens G. 2014. Global status report on noncommunicable diseases 2014. World Health Organization 1-280.

Mishra G, Singh P, Verma R, Kumar S, Srivastav S, Jha KK, Khosa RL. 2011. Traditional uses, phytochemistry and pharmacological properties of *Moringa oleifera* plant: An overview. Der Pharmacia Lettre 3:141-164.

Montazeri A, Milroy R, Hole D, McEwen J, Gillis CR. 2001. Quality of life in lung cancer patients as an important prognostic factor. Lung Cancer 31:233-240.

Mossman T. 1983. Rapid colorimetric assay for cellular growth and survival: application to proliferation and cytotoxicity assay. J Immunol Methods 65:55-63.

Ndubuaku UM, Nwankwo VU, Baiyeri KP. 2013. Influence of poultry manure application on leaf amino acid profile, growth and yield of moringa (*Moringa oleifera* Lam) plants. Int J Cur Tr Res 2:390-396.

Parveen A, Roa S. 2014. Cytotoxicity and genotoxicity of biosynthesized gold and silver nanoparticles on human cancer cell lines. J Clust Sci 1-14.

Prasad TNVKV, Elumalai EK. 2011. Biofabrication of Ag nanoparticles using *Moringa oleifera* leaf extract and their antimicrobial activity. Asian Pac J Trop Biomed 439-442.

Roth E, Oehler R, Manhart N, Exner R, Wessner B, Strasser E, Spittler A. 2002. Regulative potential of glutamine-relation to glutathione metabolism. Nutrition 18:217-221.

Salamanca-Buentello F, Persad DL, Court EB, Martin DK, Daar AS, Singer PA. 2005. Nanotechnology and the developing world. PLoS Med 2:0383-0386.

Schlegel RA, Williamson P. 2001. Phosphatidylserine, a death knell. Cell Death Diff 8:551-563.

Selim M, Hendi A. 2012. Gold nanoparticles induce apoptosis in MCF-7 human breast cancer cells. A Pac J Can Prev 13:1617-1620.

Shankar SS, Rai A, Ankamwar B, Singh A, Ahmad A, Sastry M. 2004. Biological synthesis of triangular gold nanoprisms. Nature Mater 3:482-488.

Shultz JC, Goehe RW, Murudkar CS, Wijesinghe DS, Mayton EK, Massiello A, Hawkins AJ, Mukerjee P, Pinkerman RL, Park MA, Chalfant CE. 2011. SRSF1 regulates the alternative splicing of caspase 9 via a novel intronic splicing enhancer affecting the chemotherapeutic sensitivity of non-small cell lung cancer cells. Molecular cancer reseach 9:889-900.

Shultz JC, Goehe RW, Wijesinghe DS, Murudkar C, Hawkins AJ, Shay JW, Minna JD, Chalfant CE. 2010. Alternative splicing of caspase 9 is modulated by the phosphoinositide 3-Kinase/Akt pathway via phosphorylation of SRp30a. Cancer research 70:9185-9196.

Siddiqi NJ, Abdelhalim M, El-Ansary A, Alhomida AS, Ong W. 2012. Identification of potential biomarkers of gold nanoparticle toxicity in rat brains. J Neuro 9:1-16.

Sreelatha S, Jeyachitra A, Padma PR. 2011. Antiproliferation and induction of apoptosis by *Moringa oleifera* leaf extract on human cancer cells. Food Chem Toxicol 49:1270-1275.

Stuchinskaya T, Moreno M, Cook MJ, Edwards DR, Russell DA. 2011. Targeted photodynamic therapy of breast cancer cells using antibody-phthalocyanine-gold nanoparticle conjugates. Photochem Photobiol Sci 10:822-831.

Sukirtha R, Priyanka KM, Antony JJ, Kamalakkannan S, Thangam R, Gunasekaran P, Krishnan M, Achiraman S. 2012. Cytotoxic effect of green synthesized silver nanoparticles using *Melia azedarach a*gainst *in vitro* HeLa cell lines and lymphoma mice model. Process Biochem 47:273-279.

Tay CY, Setyawati MI, Xie J, Parak WJ, Leong DT. 2014. Back to basics: exploiting the innate physico-chemical characteristics of nanomaterials for biomedical applications. Adv Funct Mater 24:5936-5955.

Tedesco S, Doyle H, Blasco J, Redmond G, Sheehan D. 2010. Oxidative stress and toxicity of gold nanoparticles in Mytilus edulis. Aquatic Toxicol 100:178-186.

Tiloke C, Phulukdaree A, Chuturgoon AA. 2013. The antiproliferative effect of *Moringa oleifera* crude aqueous leaf extract on cancerous human alveolar epithelial cells. BMC Complement Altern Med 13:1-8.

Wang X. 2001. The expanding role of mitochondria in apoptosis. Genes Dev 15:2922-2933.

Wilson K, Walker J. 2005. Principles and techniques of biochemistry and molecular biology. Cambridge University Press.

Xie J, Lee JY, Wang DIC. 2007a. Synthesis of single-crystalline gold nanoplates in aqueous solutions through biomineralization by serum albumin protein. J Phys Chem C 111:10226-10232.

Xie J, Lee JY, Wang DIC, Ting YP. 2007b. Identification of active biomolecules in the high-yield synthesis of single-crystalline gold nanoplates in algal solutions. Small 3:672-682.

Xie J, Lee JY, Wang DIC, Ting YP. 2007c. Silver nanoplates: from biological to biomimetic synthesis. ACS Nano 1:429-439.

Xie J, Zheng Y, Ying JY. 2009. Protein-directed synthesis of highly fluorescent gold nanoclusters. J Am Chem Soc 131:888-889.

Yang Y, Ma H. 2009. Western Blotting and ELISA techniques. Researcher 1:67-86.

Zhang P, Gao WY, Turner S, Ducatman BS. 2003. Gleevec (STI-571) inhibits lung cancer cell growth (A549) and potentiates the cisplatin effect *in vitro*. BMC Mol Cancer 2:1-9.

CHAPTER 5
DISCUSSION, CONCLUSION AND RECOMMENDATIONS

South Africa has a diverse range of plants and trees which are readily available for traditional medicinal use [1]. More than 3000 species are used for herbal remedies which have shown potential in treatment of various ailments including cancer. A growing interest into the local biodiversity of our plant kingdom and their medicinal potential has led to the expansion of indigenous knowledge and medical use. Although modern medicine has advanced tremendously, the rate of disease progression especially in developing countries are also advancing with uncontrollable side-effects. Traditional medicinal plants and trees may provide positive outcomes in chronic diseases with minimal side-effects. Of the many traditional medicinal trees available, MO is readily used by many South Africans.

In SA, cancer mortality (especially lung and oesophageal cancer) is increasing at a rapid rate. The high mortality rates are due to late stage detection which increases the aggressive nature of cancer cells [2, 3]. Therefore, early detection and diagnosis will allow for treatment with positive outcomes. Unfortunately, the cost associated with early detection and subsequent treatments are relatively high, in addition to the many side-effects, which necessitates for complementary and alternative medicines (CAM). CAM can be beneficial to cancer patients as it is not only cost-effective but also induces cancerous cell death. This study investigated the antiproliferative and apoptosis inducing effects of MOE and its synthesised AuNP's in human cancer cells *in vitro*.

First, it was shown that MOE possessed antiproliferative effects in A549 lung cancer cells [4]. MOE increased ROS production which compromised cellular membranes via lipid peroxidation [5]. It specifically targeted Nrf2 and significantly reduced its levels with a subsequent decrease in GSH levels. MOE induced significant oxidative stress accompanied by DNA damage and p53 upregulation. This resulted in induction of programmed cell death via the mitochondria (intrinsic pathway of apoptosis). In addition, MOE increased Smac/DIABLO expression and cleavage of PARP-1 to ensure lung cancer cell death. Similarly, in SNO oesophageal cancer cells, MOE significantly increased oxidative stress by increasing lipid peroxidation and significantly decreasing antioxidant response, viz., Nrf2, GSH and catalase levels. This led to oxidative DNA damage and execution of the apoptotic cascade via p53 activation. In addition, apoptotic markers such as PS externalisation, Smac/DIABLO and PARP-1 cleavage were significantly elevated. Interestingly, MOE had no cytotoxic effects on normal healthy PBMCs.

MOE is composed of various phytochemicals which is vital for the antiproliferative effect seen in cancer cells. Amongst the several bioactive compounds such as gallic acid, rhamnose, glucosinolates and isothiocyanates [6], niazimicin has been identified to have potent anticancer properties [7]. It has been shown that niazimicin had anticancer properties by inhibiting Epstein-Barr-virus-early antigen activation in Raji cells induced by a tumour promoter [7]. Further *in vivo* tests showed that it had anticancer effects in two-stage carcinogenesis in mouse skin. Niazimicin delayed tumour promotion by 50% and papilloma formation by 80% after 10 weeks in mice. MOE exerted anticancer activity in B16 F10 melanoma tumours in mice [8]. MOE inhibited cell proliferation and tumour growth in comparison to the control. The anticancer property was attributed to phytochemical constituents including niazimicin. It has also been shown that MOE decreased NFkB signalling pathway and inhibited cell proliferation in Panc-1 cells [9]. MOE caused cells to accumulate in the G1 phase of the cell cycle. It also worked synergistically with cisplatin to induce cytotoxicity in pancreatic cancer cells. MOE also displayed cytoprotective effects against lead induced hepatotoxicity in wistar rats [10]. Lead treatment caused increased hepatocyte damage as alkaline phosphatase, amino transferase and alanine amino transferase levels were elevated with a decrease in catalase activity. Following exposure to MOE, the damage caused by lead was reversed.

Existing chemotherapies are non-specific [11] and selective targeting by anticancer agents is ideal. MOE was then used in an environmentally friendly synthesis of gold nanoparticles (ML_{AuNP}). The GC-MS analysis showed that MOE contained many bioactive compounds such as Pyran-4-one, 2-Furancarboxaldehyde, Docosane, Tetracosane, Pentacosane, Heptacosane and Octacosane which facilitated the synthesis of ML_{AuNP}'s. A one pot green synthesis technique [12] was used to synthesise the novel ML_{AuNP} successfully. As compared to chemically synthesised $C_{AuNP,}$ ML_{AuNP} induced greater cytotoxicity in both A549 and SNO cells. The ML_{AuNP} was more effective in selective targeting, albeit in a unicellular system, and inducing apoptosis of lung and oesophageal cancer cells. Interestingly, ML_{AuNP} was not cytotoxic to normal healthy PBMCs but modulated oncogenes, tumour suppressor genes and alternate splicing of *caspase-9* to effectively induce apoptosis in A549 lung cancer cells. In cancers, there is dysregulation of oncogenes (e.g. *c-myc*) and tumour suppressor genes (e.g. *p53*) which promotes tumour progression. ML_{AuNP} significantly decreased c-myc levels with a simultaneous increase in p53 levels which signalled for apoptosis via the mitochondria. Alternate splicing is regulated by SR proteins such as SRp30a. Irregular alternate splicing in cancer cells leads to chemotherapy resistance as the isoforms expressed results in differing functionality. Cancer cells increase anti-apoptotic isoforms and decrease pro-apoptotic isoforms thereby increasing

resistance. The alternate processing of *caspase-9* gene produces two splice variants, the pro-apoptotic *caspase-9a* and the anti-apoptotic *caspase-9b* [13-15]. *Caspase-9* alternate splicing has shown that the *caspase-9b* splice variant (anti-apoptotic) enhances chemotherapy resistance [16]. ML_{AuNP} increased SRp30a which favoured *caspase-9a* splice variant and subsequently increased caspase-9 activity to effectively execute apoptosis in A549 lung cancer cells. Dysregulated alternate splicing facilitates cell growth, angiogenesis, tumour development, cancer metabolism, evasion of apoptosis and chemotherapy resistance [17]. Therefore, targeting alternate splicing in cancer cells can be effective in therapy. It has been shown that there is dysregulated alternate splicing in renal cancer cells when compared to their paired control [18]. The *caspase9a/caspase-9b* ratio was affected with higher expression of *caspase-9b* which was similar to *survivin* splice variant expression leading to inhibition of apoptosis. Also alternate splicing of *GLI1*, an oncogenic transcription factor, was dysregulated resulting in increased expression of anti-apoptotic molecules and resistance to cell death.

Cancer cells increase their resistance by inducing an antioxidant response, elevating GSH levels to reduce ROS [17]. Synthesis of GSH is dependent on the availability and functionality of cysteine and cystine transporter system (xCT and CD98hc). *CD44* has multiple functions and plays a role in inter cell and matrix interactions as well as migration and invasion. Alternate splicing of *CD44* produces *CD44 v8-10* which increases GSH levels by interacting with cystine transporter xCT. This results in reduced oxidative damage by reducing ROS levels. This was evident in *CD44v*-positive 4T1 mouse breast cancer cells. It increased xCT activity and GSH levels. These mice then developed lung metastatic lesions demonstrating its role in metastasis. The splicing factor ESRP1 is responsible for the alternate splicing of *CD44*. The decreased expression of the splicing factor prevented lung metastasis. Regulation of alternate splicing especially in cancer cells is imperative as cellular fate is thereby determined.

MO seedpods were used in the synthesis of AuNP's [19]. The seedpod extract caused the reduction of chloroauric acid resulting in AuNP's formation. The phytochemical screening of the extract also showed it contained flavonoids, alkaloids, terpenes, saponins and phenols. The extract possessed antibacterial effects against *B. subtilis, S. aureus, E. coli and K. pneumonia.* The synthesised AuNP's showed hepatoprotective properties in $HepG_2$ cells. B-chronic lymphocytic leukaemia is resistant to apoptosis as a result of increased VEGF secretion from cancerous cells [20]. VEGF causes neovascularisation and cell survival therefore anti-VEGF antibody can be utilised to induce apoptosis in cancer cells. Anti-VEGF antibody were conjugated to gold nanoparticles to assess whether it enhanced the apoptotic cascade [20]. The

synthesised conjugated AuNP's decreased anti-apoptotic molecules and caused a significant cleavage of PARP-1 showing potential of AuNP's as an anticancer agent.

A study conducted on AuNP's effects on Vero, MRC-5 and NIH3T3 cells showed that AuNP's specifically induced apoptosis only in Vero cells [21]. However, in MRC-5 cells, AuNP's caused DNA damage and induced a cellular repair response. AuNP's induced autophagy in NIH3T3 cells as cell growth was slowed. It has been shown that stable AuNP's can be synthesised using MOE [22]. However biocompatibility and cytotoxicity of the synthesised AuNP's required further investigations.

It was shown that MOE, possess antiproliferative properties *in vitro* by inducing apoptosis (the intrinsic apoptotic pathway) in both lung and oesophageal cancer cell lines via increased oxidative stress, DNA fragmentation and pro-apoptotic molecules. Interestingly, both MOE and ML_{AuNP} were only cytotoxic to cancer cells and not on normal healthy cells (PBMCs). This shows the selective targeting of MOE and ML_{AuNP} to cancerous cells. In addition, exposure to MOE had a greater increase in PBMCs cell viability as compared to ML_{AuNP}. This can be attributed to MOE's constituents i.e. glutamine which plays a role in nutrition and cellular metabolism [23, 24]. Glutamine is required by lymphocytes for cellular proliferation and activation. Also, exposure to glutamine stimulated DNA, RNA and protein synthesis in hepatocytes [24], demonstrating its role in cell proliferation. Taken together the results from our study indicate the potential use of MOE as a complementary and alternative medicine for lung and oesophageal cancer. Further, ML_{AuNP} also induced apoptosis in A549 lung cancer cells via classical splicing and up-regulation of the pro-apoptotic *caspase-9a* variant. In addition, ML_{AuNP} induced caspase activity for the induction of apoptosis in SNO oesophageal cancer cells.

In conclusion, both MOE and ML_{AuNP} have potential against cancer as they displayed the potent apoptotic inducing properties. Fractionation and purification studies of the crude extract are further recommended for future studies. In addition, an assessment of the safety and efficacy of MOE and ML_{AuNP} in an *in vivo* and cancer model will be beneficial. Gallic acid was identified as a bioactive compound present in the leaf extract which is a potential compound for future tests. Cancer cell resistance to therapy can be due to membrane transport proteins such as the ABCC family and p-glycoprotein which causes an efflux of anticancer drugs preventing their therapeutic potential. By targeting these membrane transport proteins, there will be an intracellular accumulation of the anticancer agent for the effective activation and execution of

apoptosis. In addition, the cell cycle, cyclin-CDK complex and IAP's are also possible target points which are further recommended for investigation.

The main limitation of this study is the use of a unicellular/monolayer cell culture system. In order to show selective cancer cell targeting by MOE and its synthesised ML_{AuNP}'s, an assessment in an *in vivo* rodent model (with induced lung cancer) will be beneficial. Further, an evaluation in a healthy model will assess the safety, bio-distribution and efficacy of MOE and ML_{AuNP}. Furthermore, by inducing lung cancer in the rodents (*in vivo* testing), we can assess the antiproliferative effect and selective cancer cell targeting in a multicellular system.

References

1. Rybicki, E.P., Chikwamba, R., Koch, M., Rhodes, J.I., Groenewald, J. Plant-made therapeutics: An emerging platform in South Africa. Biotechnol Adv, 2012, 30:449-459.
2. Billeter, A.T., Barnett, R.E., Druen, D., Polk, H.C., van Berkel, V.H. MicroRNA as a new factor in lung and esophageal cancer. Semin Thoracic Surg, 2012, 24:155-165.
3. Zhang, Y. Epidemiology of esophageal cancer. World J Gastroenterol, 2013, 19:5598-5606.
4. Tiloke, C., Phulukdaree, A., Chuturgoon, A.A. The antiproliferative effect of *Moringa oleifera* crude aqueous leaf extract on cancerous human alveolar epithelial cells. BMC Complement Altern Med, 2013, 13:1-8.
5. Bartosz, G. Reactive oxygen species: destroyers or messengers? Biochem Pharmacol, 2009, 77:1303-1215.
6. Fahey, J.W. *Moringa oleifera*: A review of the medical evidence for its nutritional, therapeutic, and prophylactic properties. part 1. Trees for Life J, 2005, 1-5.
7. Guevara, A.P., Vargas, C., Sakurai, H., Fujiwara, Y., Hashimoto, K., Maoka, T., Kozuka, M., Ito, Y., Tokuda, H., Nishino, H. An antitumor promoter from *Moringa oleifera Lam.* Mutat Res, 1999, 440:181-188.
8. Purwal, L., Pathak, A.K., Jain, U.K. *In vivo* anticancer activity of the leaves and fruits of *Moringa oleifera* on mouse melanoma. Pharmacologyonline, 2010, 1:655-665.
9. Berkovich, L., Earon, G., Ron, I., Rimmon, A., Vexler, A., Lev-Ari, S. *Moringa oleifera* aqueous leaf extract down-regulates nuclear factor-kappaB and increases cytotoxic effect of chemotherapy in pancreatic cancer cells. BMC Complement Altern Med, 2013, 13:1-7.

10. Omotoso, B.R., Abiodun, A.A., Ijomone, O.M., Adewole, S.O. Lead-induced damage on hepatocytes and hepatic reticular fibres in rats; protective role of aqueous extract of *Moringa oleifera* leaves (Lam). J Biosci Med, 2015, 3:27-35.
11. Lim, Z.J., Li, J.J., Ng, C., Yung, L.L., Bay, B. Gold nanoparticles in cancer therapy. Acta Pharmacol Sin, 2011, 32:983-990.
12. Anand, K., Gengan, R.M., Phulukdaree, A., Chuturgoon, A. Agroforestry waste *Moringa oleifera* petals mediated green synthesis of gold nanoparticles and their anti-cancer and catalytic activity. J Ind Eng Chem, 2014, 21:1105-1111.
13. Shultz, J.C., Goehe, R.W., Murudkar, C.S., Wijesinghe, D.S., Mayton, E.K., Massiello, A., Hawkins, A.J., Mukerjee, P., Pinkerman, R.L., Park, M.A., Chalfant, C.E. SRSF1 regulates the alternative splicing of caspase 9 via a novel intronic splicing enhancer affecting the chemotherapeutic sensitivity of non-small cell lung cancer cells. Mol Cancer Res, 2011, 9:889-900.
14. Massiello, A., Chalfant, C.E. SRp30a (ASF/SF2) regulates the alternative splicing of caspase-9 pre-mRNA and is required for ceramide-responsiveness. J Lipid Res, 2006, 47:892-897.
15. Shultz, J.C., Goehe, R.W., Wijesinghe, D.S., Murudkar, C., Hawkins, A.J., Shay, J.W., Minna, J.D., Chalfant, C.E. Alternative splicing of caspase 9 is modulated by the phosphoinositide 3-kinase/Akt pathway via phosphorylation of SRp30a. Cancer Res, 2010, 70:9185-9196.
16. Srinivasula, S.M., Ahmad, M., Fernandes-Alnemri, T., Alnemri, E.S. Autoactivation of procaspase-9 by Apaf-1-mediated oligomerization. Mol Cell, 1998, 1:949-957.
17. Bonomi, S., Gallo, S., Catillo, M., Pignataro, D., Biamonti, G., Ghigna, C. Oncogenic alternative splicing switches: role in cancer progression and prospects for therapy. Int J Cell Biol, 2013, 2013:1-17.
18. Piekielko-Witkowska, A., Wiszomirska, H., Wojcicka, A., Poplawski, P., Boguslawska, J., Tanski, Z., Nauman, A. Disturbed expression of splicing factors in renal cancer affects alternative splicing of apoptosis regulators, oncogenes, and tumor suppressors. PLoS one, 2010, 5:1-12.
19. Belliraj, T.S., Nanda, A., Ragunathan, R. *In-vitro* hepatoprotective activity of *Moringa oleifera* mediated synthesis of gold nanoparticles. J Chem Pharm Res, 2015, 7:781-788.
20. Mukherjee, P., Bhattacharya, R., Bone, N., Lee, Y.K., Patra, C.R., Wang, S., Lu, L., Secreto, C., Banerjee, P.C., Yaszemski, M.J., Kay, N.E., Mukhopadhyay, D. Potential therapeutic application of gold nanoparticles in B-chronic lymphocytic leukemia (BCLL): enhancing apoptosis. J Nanobiotechnology, 2007, 5:1-13.

21. Chueh, P.J., Liang, R., Lee, Y., Zeng, Z., Chuang, S. Differential cytotoxic effects of gold nanoparticles in differentmammalian cell lines. J Hazard Mater, 2014, 264:303-312.
22. Chakraborty, A., Das, D., Sinha, M., Dey, S., Bhattacharjee, S. *Moringa oleifera* leaf extract mediated green synthesis of stabilized gold nanoparticles. J Bionanosci, 2013, 7:1-5.
23. Ndubuaku, U., Nwankwo, V.U., Baiyeri, K.P. Influence of poultry manure application on leaf amino acid profile, growth and yield of moringa (*Moringa oleifera* Lam) plants. Int J Cur Tr Res, 2013, 2:390-396.
24. Roth, E., Oehler, R., Manhart, N., Exner, R., Wessner, B., Strasser, E., Spittler, A. Regulative potential of glutamine - relation to glutathione metabolism. Nutrition, 2002, 18:217-221.

APPENDIX 1

Moringa oleifera **leaves were collected from the KwaZulu-Natal region (Durban, South Africa) and verified by the KwaZulu-Natal herbarium (Figure 1)**

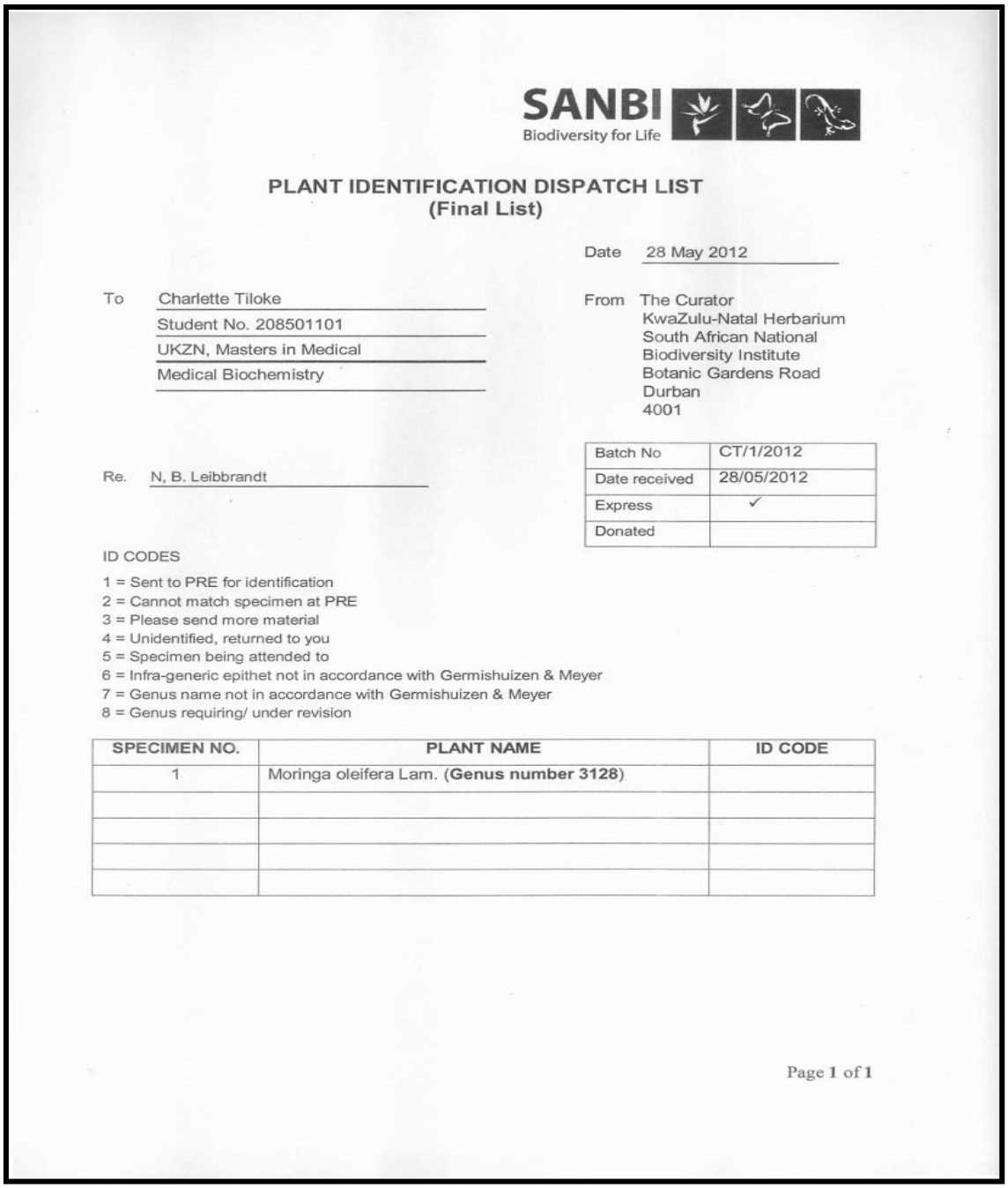

SANBI
Biodiversity for Life

PLANT IDENTIFICATION DISPATCH LIST
(Final List)

Date 28 May 2012

To Charlette Tiloke
Student No. 208501101
UKZN, Masters in Medical
Medical Biochemistry

From The Curator
KwaZulu-Natal Herbarium
South African National
Biodiversity Institute
Botanic Gardens Road
Durban
4001

Batch No	CT/1/2012
Date received	28/05/2012
Express	✓
Donated	

Re. N, B. Leibbrandt

ID CODES

1 = Sent to PRE for identification
2 = Cannot match specimen at PRE
3 = Please send more material
4 = Unidentified, returned to you
5 = Specimen being attended to
6 = Infra-generic epithet not in accordance with Germishuizen & Meyer
7 = Genus name not in accordance with Germishuizen & Meyer
8 = Genus requiring/ under revision

SPECIMEN NO.	PLANT NAME	ID CODE
1	Moringa oleifera Lam. (**Genus number 3128**)	

Page 1 of 1

Figure 1 *Moringa oleifera* leaves verification certificate obtained from the KwaZulu-Natal herbarium.

APPENDIX 2

Chapter 2 - The antiproliferative effect of *Moringa oleifera* crude aqueous leaf extract on cancerous human alveolar epithelial cells - Supplementary material

DNA damage

DNA damage was determined using the Comet assay. Following treatment of cells (20,000 cells/well) in a 6-well plate, supernatants were removed and cells were trypsinized. Three slides per sample were prepared as the first layer of 1% low melting point agarose (LMPA, 37°C), second layer of 25µl of cells (20,000) from the samples with 175µl of 0.5% LMPA (37°C) and third layer of 0.5% LMPA (37°C) covered the slides. After solidification, the slides were then submerged in cold lysing solution [2.5M NaCl, 100mM EDTA, 1% Triton X-100, 10mM Tris (pH 10), 10% DMSO] and incubated (4°C, 1h). Following incubation the slides were placed in electrophoresis buffer [300mM NaOH, 1mM Na_2EDTA (pH 13)] for 20min and thereafter subjected to electrophoresis (25V, 35min, RT) using Bio-Rad compact power supply. The slides were then washed 3 times with neutralisation buffer [0.4M Tris (pH 7.4)] for 5min each. The slides were stained overnight (4°C) with 40µl ethidium bromide (EtBr) and viewed with a fluorescent microscope (Olympus IXSI inverted microscope with 510-560nm excitation and 590nm emission filters). Images of 50 cells and comets were captured per treatment and the comet tail lengths were measured using Soft imaging system (Life Science - ©Olympus Soft Imaging Solutions v5) and expressed in µm.

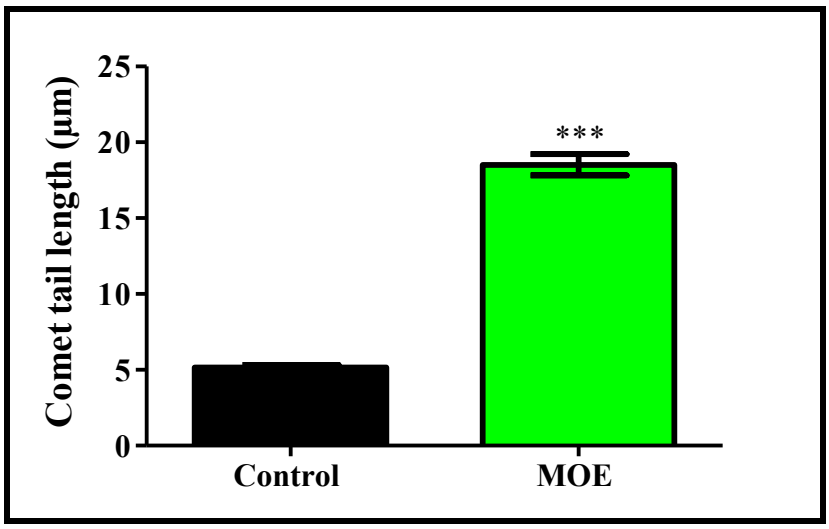

Figure 1 DNA damage was assessed using the Comet assay and comet tails length were measured and compared between the control and treatment groups. MOE significantly increased

comet tail length as compared to the untreated control (18.52 ± 4.90µm vs 5.15 ± 1.18µm, $p < 0.0001$).

Western blotting

Western Blots were performed to determine the expression of Nrf2, p53, Smac/DIABLO and PARP-1. Briefly, total protein was isolated using Cytobuster™ reagent supplemented with protease inhibitor (Roche, cat. no. 05892791001) and phosphatase inhibitor (Roche, cat. no. 04906837001). The bicinchoninic acid assay (Sigma, Germany) was used to quantify the protein and was standardised to 2.042mg/ml. The samples were prepared in Laemmli buffer, boiled (100°C, 5min) and electrophoresed (150V, 1h) in 7.5% sodium dodecyl sulfate polyacrylamide gels using a Bio-Rad compact power supply. The separated proteins were electro-transferred to nitrocellulose membrane using the Trans-Blot® Turbo Transfer system (Bio-Rad) (20V, 45min). The membranes were blocked (1h) using 3% BSA in Tris-buffered saline containing 0.5% Tween20 (TTBS - NaCl, KCL, Tris, Tween 20, dH_2O, pH 7.4). Thereafter, the membranes were immune-probed with primary antibody [Nrf2 (ab89443), p53 (ab26), PARP-1 (ab110915), 1:1,000; Smac/DIABLO (ab68352), 1:200] at 4°C overnight. The membranes were then washed 4x with TTBS (10min each) and incubated with the secondary antibody (ab97046; 1:2,000) at RT for 1h. The membranes were finally washed 4x with TTBS (10min each). To correct for loading error and to normalise the expression of the proteins, β-actin was assessed (ab8226; 1:5,000). Horse radish peroxidase (HRP) chemiluminescence detector and enhancer solution was used for the antigen-antibody complex and the signal was detected with the Alliance 2.7 image documentation system (UViTech). The expression of the proteins were analysed with UViBand Advanced Image Analysis software v12.14 (UViTech). The data was expressed as relative band density (RBD) and fold change.

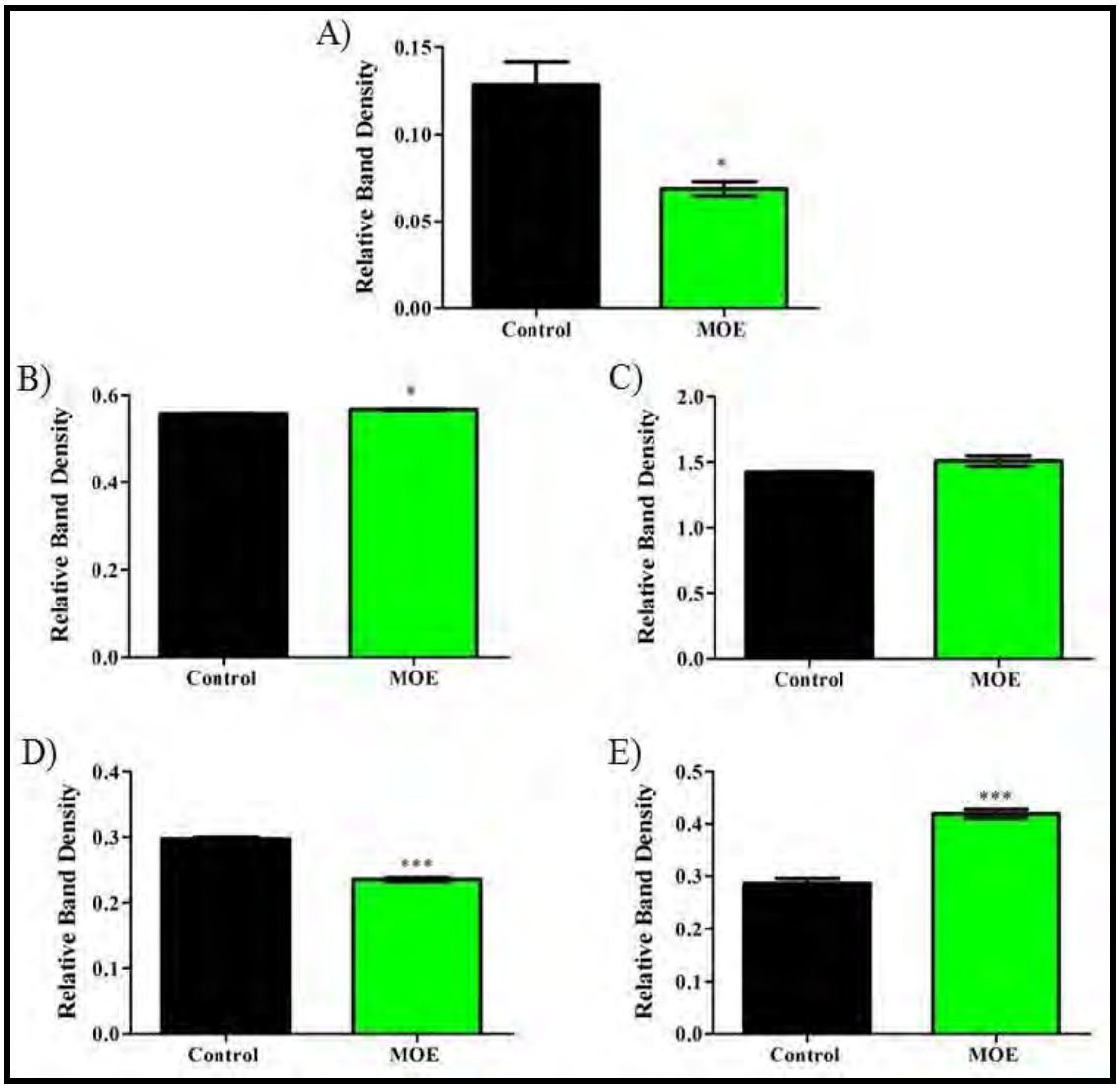

Figure 2 Western blot was used to determine the expression of proteins in relative band density (RBD) of Nrf2 (A), p53 (B), Smac/DIABLO (C), PARP-89 kDa (D) and 24 kDa (E) fragment in A549 cells after treatment with MOE. The expression of Nrf2 in MOE treated cells were significantly decreased compared to the untreated control [Figure 2A (0.069 ± 0.007 RBD vs 0.129 ± 0.022 RBD, $p < 0.05$). There was a significant increase in p53 expression [Figure 2B (0.567 ± 0.002 RBD vs control: 0.558 ± 0.002 RBD, $p < 0.05$)] and Smac/DIABLO expression [Figure 2C (1.509 ± 0.055 RBD vs control: 1.425 ± 0.007 RBD, $p = 0.162$)]. MOE caused PARP cleavage into an 89 kDa and 24 kDa fragment with a significant decrease in PARP 89 kDa fragment expression compared to the control [Figure 2D (0.234 ± 0.005 RBD vs 0.297 ± 0.005 RBD, $p < 0.0001$)]. The PARP 24 kDa fragment was significantly increased [Figure 2E (0.419 ± 0.014 RBD vs 0.286 ± 0.016 RBD, $p < 0.0001$)].

Data analysis for western blot

1) Nrf2

Table 1 The normalisation of the expression of Nrf2 in the control

Treatments	RBD 1	RBD 2	RBD 3
Control	23118944	31714632	24647880
β-actin	205612604	205612604	205612604
	0.112	0.154	0.120

Table 2 The normalisation of the expression of Nrf2 in the MOE treatment

Treatments	RBD 1	RBD 2	RBD 3
MOE	16219257	17313580	13970162
β-actin	230473898	230473898	230473898
	0.070	0.075	0.061

Table 3 The expression of Nrf2 in A549 cells treated with MOE for 24h

Treatments	RBD 1	RBD 2	RBD 3	Mean RBD	SD	Fold change
Control	0.112	0.154	0.120	0.129	0.022	1
MOE	0.070	0.075	0.061	0.069	0.007	1.89

2) p53

Table 4 The normalisation of p53 expression in the control

Treatments	RBD 1	RBD 2	RBD 3
Control	8609	8566	8636
β-actin	15394	15394	15394
	0.559	0.556	0.561

Table 5 The normalisation of p53 expression in the MOE treatment

Treatments	RBD 1	RBD 2	RBD 3
MOE	9661	9606	9648
β-actin	16986	16986	16986
	0.569	0.566	0.568

Table 6 The expression of p53 in A549 cells treated with MOE for 24h

Treatments	RBD 1	RBD 2	RBD 3	Mean RBD	SD	Fold change
Control	0.559	0.556	0.561	0.558	0.002	1
MOE	0.569	0.566	0.568	0.567	0.002	1.02

3) Smac/DIABLO

Table 7 The normalisation of the expression of Smac/DIABLO in the control

Treatments	RBD 1	RBD 2	RBD 3
Control	22059	21905	21969
β-actin	15428	15428	15428
	1.430	1.420	1.424

Table 8 The normalisation of the expression of Smac/DIABLO in the MOE treatment

Treatments	RBD 1	RBD 2	RBD 3
MOE	22551	23743	22266
β-actin	15335	15335	15335
	1.471	1.548	1.509

Table 9 Smac/DIABLO expression in A549 cells treated with MOE for 24h

Treatments	RBD 1	RBD 2	RBD 3	Mean RBD	SD	Fold change
Control	1.430	1.420	1.424	1.425	0.007	1
MOE	1.471	1.548	1.509	1.509	0.055	1.06

4) *PARP 89 kDa

Table 10 The normalisation of PARP 89 kDa expression in the control

Treatments	RBD 1	RBD 2	RBD 3
Control	6521	6369	6299
β-actin	21520	21520	21520
	0.303	0.296	0.293

Table 11 The normalisation of PARP 89 kDa expression in the MOE treatment

Treatments	RBD 1	RBD 2	RBD 3
MOE	4495	4644	4662
β-actin	19623	19623	19623
	0.229	0.237	0.238

Table 12 The expression of PARP 89 kDa in A549 cells treated with MOE for 24h

Treatments	RBD 1	RBD 2	RBD 3	Mean RBD	SD	Fold change
Control	0.303	0.296	0.293	0.297	0.005	1
MOE	0.229	0.237	0.238	0.234	0.005	1.27

* PARP 24 kDa

Table 13 The normalisation of the expression of PARP 24 kDa in the control

Treatments	RBD 1	RBD 2	RBD 3
Control	6559	5977	5941
β-actin	21520	21520	21520
	0.305	0.278	0.276

Table 14 The normalisation of the expression of PARP 24 kDa in the MOE treatment

Treatments	RBD 1	RBD 2	RBD 3
MOE	8452	8291	7913
β-actin	19623	19623	19623
	0.431	0.423	0.403

Table 15 PARP 24 kDa expression in A549 cells treated with MOE for 24h

Treatments	RBD 1	RBD 2	RBD 3	Mean RBD	SD	Fold change
Control	0.305	0.278	0.276	0.286	0.016	1
MOE	0.431	0.423	0.403	0.419	0.014	1.46

APPENDIX 3

Phytochemical analysis of *Moringa oleifera* aqueous leaf extract

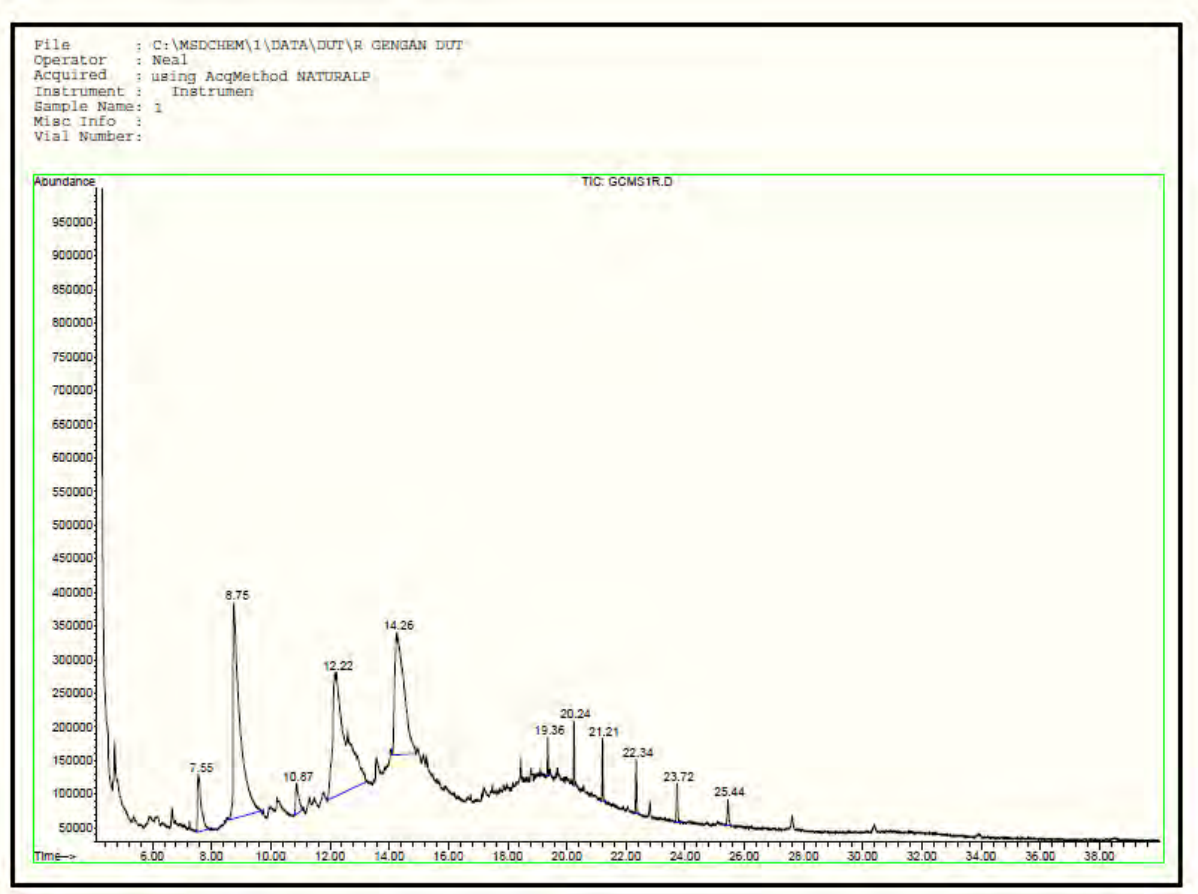

Figure 1 Chemical composition of MOE by GC-MS analysis

MOE showed eleven peaks in the GC-MS chromatogram. The compounds were separated according to their retention time on fused silica capillary column. The total ion chromatogram (TIC) indicates the presence of various organic compounds with significant abundant peaks at retention time 7.55, 8.75, 10.87, 12.22, 14.26, 19.36, 20.24, 21.21, 22.34, 22.72 and 25.44 min having molecular ions (m/z) of 144.0, 126.0, 142.0, 58.0, 60.0, 310.0, 338.0, 352.0, 279.0, 366.0 and 380.0 respectively. These compounds mainly comprised of hydrocarbons and phenolic compounds. Pyran-4-one (7.55), 2-Furancarboxaldehyde (8.75), Docosane (19.36), Tetracosane (21.21), Pentacosane (22.34), Heptacosane (23.72) identified as major chemical constituents followed by Octacosane (25.44) [1]

References

1. Al-Owaisi, M., Al-Hadiwi, N., Khan, S.A. GC-MS analysis, determination of total phenolics, flavonoid content and free radical scavenging activities of various crude extracts of *Moringa peregrina* (Forssk.) Fiori leaves. Asian Pac J Trop Biomed, 2014, 4:964-970.

APPENDIX 4

SNO cell viability assay

SNO cell viability was determined using the 3-(4, 5-Dimethyl-2-thiazolyl)-2, 5-diphenyl-2H-tetrazolium bromide (MTT) assay. Cells (20,000cells/well) were seeded into a 96-well microtitre plate. The cells were incubated with varying MOE dilutions (0.1-10mg/ml) in six replicates (300µl/well) and incubated (37ºC, 5% CO_2) for 48 and 72h. Control cells were incubated with CCM only. A CCM/MTT salt solution (5mg/ml) was added (120µl/well) and the plate was incubated (37ºC, 4h). Thereafter, supernatants were removed; dimethyl sulphoxide (DMSO) 100µl/well was added and incubated (1h). The optical density of the formazan product was measured (570/690nm) using a spectrophotometer (Bio Tek µQuant). The results were expressed as percentage cell viability relative to the control. This experiment was repeated on two separate occasions before the concentration of half the maximum inhibition (IC_{50}) of MOE for SNO cells were determined.

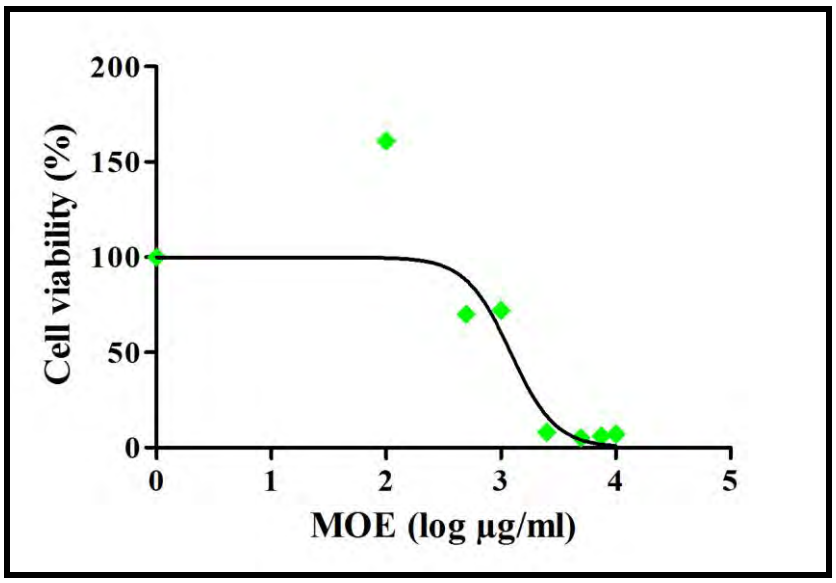

Figure 1 SNO cell viability treated with MOE for 48h

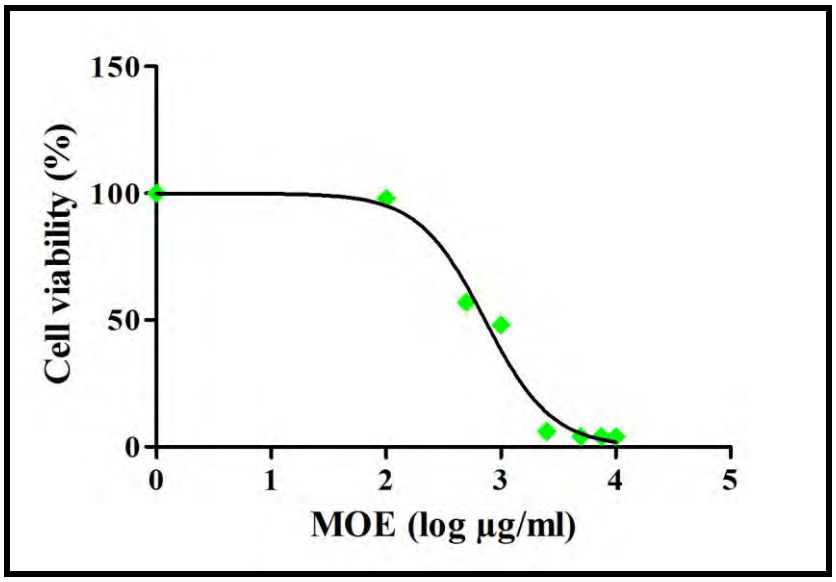

Figure 2 SNO cell viability treated with MOE for 72h

A dose-dependent decline in SNO cell viability was seen after exposure to MOE for 48 and 72h. An IC_{50} of 1214µg/ml (48h, Figure 1) and 727.2µg/ml (72h, Figure 2) was determined.

APPENDIX 5

Protein quantification and standardisation

The bicinchoninic acid assay (BCA) (Sigma, Germany) was used to quantify the isolated protein. Bovine serum albumin (BSA) standards (0-1mg/ml) were prepared in dH_2O. 25µl of each BSA standards, samples and 202µl BCA working solution (BCA, $CuSO_4$) was added per well and incubated (37°C, 30min). The optical density was measured on a spectrophotometer (Bio Tek µQuant) at 562nm. The data was analysed and expressed in mg/ml from the linear equation generated from the standard curve. The concentration of protein for each sample was determined and subsequently standardised.

1) The antiproliferative effect of *Moringa oleifera* crude aqueous leaf extract on cancerous human alveolar epithelial cells

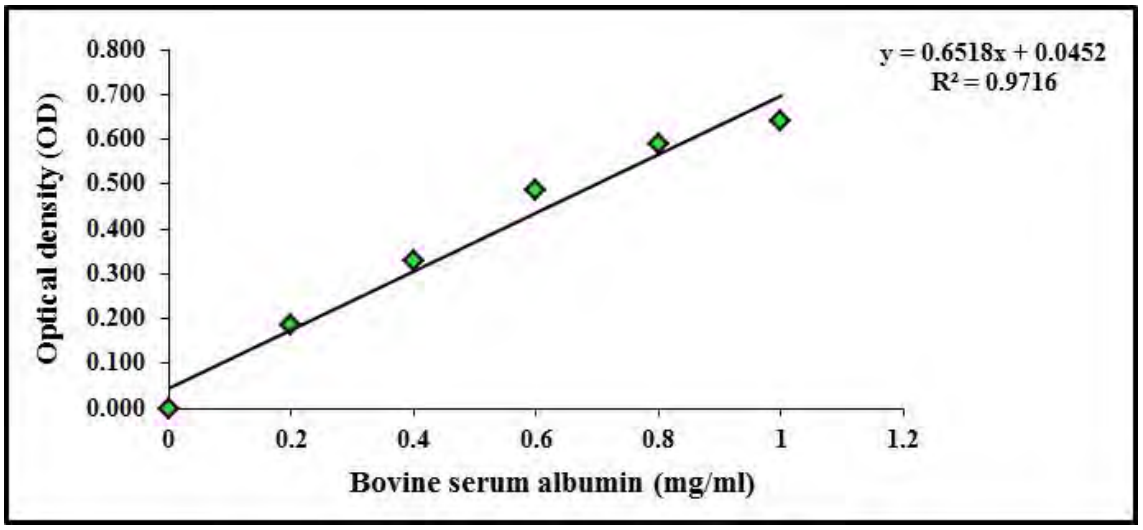

Figure 1 Standard curve using known concentrations of bovine serum albumin for determining sample protein concentration using bicinchoninic acid assay

Table 1: Standardisation of protein samples (A549 cells exposed to MOE) using the standard curve for Western blotting

Treatments	Average absorbance (OD)	Protein concentration (mg/ml)	C2 (mg/ml)	V1 (µl)	V2 (µl)
Control	1.377	2.042	2.042	100	100
MOE	1.538	2.290	2.042	89.17	100

2) The antiproliferative effect of *Moringa oleifera* crude aqueous leaf extract on human oesophageal cancer cells

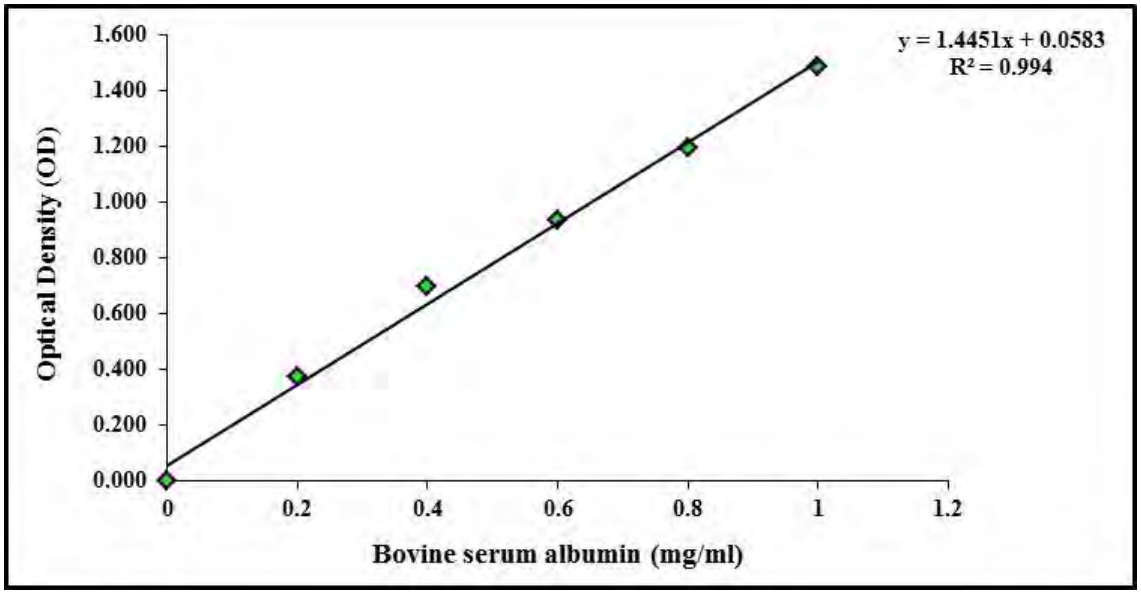

Figure 2 Standard curve using known concentrations of bovine serum albumin for determining sample protein concentration using bicinchoninic acid assay

Table 2: Standardisation of protein samples (SNO cells exposed to MOE) using the standard curve for Western blotting

Treatments	Average absorbance (OD)	Protein concentration (mg/ml)	C2 (mg/ml)	V1 (µl)	V2 (µl)
Control	2.306	1.555	1	64.3	100
MOE	2.281	1.538	1	65	100

3) *Moringa oleifera* gold nanoparticles modulate oncogenes, tumor suppressor genes and *caspase-9* splice variants in A549 cells.

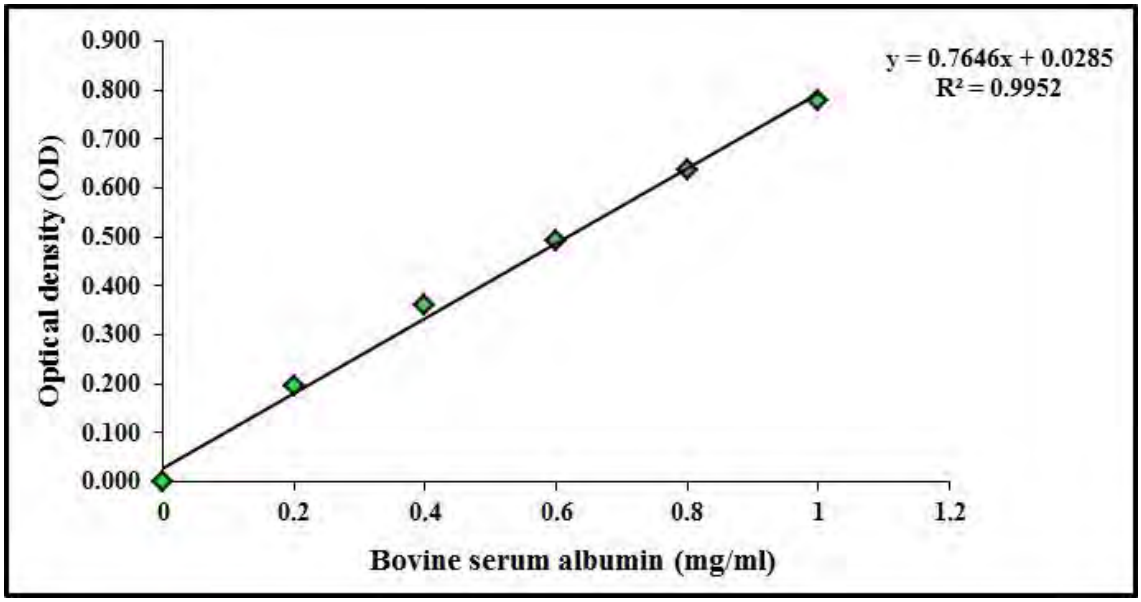

Figure 3 Standard curve using known concentrations of bovine serum albumin for determining sample protein concentration using bicinchoninic acid assay

Table 3: Standardisation of protein samples (A549 exposed to ML_{AuNP}) using the standard curve for Western blotting

Treatments	Average absorbance (OD)	Protein concentration (mg/ml)	C2 (mg/ml)	V1 (µl)	V2 (µl)
Control	2.312	2.986	1.066	71.4	200
MOE	1.892	2.437	1.066	87.5	200